

University of Alberta

Applications of nonautonomous infinite-dimensional systems control
theory for parabolic PDEs

by

James Choon-sun Ng

A thesis submitted to the Faculty of Graduate Studies and Research
in partial fulfillment of the requirements for the degree of

Doctor of Philosophy

in

Process Control

Department of Chemical and Materials Engineering

©James Choon-sun Ng

Fall 2013

Edmonton, Alberta

Permission is hereby granted to the University of Alberta Libraries to reproduce single copies of this thesis and to lend or sell such copies for private, scholarly or scientific research purposes only. Where the thesis is converted to, or otherwise made available in digital form, the University of Alberta will advise potential users of the thesis of these terms.

The author reserves all other publication and other rights in association with the copyright in the thesis and, except as herein before provided, neither the thesis nor any substantial portion thereof may be printed or otherwise reproduced in any material form whatsoever without the author's prior written permission.

Dedication

To my parents, Heng-joo and Ku-Leong

Abstract

Parabolic partial differential equations (PDEs) are used as models of transport-reaction phenomena in a variety of different industrial chemical and materials engineering processes, and can yield precise descriptions of process variables with complex temporal and spatially dependent system dynamics. In many cases, the process dynamics are also affected by time-dependent features of the system which arise from the underlying physical characteristics of the process or the methods utilized in the formation and treatment of materials which may result in phase transitions, deformations or a combination of these behaviours. The dynamical analysis of these processes provides a fundamental basis for development of model based control strategies through a number of approaches including from within the framework of infinite-dimensional systems control theory. However, each class of transport-reaction system presents its own unique challenges and requires the development of new strategies within the existing framework.

The focus of this thesis is the systematic treatment and realization of the feedback control design for two general classes of problems. The first class deals with the optimal boundary control problem for unstable parabolic PDEs with nonautonomous and nonhomogeneous infinite-dimensional system representation, and is considered within the context of a lithium-ion battery thermal regulation problem. The key challenges addressed include the time-dependence of system parameters, system instability, the restriction of the input along a portion of the battery domain boundary, the observer based optimal boundary control design, and the realization of the outback feedback control problem based on state measurement and interpolation methods. The second class of problems is the optimal distributed and boundary control of parabolic PDEs on time-varying spatial domains with nonautonomous infinite-dimensional system representation. The key challenges addressed include the development of an appropriate function space setting to handle the time-dependence of the spatial domain, the formulation of the infinite-dimensional system representation of the PDE control problem within this function space setting, and the realization of the optimal distributed and boundary control problems within the context of the Czochralski crystal temperature stabilization problem.

Acknowledgements

I would like to thank my supervisors Dr. Stevan Dubljevic and Dr. Sirish L. Shah for all of their guidance and support. The many insightful discussions which we have shared over the years have played a huge role in shaping this current work. I would also like to give special thanks to Dr. Yau-shu Wong for all of his thoughtfulness and encouragement throughout my studies and research endeavours.

To my family, words cannot fully express how deeply grateful I am for all of your love and support. For my mother, Ku-Leong, and father, Heng-joo, thank you for believing in me and for encouraging me to pursue this path. Without all of your patience and empathy, I would not have been able to see this through. I hope to have made you proud.

To my friends, I cannot imagine a more amazing group of people who's diverse interests and talents have been a profound source of inspiration throughout the many years which we have enjoyed together. I am truly fortunate to be in the company of such compassionate individuals, and I wish the very best in life for each and every one of you.

Contents

1	Introduction	1
1.1	Control theory for PDEs: A brief historical overview	3
1.2	PDE process models and control systems	7
1.2.1	Examples	10
1.2.2	Infinite-dimensional system representation	13
1.3	Thesis motivation	15
1.3.1	Thermal regulation of lithium-ion batteries	16
1.3.2	Czochralski crystal temperature stabilization	17
1.4	Thesis scope and contributions	20
	Bibliography	22
2	Boundary control synthesis for a lithium-ion battery thermal regulation problem	31
2.1	Introduction	31
2.2	Model description	35
2.3	Boundary control and infinite-dimensional system representation	41
2.3.1	Infinite-dimensional system representation	44
2.3.2	Boundary control formulation as an infinite-dimensional system	47

2.4	State estimation and output feedback control	52
2.4.1	Observer design	54
2.4.2	Interpolation based output feedback controller design	58
2.5	Numerical Simulation and Case Studies	62
2.5.1	Case 1 and Case 2	66
2.5.2	Case 3 and Case 4	68
2.6	Summary	72
2.7	Proof of Proposition 1	74
2.8	Proof of Proposition 2	77
	Bibliography	80
3	Control of parabolic PDEs with time-varying spatial domain:	
	Czochralski crystal growth process	84
3.1	Introduction	84
3.2	Preliminaries	88
3.3	Parabolic PDE on time-dependent spatial domain	90
3.3.1	Model formulation	90
3.3.2	General class of PDE	94
3.3.3	CZ crystal temperature model	96
3.4	Infinite-dimensional system representation	98
3.5	The optimal control problem	107
3.6	Numerical results	111
3.7	Summary	113
	Bibliography	115
4	Optimal control of convection-diffusion process with time-varying spatial domain: Czochralski crystal growth process	120

4.1	Introduction	120
4.2	Model description	124
4.3	Infinite-dimensional system representation	126
4.3.1	Function space description	127
4.3.2	Nonautonomous evolution system representation	128
4.4	Controller design	134
4.4.1	Optimal boundary control formulation	134
4.5	Numerical implementation	136
4.5.1	Galerkin approximation	136
4.5.2	Optimal control problem for coupled systems	138
4.6	Simulation and results	139
4.6.1	Crystal temperature regulation	140
4.6.2	Comparison to fixed-gain controllers	143
4.7	Conclusions	146
4.8	Appendix	147
	Bibliography	152

5 Optimal boundary control of a diffusion-convection-reaction PDE model with time-dependent spatial domain: Czochralski crystal growth process 155

5.1	Introduction	155
5.2	Preliminaries	159
5.2.1	Model formulation	160
5.2.2	Notation and function space description	163
5.2.3	Parabolic PDE with time-dependent spatial domain	165
5.3	Optimal boundary controller synthesis	168
5.3.1	System representation	169

5.3.2	Linear Quadratic Regulator synthesis	171
5.4	Application of optimal boundary control to CZ crystal growth process	172
5.4.1	Eigenfunctions and eigenvalues	173
5.4.2	The optimal boundary control problem synthesis	177
5.4.3	Numerical implementation	179
5.4.4	Simulation results	181
5.5	Summary	186
	Bibliography	187
6	Conclusions and Future Work	191
6.1	Conclusions	192
6.2	Future Work	195
	Bibliography	197

List of Tables

2.1	Case 1 and Case 2: measurement and control parameters . . .	66
2.2	Case 3 and Case 4: measurement and control parameters . . .	68
2.3	Nomenclature	73
2.4	Physical properties	73
5.1	Table of physical and numerical parameters	182

List of Figures

1.1	Tubular reactor system example	10
1.2	Annealing process diagram	12
2.1	Entropy changes as functions of state of charge (SOC)	38
2.2	Battery system schematic with boundary actuation.	41
2.3	Actual and reconstructed initial temperature distributions	59
2.4	Open loop temperature distributions.	63
2.5	Solutions of the differential and auxiliary Riccati equations	65
2.6	Input and energy profiles for Case 1 and Case 2.	67
2.7	Input and energy profiles for Case 3 and Case 4.	69
2.8	Closed loop temperature distributions for Case 1 and Case 3.	71
3.1	Czochralski crystal growth process components and evolution	96
3.2	Crystal length and boundary velocity 1D	112
3.3	Input and closed loop energy profiles 1D	113
3.4	Crystal temperature evolution 1D	114
4.1	Czochralski crystal growth process diagram 2D	125
4.2	Crystal boundary evolution	140
4.3	Initial crystal temperature distribution 2D	141
4.4	Crystal temperature distribution at $t = 5$ and $t = 25$	142

4.5	Crystal temperature distribution at $t = 50$ and $t = 75$	143
4.6	Crystal temperature distribution at $t = 100$ and $t = 150$	143
4.7	Input profiles for different controllers	144
4.8	Energy profiles for different controllers	144
5.1	Bridgman-Stockbarger crystal growth method process schematic	158
5.2	Czochralski process diagram with boundary input	174
5.3	Boundary length and velocity	183
5.4	Boundary input	183
5.5	Energy profiles	184
5.6	Crystal temperature distribution $t = 0$ and $t = 5$	185
5.7	Crystal temperature distribution $t = 20$ and $t = 50$	185

List of Common Notation

Ω	Spatial domain
Ω_t	Time varying spatial domain
$\partial\Omega$	Spatial domain boundary
$\partial\Omega_t$	Time varying spatial domain boundary
$\mathcal{L}(\mathcal{Z})$	Bounded linear operator from \mathcal{Z} to \mathcal{Z}
$\mathcal{L}(\mathcal{Z}, \mathcal{Y})$	Bounded linear operator from \mathcal{Z} to \mathcal{Y}
\mathcal{U}	Input space
\mathcal{Y}	Output space
\mathcal{Z}	State space
\mathbb{C}	Set of complex numbers
\mathbb{N}	Set of positive integers
\mathbb{R}	Set of real numbers
\mathbb{R}^m	m-dimensional space
$\Pi(t)$	Operator valued solution of the differential Riccati Equation
ξ	Spatial variable
$A(\xi, t)$	PDE spatial operator
$A(t)$	Nonautonomous state linear operator
$B(\xi, t)$	PDE input operator
$B(t)$	Nonautonomous state input operator

$C(t)$	Nonautonomous state measurement operator
$D(A(t))$	Domain of the operator $A(t)$
$S(t)$	One parameter semigroup
t	Time variable
$u(t)$	Input function
$U(t, s)$	Two-parameter semigroup
$y(t)$	State measurements
$z(\xi, t)$	Distributed state
$z(t)$	System state

Chapter 1

Introduction

In chemical and materials engineering sciences, Partial Differential Equations (PDEs) are widely used as models of transport-reaction phenomena in formation, synthesis, separation, and electrochemical processes. There continues to be a rich and active research interest in this field which draws upon the well established classical tools of mathematical analysis, and also employ the recent advancements in computer technology for process simulation and numerical studies of complex problems. Modern applications include many examples in the petroleum industry such as reservoir modelling for heavy oil recovery, and tubular and plug-flow reactor systems which are used for the production and the refinement of large volume chemicals such as hydrogen, methanol, and synthetic hydrocarbons by the catalysis of various types of feedstocks. In the electronics, automotive, and power distribution industries, electrochemical devices such as fuel cells and lithium-ion battery technology, are revolutionizing the way in which energy is being stored and utilized. In manufacturing industries, phase transitions and thermal treatment are critical factors in the fabrication and processing of materials, such as in semiconductor production by crystal growth methods.

One broad area of applied mathematics is control systems science which deals with the analysis and design of controllers for dynamical systems, and is closely aligned with and intersects the engineering disciplines on many different levels. Contemporary advancements in the field have also been greatly aided by the advent, development, and proliferation to computer technology which has facilitated the implementation of digital control systems in many industrial applications. In the context of chemical and materials engineering, the basic premise underlying the control of processes described by PDEs is that one can affect the transport-reaction process dynamics by manipulating certain parameters of the system. One would like to then be able to predict the response of the dynamical system and achieve, as close as possible, some kind of desired behaviour. Consequently, an understanding of the process dynamics given by the PDE is a prerequisite to the development of model based control schemes to obtain these objectives. As such, the fundamental mathematical tools utilized in the dynamical analysis of these types of systems are also necessary in the development of control methodologies, and the results of which form the cornerstone of control theory for PDEs. While there has been a considerable effort in this research area, there remain many open problems and challenges not only in understanding the fundamental control related questions, but also in the feasible implementation of control schemes. The following sections provide a brief background in this area, and describe some of the challenges which are associated with the related control problems for the classes of PDEs considered in this work.

1.1 Control theory for PDEs: A brief historical overview

Some of the most important developments in control theory for PDEs occurred in the 1960s-1970s and are documented in several well known monographs and review papers from that time era [1, 2, 3, 4]. A more complete account of the historical developments in control theory for PDEs can be found in review articles [5, 6]. The early works focused on control systems for linear PDEs from a mathematical point of view and dealt with the rudimentary notions of stability, stabilizability, and controllability, in the generalization of some of the key concepts from control theory for processes described by ordinary differential equations (ODEs) and their finite-dimensional state space representation. To this end, one of the approaches taken was the functional analytic description of the PDE control problems as abstract evolution systems in Banach spaces which formed the basis of infinite-dimensional systems control theory. Essentially, this approach facilitated the state space representation of PDEs which enabled the dynamical analysis of the the related control problems within the context of operator semigroup theory. Moreover, results developed within the infinite-dimensional systems framework could now be interpreted in a familiar setting with direct comparisons to the analogous results from their finite-dimensional system counterparts. However, not all concepts from finite-dimensional systems could be carried over, and in fact, many negative results and pathological phenomena appeared out of the infinite-dimensional system representation of the PDE control problems.

Although early obstacles which prevented the formation of a comprehensive and generalized control theory for PDEs included issues similar to those faced

in dealing with control problems for ODEs, such as in nonautonomous (time-varying) and nonlinear systems, many other obstacles were unique to PDE control problems and also varied between the different PDE classes.¹ One of the most important issues was that the spatially distributed nature of PDE models required the inclusion of geometric considerations in the overall theory. For example, the geometry of the physical spatial domain required a distinction between the types of distributed control problems (actuation within domain), and those belonging to the types of boundary control problems (actuation at the boundary). The number and placement of actuators and sensors yielded a host of new factors to consider in both control and observation problems within each of these categories. A concerted effort shared between the mathematics and mathematical control communities was required to resolve many of the technical and often subtle mathematically abstract issues pertaining to the existence, uniqueness, and regularity of solutions for specific cases and examples in both distributed and boundary control problems.

During the same time period, there was also a large effort by researchers looking at control problems involving PDEs from a more conventional engineering mathematics perspective. One of the most common approaches taken for these problems utilized so called early lumping methods through modal analysis and modal decomposition to approximate the PDEs by finite-dimensional systems of ODEs, and subsequently enabled the application of well developed finite-dimensional systems control theory [7, 8]. While this has proven to be both an attractive means for controller design and readily

¹For example, from the spectral analysis of finite-dimensional systems from ODEs and infinite-dimensional systems from the class of parabolic PDEs, the position of the spectrum determines the growth of the semigroup formed by each, but the same cannot be said for time-varying operators (nonautonomous systems) and the class of hyperbolic PDEs.

implementable in industrial applications, the limitations of the early lumping approach were quickly realized. Early lumping techniques often resulted in a mismatch in the dynamical properties of the original PDE and the approximated system which led to poor controller performance. The source of this issue lay in the intrinsically distributed nature of the PDE control problems which could not be completely accounted for through finite-dimensional approximations of the systems. However, the foundation which provided a basis for the necessary theoretic framework on which to study the issue was being concurrently built within the mathematical control community. In particular, infinite-dimensional systems theory provided a viable methodology to capture the complete dynamical picture for PDE systems while preserving the ability to subsequently develop more practically oriented and implementable control schemes through methods often referred to as late lumping techniques for controller design [9, 10, 11, 12].

The reconciliation of control theory from the abstract mathematical perspective with the pragmatic engineering perspective continues to be a major topic in control theory for PDEs. While the convergence of these two points of view has led to advanced model based control strategies for PDEs, there remains key barriers to their mainstream adoption in industrial settings. By the mid 1990s, many key fundamental issues had been resolved to the extent that several important classes of problems could be handled by a sufficiently robust and generalized infinite-dimensional systems control framework, including stabilizability, exact controllability, and optimality conditions for distributed, point and boundary control systems, and also related infinite-dimensional LQR and LQG controller design problems [1, 13, 14, 15]. On the other hand, the use of these theoretic results remains somewhat restricted by the specific technical criteria requiring satisfaction for the control schemes to be correctly applied or

well-posed, at least in the mathematical sense, and often result in seemingly intractable control designs which are impractical, in the physical sense. The set of problems which can be handled by this approach also requires some care when taking into account the physical nature of the processes being described by the PDE. Assumptions are inevitably required to deal with the inherent complexity of the actual physical system itself, all of which lead to some degree of plant-model mismatch. For example, in situations where the system parameters themselves must often be estimated, the actual spatial geometry of the system is irregular, and because nonlinearities are present everywhere in nature. That is not to say these assumptions about the process invalidate their description by the PDEs, nor do they prohibit model based control design since even simplified PDEs can provide good models of complex processes and are able to capture the dominant dynamics of the systems. Moreover, infinite-dimensional systems theory still remains a fundamental tool in linear and nonlinear analysis of PDEs, which can be utilized in control development for these types of systems. Indeed there is a wide range of useful applications made available by careful consideration of both theoretic and practical aspects of specific problems. The infinite-dimensional systems approach to PDE control problems, as well as other frameworks such as proper orthogonal decomposition [16], backstepping methods [17, 18], and sliding mode control [19], are all valuable methodologies towards the vast array of different processes. Each approach has also been greatly augmented by the continual advancement in computer technology which has provided a wealth of resources from numerical analysis, and has also afforded the control engineer the ability to realize otherwise abstract and inaccessible control implementations.

1.2 PDE process models and control systems

From a mathematical perspective, a PDE is a differential equation for a function which contains one or more partial derivatives of the dependent variable [20, 21, 22]. As an example, consider the dependent variable $z(\xi, t)$ which is a function of the independent variables ξ corresponding to spatial points $\xi = (\xi_1, \dots, \xi_m)$ in an m -dimensional domain $\Omega \subset \mathbb{R}^m$ with boundary $\partial\Omega$, and also the independent variable of time $t \in [0, T]$. The general expression for a second order PDE for the function $z(\xi, t)$ is:

$$F\left(\xi_1, \dots, \xi_m, t, z, \frac{\partial z}{\partial t}, \frac{\partial z}{\partial \xi_1}, \dots, \frac{\partial z}{\partial \xi_m}, \frac{\partial^2 z}{\partial \xi_1^2}, \dots, \frac{\partial^2 z}{\partial \xi_m^2}, \frac{\partial^2 z}{\partial \xi_1 \partial \xi_2}, \dots\right) = 0 \quad (1.2.1)$$

The *order* of the PDE is the order of the highest derivative in the equation. All PDEs can be classified as belonging to one of three major types of equations: *parabolic*, *hyperbolic*, and *elliptic*, and describe a wide range of different processes where the complexity of each model is dependent on the assumptions made about the process itself. The function $z(\xi, t)$ gives the state of the system at some time t which is distributed over the space, and represents a process variable of interest (e.g. temperature or concentration). The distributed nature of the state is a distinguishing feature of process variables modelled by PDEs in contrast to those modelled by ODEs for which the process variables are represented by functions of only a single independent variable, for example $z(t)$ which is spatially invariant. Consequently, PDEs belong to a class referred to as *distributed parameter systems* (DPS), whereas ODEs belong to the class of *lumped parameter systems* (LPS). Many transport-reaction processes in chemical and materials engineering can be described by the second

order linear parabolic PDE:

$$\frac{\partial z}{\partial t} = A(\xi, t)z + B(\xi, t)u(t) + q(\xi, t) \quad (1.2.2)$$

The operator $A(\xi, t)$ is often referred to as the *spatial operator* and is expressed as:

$$A(\xi, t) := \sum_{i,j=1}^m \frac{\partial}{\partial \xi_i} \left(d_{ij}(\xi) \frac{\partial}{\partial \xi_j} \right) + \sum_{k=1}^m v_{\xi_k}(t) \frac{\partial}{\partial \xi_k} + g(\xi, t) \quad (1.2.3)$$

Two important transport mechanisms included in the PDE process model in Eqs.1.2.2-Eq.1.2.3 are *diffusion* and *convection*. In the context of a chemical-reaction system, $z(\xi, t)$ represents the concentration of a chemical species, $d_{ij}(\xi)$ are the diffusion coefficients which relate the change in the concentration at any point to it's gradient, $v_{\xi_k}(t)$ are the velocity field components in the ξ_k direction which relate the convective transport of the chemical species to the flow of it's fluid medium, $g(\xi, t)$ is the state related linearized generation/consumption term, and $q(\xi, t)$ is the nonhomogeneous generation/consumption term.²

In the context of heat transport where $z(\xi, t)$ represents the temperature distribution of the system, the Eqs.1.2.2-Eq.1.2.3 describe the diffusion and convection of heat through a conducting material, and are formulated from energy balance relationships which are dependent on the material physical properties such as density, pressure, thermal conductivity, and specific heat capacity. For solids, the mechanism for energy interchange is usually conduction only, however, energy transport in a moving fluid is due to both conduction and convection. Convective transport also occurs in a special class

²For example, in the case of nonisothermal tubular reactor models, the generation/consumption terms are typically nonlinearly dependent on the concentration of other chemical species, kinetics of reaction, and on the temperature of the system.

of PDE defined on time-dependent spatial domains. In the latter case, the convective heat transfer is due to the thermal interaction between a surface and an adjacent moving fluid. The function $B(\xi, t)u(t)$ in Eq.1.2.2 can be seen as a heat source or sink within the domain Ω , which can be manipulated by a controller input $u(t)$ to affect the temperature distribution of the system. This type of system is representative of the class of distributed control problems for parabolic PDEs.

On the other hand, in order for the problem to be properly stated, one must impose additional restrictions on the system in the form of initial conditions, given by the initial temperature distribution $z(\xi, 0)$, and also the boundary conditions, which describe what happens on the boundary of the domain $\partial\Omega$. Boundary conditions referred to as mixed or Robin boundary conditions for heat transport systems are given by:

$$K_0 \frac{\partial z}{\partial n} + hz = b_{\text{ctr}}(\xi)u(t) \quad (1.2.4)$$

where n is the unit outward normal vector to $\partial\Omega$. The parameters specified for the boundary conditions in this are the thermal conductivity of the material K_0 , and the convective heat transfer coefficient h . The control function $b_{\text{ctr}}(\xi)$ describes the region of $\partial\Omega$ over which the input $u(t)$ is applied to the boundary. In the absence of convective heat transfer ($hz = 0$) the boundary conditions are referred to as zero-flux (Neumann) boundary conditions. In the context of PDE control problems with $B(\xi, t) = 0$, the Eqs.1.2.2-1.2.4 is representative of the class of boundary control problems for parabolic PDEs.

1.2.1 Examples

The following examples illustrate two types of chemical and heat transport systems described by parabolic PDEs in the form of Eqs.1.2.2-1.2.4.

Example 1: Tubular Reactor model

Consider the PDE model for a chemical reaction:



where b_{stoic} is the stoichiometric reaction coefficient. The non steady state concentration profiles of the reactant c_A and product c_B are given by $z_A(r, \xi, t)$ and $z_B(r, \xi, t)$ respectively. The isothermal tubular reactor is depicted in Fig.1.1 where $\Omega = [0, r] \times [0, L]$ is axisymmetric, $0 \leq r \leq R$ and $0 \leq \xi \leq L$.

The system requires solving the equations corresponding to the mass balance for the species concentration and a set of momentum balance equations for the fluid motion, which can be simplified under the following assumptions: (i) the diffusion coefficients are directionally independent and constant, $d_{ij} = D_c$ for $i = j$ and $d_{ij} = 0$ for $i \neq j$; (ii) the convective transport is only due

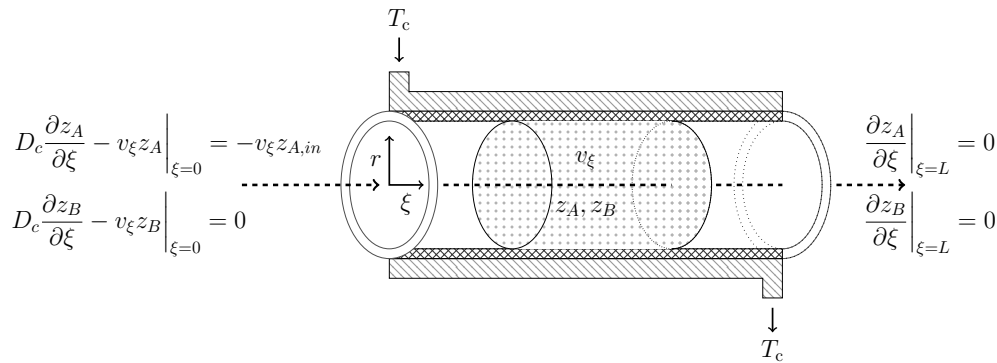


Figure 1.1: Tubular reactor system example

to the constant fluid superficial velocity, v_ξ , so that the radial velocity profile is constant; (iii) the reaction kinetics are first order and depend only on z_A , such that the reaction rate model is given by $k_{\text{rxn}}z_A$, where k_{rxn} is the kinetic reaction rate constant (i.e. the species A is consumed such that $g_A = -k_{\text{rxn}}z_A$ and the species B is generated with $g_B = b_{\text{stoic}}k_{\text{rxn}}z_A$); and (iv) the fluid motion is relatively slow such that the density is taken as constant.

Under these assumptions, the coupled system of PDEs for the concentrations of species c_A and c_B is given as:

$$\begin{aligned}\frac{\partial z_A}{\partial t} &= D_c \left(\frac{1}{r} \frac{\partial}{\partial r} \left(r \frac{\partial z_A}{\partial r} \right) + \frac{\partial^2 z_A}{\partial \xi^2} \right) - v_\xi \frac{\partial z_A}{\partial \xi} - k_{\text{rxn}} z_A \\ \frac{\partial z_B}{\partial t} &= D_c \left(\frac{1}{r} \frac{\partial}{\partial r} \left(r \frac{\partial z_B}{\partial r} \right) + \frac{\partial^2 z_B}{\partial \xi^2} \right) - v_\xi \frac{\partial z_B}{\partial \xi} + b_{\text{stoic}} k_{\text{rxn}} z_A\end{aligned}\tag{1.2.6}$$

The reactor outlet ($\xi = L$), the reactor wall ($r = R$) and the reactor centre ($r = 0$) are specified as having zero flux boundary conditions. The boundary conditions for z_A and z_B at the reactor inlet ($\xi = 0$) are given by:

$$D_c \frac{\partial z_A}{\partial \xi} - v_\xi z_A = -v_\xi z_{A,in}, \quad D_c \frac{\partial z_B}{\partial \xi} - v_\xi z_B = 0\tag{1.2.7}$$

where $z_{A,in}$ is the concentration of the reactant influent which can be utilized as an input to the system, i.e. $u(t) = -v_\xi z_{A,in}$. In some processes which are convection-dominated, the diffusion terms in Eq.1.2.6 are neglected, and the equations are reduced to a system of first order *hyperbolic* PDEs [23, 24].

Example 2: Annealing process

Consider the annealing process depicted in Fig.1.2 in which a thin solid slab is being lowered into a fluid medium by a mechanical pulling arm. The slab

length above the fluid medium surface changes in time and the one-dimensional model for the temperature dynamics in this time-varying region $\Omega_t = [0, l(t)]$ with moving boundary $\partial\Omega_t$ are described by the parabolic PDE model given by:

$$\frac{\partial z}{\partial t} = \kappa \frac{\partial^2 z}{\partial \xi^2} - v_\xi(t) \frac{\partial z}{\partial \xi} \quad (1.2.8)$$

with $\kappa = D_c/(\rho C_p)$ where ρ is the mass density, and C_p is the specific heat capacity. The boundary input $u(t)$ is applied by the heater attached to the pulling arm. One can notice that the temperature dynamics are influenced by the change in the material domain which is manifested in the convective transport term $v_\xi(t)\partial z/\partial \xi$ associated with the boundary velocity $v_\xi(t)$ which in turn is determined by the rate at which the slab is lowered into the melt by the pulling arm. In addition to being a thermal boundary control problem, this type of system is also representative of a large number and variety of *moving boundary problems* where the PDE system is defined on a *time-varying spatial domain*.

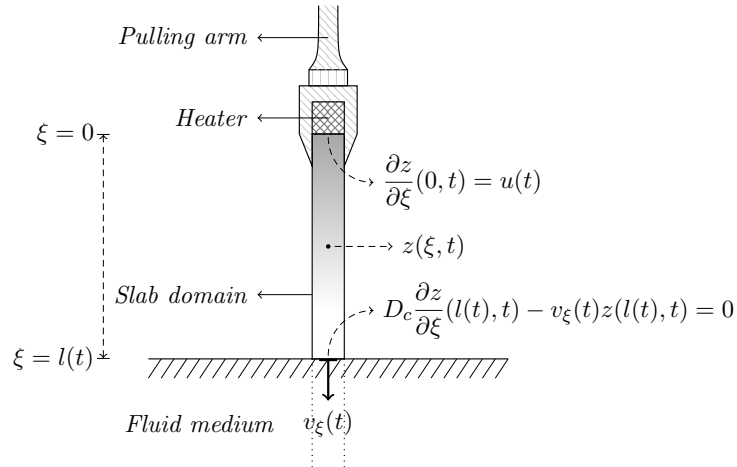


Figure 1.2: Annealing process diagram

1.2.2 Infinite-dimensional system representation

There are many excellent works on infinite-dimensional systems theory which utilize the methodologies and tools of linear functional analysis as a powerful means in the analysis of PDE dynamics and the properties of solutions [25, 26, 1, 27, 28, 14, 29, 22, 21]. The general idea behind this approach is the representation of the PDE initial and boundary value problem as an abstract evolution system on some Banach or Hilbert space. One can think of this type of representation analogous to the representation of an ODE on a finite-dimensional vector space, except that the state evolution is determined by the PDE spatial operator on an infinite-dimensional state-space \mathcal{Z} which consists of a certain class of functions, rather than vectors in a finite-dimensional state vector space. The initial and boundary value problem given by the general parabolic PDE in Eq.1.2.2-1.2.4 with distributed input can be represented as the nonautonomous and nonhomogeneous initial value problem:

$$\frac{dz(t)}{dt} = A(t)z(t) + B(t)u(t) + g(t), \quad z(0) = z_0 \quad (1.2.9)$$

The state in Eq.1.2.9 is defined as $z(t) := [z(\xi)](t)$ and the linear operator $A(t)$ is related to the PDE spatial operator where $A(t) := [A(\xi)](t)$. This operator is defined along with a domain $D(A(t))$ which consists of a class of functions for which $A(t)$ is associated and also those functions which satisfy the boundary conditions of the PDE. Typically the domain of the operator is a subset of the state space such that $A(t)$ maps elements from the domain $D(A(t))$ to the state space \mathcal{Z} . Similar to the idea in finite-dimensional systems theory, the input operator $B(t)$ takes the functions from the space of inputs \mathcal{U} to the state space \mathcal{Z} . The initial value problem in Eq.1.2.9 is nonhomogeneous due to the presence of the function $g(t)$ which represents the evolution of the non-state

related generation term on the state space. In the absence of this generation term, the state evolution is determined simply from the homogeneous version of the initial value problem in Eq.1.2.9. The output measurements $y(t)$ of the system in Eq.1.2.9 are given by $y(t) = C(t)z(t)$, where $C(t)$ is the output operator which takes functions from \mathcal{Z} to the space of outputs \mathcal{Y} .

The system in Eq.1.2.9 is nonautonomous, where the time-dependence of the operators $A(t)$ and $B(t)$ are due to the time-dependence of the PDE coefficients in the Eq.1.2.2. This type of problem is representative of a class of nonautonomous infinite-dimensional system which is a generalization of autonomous (time-invariant) infinite-dimensional systems theory. In some cases, the time-dependence of the operator $A(t)$ can often be viewed as a perturbation of some autonomous operator, i.e. $A(t) = A + P(t)$ where A is the autonomous operator and $P(t)$ is the perturbation [30]. However, there are many works which deal with theoretical consideration of the complete nonautonomous system [31, 28, 29], including those dedicated to the related control problem [32, 14, 33, 34]. Abstract results on the existence and uniqueness of solutions to control problems for parabolic PDEs where the input is specified at the boundary as in Eq.1.2.4 have also been rigorously developed in several studies, including some optimal boundary control problems [35, 36, 37]. Other works have considered the boundary control problem utilizing transformations of the PDE system itself [7], and also through the use of state transformations [38, 39, 40]. In the cases where the operators are autonomous, the solution of the initial value problems are provided through semigroup theory in which a (one-parameter) semigroup governs the temporal state evolution from the initial state $z(0)$ to the state $z(t)$ at some future time. However, in the cases where the operators are nonautonomous, the solutions are provided in terms of two-parameter semigroups which govern the state evolution.

1.3 Thesis motivation

The use of PDEs as models for many important industrial processes has gained more attention in recent years, and this is due in part to the increasing necessity for precise descriptions of process variables with complex temporal and spatially dependent system dynamics which is generally unattainable by the use of lumped parameter models. Often, the process variables of interest are also affected by time and/or spatially varying features of the system which are manifested as time and/or spatially varying coefficients of the PDE models. These features arise from the underlying physical characteristics of the process, chemical reactions, or the methods utilized in the formation and treatment of materials which may result in phase transitions, deformations or a combination of these behaviours in processes such as crystal growth, metal casting, solid-gas reaction systems, and other diverse problems arising in fluid mechanics, and biological systems.

The objective of this research work is the development and the application of optimal control methods for thermal transport-reaction systems modelled by parabolic PDEs within the infinite-dimensional systems theory framework. A systematic treatment within this framework is provided for two general classes of control problems:

1. Optimal boundary control of unstable parabolic PDEs with nonautonomous and nonhomogeneous infinite-dimensional system representation;
2. Optimal distributed and boundary control of parabolic PDEs on time-varying spatial domains with nonautonomous infinite-dimensional system representation;

The investigation, development and implementation of the model based control methodology is presented within the context of a specific pair of physically relevant and illustrative processes: (i) the lithium-ion battery thermal regulation problem; (ii) the crystal temperature stabilization problem in the Czochralski crystal growth.

1.3.1 Thermal regulation of lithium-ion batteries

Lithium-ion (Li-ion) batteries are among the most critical components in many different modern industrial systems including consumer electronics and in larger scale commercial applications, such as electric vehicles (EVs) and hybrid electric vehicles (HEVs). One of the key issues in the application of the battery technology as electrochemical energy storage devices for high-performance electronics, HEVs, and EVs, is battery thermal management. Li-ion batteries generate a significant amount of heat at high-discharge rates which is a major problem since excessive heat and uneven temperature distributions prolonged over can have several severe consequences, including those associated with the well-known dangers of thermal runaway [41, 42].

The use of PDE models of Li-ion battery thermal dynamics is advantageous because they capture the distributed nature of the battery temperature evolution, rather than the non distributed dynamics provided by lumped parameter models, and yields a more complete picture of the physical system. A large amount of literature is dedicated to the thermal analysis of Li-ion batteries which employ experimental and computation techniques to model the complex electrochemical reactions responsible for heat generation under a variety of operating conditions [43, 44, 45]. Other works have discussed the various approaches in the thermal management of Li-ion batteries [46, 47]. Both passive

and active temperature control strategies have been proposed utilizing combinations of air and fluids as the means of heating/cooling, and also the use of phase change materials (PCMs) which act as heat sinks within the devices. However, there are only a few works scattered throughout the literature which deal with model based control design for the Li-ion battery thermal regulation problem, and to the authors knowledge, none which consider the problem in the context of infinite-dimensional systems theory.

PDE model based control design has the potential of providing new methods and insights into the Li-ion battery thermal regulation problem, and also to greatly improve existing control schemes. However, there are several key issues which arise from each of the system design engineering perspective, and the mathematical control perspective. From the former perspective, the battery system setup plays a significant role in determining the feasibility of heating/cooling implementations which must be accounted for in terms of both actuator and sensor placement. From the mathematical control perspective, one needs to consider each of the physical design restrictions which must be incorporated into the mathematical model of the system, while developing an appropriate feedback control strategy to handle the unstable dynamical behaviour of the system.

1.3.2 Czochralski crystal temperature stabilization

The Czochralski (CZ) crystal growth process is a method of crystal growth in which large boules of single crystals, typically Si, GaAs, InP, and CdTe, are formed by drawing a seed crystal from a pool of melt using a mechanical pulling arm in a thermal environment. The grown crystals are subsequently processed into wafers which form the basis of the vast majority of integrated

circuits in the microelectronics industry, and also in the solar cell industry. The overall crystal quality is affected by the rate of growth and variations in the thermal fields of the processing environment [48, 49, 50, 51]. While there are many studies which deal with the effect of the pulling rate on the crystal growth [52, 53, 54], much less attention has been given to developing control methods to stabilize the crystal temperature during the crystal growth process.

The most predominant feature about the CZ crystal temperature stabilization problem is that the transport phenomena of the crystal temperature is described by a parabolic PDE which is defined on time-varying spatial domain, and represents a special class of nonautonomous problem. In these types of processes, the system is inherently nonautonomous even if the PDE coefficients are constant, due to the change of the underlying spatial domain. On the other hand, the formulation of the process model from first-principles balance equations and continuum mechanics yields PDE models characterized by the presence of a convective transport term associated with the domain boundary motion [55, 56]. There are many peculiar and interesting aspects which arise from the fact that the spatial domain itself changes over time, and these initial and boundary value problems are sometimes referred to as being defined on non-cylindrical domains, i.e. the space-time domains form a non-cylindrical set. Numerous authors have studied these types of problems from a variety of approaches to ascertain results on existence and uniqueness of solutions and to analyze the dynamical behaviour of the system under different assumptions regarding the motion of the boundaries. Some recent results can be found in [57, 58, 59, 60, 61, 62, 63, 64, 65]. However, only a limited number of works have considered control problems for PDEs on time-varying spatial domains using robust control methods [66, 67], stabilization of the boundary

motion by manipulation of the temperature field [68], and control problems related to the two-phase Stefan problem [69]. A similar system to the annealing process depicted in Fig.1.2 is considered in [70, 71], where the motion of the mechanical pulling arm is utilized to optimally stabilize the temperature in the time-varying spatial domain. Analogously, the dynamics of the pulling arm are also coupled with the dynamics of the crystal temperature in the CZ crystal growth process. The influence of the mechanical subsystem which draws the crystal from the melt appears as the boundary velocity coefficient associated with a convective transport term in the PDE model of the crystal temperature. However, rather than controlling the temperature utilizing the pulling arm motion, one can consider the optimal control problem by input actuation along the crystal boundary.

There are very few results on the optimal distributed or boundary control of parabolic PDEs on time-varying spatial domains within the context of infinite dimensional systems control theory. One of the primary challenges in considering the control problem within this framework is overcoming the spatial domain motion which affects the underlying function space setting utilized to represent the PDE system as an abstract evolution system. There are two general approaches in dealing with this issue: First, one can consider a change of variable technique which essentially maps the system back to a cylindrical space-time domain [72]. Using this transformed system, the control problem can then be considered taking care that one is able to map the solution forward to the appropriate space-time domain. The second technique does not employ a change of variables, but rather appeals to the idea of nested spatial domains in which there exists a set which contains all of the time-varying sets (spatial domains), and forms a cylindrical space-time domain [34]. In this way, one is able to represent the evolution system on a family of time-varying function

spaces which are embedded into a static family of appropriately defined function spaces [27]. While rather abstract in nature, these notions are required to formally pose the CZ crystal temperature stabilization problem and to utilize the optimal control theory provided within the infinite-dimensional systems framework.

1.4 Thesis scope and contributions

The focus of this thesis is the feedback control of a class of reaction-diffusion process in the context of a Li-ion battery temperature regulation problem, and the feedback control of a class of convection-diffusion process in the context of the CZ crystal temperature stabilization problem. The models of the transport phenomena are given by a parabolic PDEs, and in the latter case of the CZ crystal stabilization problem, is defined on a time-varying spatial domain. The classes of problems considered are characterized by a variety of distinguishing features while the methodologies developed in this thesis are applicable to a broad number of different processes. In each case considered, the optimal control problems are addressed within the infinite-dimensional systems theoretic framework, and together with the development, formulation, and numerical realization, are explored within the following chapters.

Chapter 2 deals with the Li-ion battery thermal regulation problem with boundary control actuation. The model of the transient temperature dynamics of the battery is given by a non-homogeneous parabolic PDE on a 2-dimensional spatial domain which accounts for the time-varying heat generation during the battery discharge cycle. The spatial domain is given as a disk with radial and angular coordinates which captures the non-radially symmetric heat transfer phenomena due to the application of the control input

along a portion of the spatial domain boundary. The Li-ion battery model is formulated within an appropriately defined infinite-dimensional function space setting which is suitable for spectral controller synthesis. The key challenges in the output feedback model based controller design addressed in this work are: the dependence of the state on time-varying system parameters, the restriction of the input along a portion of the battery domain boundary, the observer based optimal boundary control design where the separation principle is utilized to demonstrate the stability of the closed loop system, and the realization of the outback feedback control problem based on state measurement and interpolation of the temperature field. Numerical results for simulation case studies are presented.

Chapters 3-5 deal with the control of a class of parabolic PDEs on time-varying spatial domains within the context of the CZ crystal temperature stabilization problem. The class of PDEs is characterized by the presence of a time-dependent convective-transport term which is associated with the time-evolution of the spatial domain boundary. Chapter 3 provides an introduction and details on both the model formulation for PDEs defined on time-varying spatial domains from the first principles continuum mechanics, and also the concept of nested spatial domains which provide the basis for the definition of an appropriate function space setting in which the control problems can be considered within the infinite-dimensional systems framework. The optimal distributed control problem is considered for the PDE model posed on a 1-dimensional time-varying spatial domain and the numerical realization is provided. Chapter 4 considers the boundary control problem where the PDE model of the CZ crystal temperature is posed on a 2-dimensional time-varying

spatial domain in cylindrical coordinates. The dynamics of the domain boundary evolution, which is determined by the mechanical subsystem pulling the crystal from the melt, are described an ordinary differential equation and are unidirectionally coupled to the convection-diffusion process described by the PDE system. The optimal control problem setup for the PDE coupled with the finite-dimensional subsystem is presented, and numerical results demonstrate the stabilization of the two-dimensional crystal temperature distribution in the time-varying spatial domain. Chapter 5 also considers the boundary control of the CZ crystal temperature where the PDE model is posed on a 2-dimensional time-varying spatial domain. In this case, an exact transformation is developed for the infinite-dimensional boundary control system representation and the LQR optimal control synthesis. Numerical results demonstrate optimal stabilization of the two-dimensional temperature distribution in the crystal.

Bibliography

- [1] Lions JL. *Optimal control of systems governed by partial differential equations*. New York: Springer-Verlag. 1971.
- [2] Russell D. Controllability and Stabilizability Theory for Linear Partial Differential Equations: Recent Progress and Open Questions. *SIAM Review*. 1978;20(4):639–739.
- [3] Wang PKC. Theory of Stability and Control for Distributed Parameter Systems (a Bibliography). *International Journal of Control*. 1968; 7(2):101–116.
- [4] Butkovskii AG. *Distributed control systems*. New York: American Elsevier. 1969.

- [5] Lasiecka I. Control of Systems Governed by Partial Differential Equations: A Historical Perspective. In: *Proceedings of 34th IEEE Conference on Decision and Control*. New Orleans, LA. 1995; pp. 2792–2797.
- [6] Padhi R, Ali SF. An account of chronological developments in control of distributed parameter systems. *Annual Reviews in Control*. 2009; 33(1):59–68.
- [7] Ray W. *Advanced Process Control*. New York: McGraw-Hill. 1981.
- [8] Ogunnaike BA, Ray WH. *Process Dynamics, Modeling, and Control*. New York: Oxford University Press. 1994.
- [9] Balas M. Exponentially stabilizing finite-dimensional controllers for linear distributed parameter systems: Galerkin approximation of infinite-dimensional controllers. *J Math Anal Appl*. 1986;117:358–384.
- [10] Gu G, Khargonekar PP, Lee EB. Approximation of Infinite Dimensional Systems. *IEEE Trans Automat Contr*. 1989;34:610–618.
- [11] Gu G, Khargonekar PP, Lee EB, Mistra P. Finite-dimensional Approximations of Unstable Infinite-dimensional Systems. *SIAM J Contr & Opt*. 1992;30:704–716.
- [12] Ito K. Finite-Dimensional Compensators for Infinite-Dimensional Systems via Galerkin-Type Approximation. *SIAM J Control Optim*. 1990; 28:1251–1269.
- [13] Lasiecka I. Unified theory for abstract parabolic boundary problems: A semigroup approach. *Appl Math & Optim*. 1980;6:287–333.

- [14] Acquistapace P. Evolution operators and strong solutions of abstract linear parabolic equations. *Diff Int Eqns.* 1988;1:433–457.
- [15] Curtain RF, Zwart H. *An introduction to infinite-dimensional linear systems theory.* New York, NY, USA: Springer-Verlag New York, Inc. 1995.
- [16] Atwell JA, King BB. Proper Orthogonal Decomposition for Reduced Basis Feedback Controllers for Parabolic equations. *Mathematical and Computer Modeling.* 2001;33:1–19.
- [17] Smyshlyaev A, Krstic M. Explicit formulae for boundary control of parabolic PDEs. *Lecture Notes In Control & Information Sciences.* 2004; 301:231–249.
- [18] Krstic M. *Boundary Control of PDEs: A Course on Backstepping Designs.* Philadelphia, PA, USA: Society for Industrial and Applied Mathematics. 2008.
- [19] Orlov Y, Utkin V. Sliding mode control in indefinite-dimensional systems. *Automatica.* 1987;23(6):753 – 757.
- [20] Debnath L, Bhatta D. *Integral transforms and their applications 2nd Ed.* USA: Chapman & Hall/CRC. 2007.
- [21] McOwen R. *Partial differential equations: methods and applications, 2nd ed.* USA: Prentice Hall. 2002.
- [22] Evans L. *Partial differential equations.* USA: American Mathematical Society. 1998.
- [23] Winkin J, Dochain D, Ligarius P. Dynamical analysis of distributed parameter tubular reactors. *Automatica.* 2000;36:349–361.

- [24] Laabissi M, Achhab M, Winkin J, Dochain D. Trajectory analysis of nonisothermal tubular reactor nonlinear models. *Systems and Control Letters*. 2001;42:169–184.
- [25] Kato T. On linear differential equations in Banach spaces. *Comm Pure Appl Math*. 1956;9:479–486.
- [26] Tanabe H. Evolution equations of parabolic type. *Proc Japan Acad*. 1961;37:610–613.
- [27] Adams R. *Sobolev Spaces*. New York, U.S.A.: Academic Press. 1978.
- [28] Pazy A. *Semigroups of Linear Operators and Applications to Partial Differential Equations*. New York, U.S.A.: Springer-Verlag. 1983.
- [29] Tanabe H. *Functional analytic methods for partial differential equations*. New York: Marcel Dekker Inc. 1997.
- [30] Kato T. *Perturbation theory for linear operators*. New York: Springer-Verlag. 1966.
- [31] Henry D. *Geometric Theory of Semilinear Parabolic Equations*. New York, NY, USA: Springer. 1981.
- [32] Acquistapace P, Terreni B. A unified approach to abstract linear non-autonomous parabolic equations. *Rend Sem Univ Padova*. 1987;78:47–107.
- [33] Acquistapace P, Flandoli F, BTerreni. Initial boundary value problems and optimal control for nonautonomous parabolic systems. *SIAM J Math Anal*. 1991;29:89–118.

- [34] Bensoussan A, Prato GD, Delfour M, Mitter S. *Representation and Control of Infinite Dimensional Systems*. Boston: Birkhäuser. 2007.
- [35] Acquistapace P, Terreni B. Infinite-horizon linear-quadratic regulator problems for nonautonomous parabolic systems with boundary control. *SIAM J Math Anal*. 1996;34:1–30.
- [36] Acquistapace P, BTerreni. Classical solutions of nonautonomous Riccati equations arising in parabolic boundary control problems. *Appl Math Optim*. 1999;39:361–409.
- [37] Acquistapace P, BTerreni. Classical solutions of nonautonomous Riccati equations arising in parabolic boundary control problems, II. *Appl Math Optim*. 2000;41:199–226.
- [38] Fattorini HO. Boundary control systems. *SIAM Journal on Control*. 1968; 6:349–385.
- [39] Sun S. On spectrum distribution of completely controllable linear systems. *Acta Mathematica Sinica*. 1981;21:193–205.
- [40] Curtain RF. On stabilizability of linear spectral systems via state boundary feedback. *SIAM J Control and Optimization*. 1985;23:144–152.
- [41] Balakrishnan P, Ramesh R, Kumar TP. Safety mechanisms in lithium-ion batteries. *Journal of Power Sources*. 2006;155(2):401 – 414.
- [42] Wang Q, Ping P, Zhao X, Chu G, Sun J, Chen C. Thermal runaway caused fire and explosion of lithium ion battery. *Journal of Power Sources*. 2012; 208(0):210 – 224.

- [43] Gu W, Wang C. Thermal-Electrochemical Modeling of Battery Systems. *Journal of The Electrochemical Society*. 2000;147(8):2910–2922.
- [44] Chen S, Wan C, Wang Y. Thermal analysis of lithium-ion batteries. *Journal of Power Sources*. 2005;140(1):111 – 124.
- [45] Bandhauer T, Garimella S, Fuller T. A Critical Review of Thermal Issues in Lithium-Ion Batteries. *Journal of the Electrochemical Society*. 2011; 158(3):R1–R25.
- [46] Lu L, Han X, Li J, Hua J, Ouyang M. A review on the key issues for lithium-ion battery management in electric vehicles. *Journal of Power Sources*. 2013;226(0):272 – 288.
- [47] Rao Z, Wang S. A review of power battery thermal energy management. *Renewable and Sustainable Energy Reviews*. 2011;15(9):4554 – 4571.
- [48] Brown R. Theory of transport processes in single crystal growth from the melt. *AIChE J*. 1988;34:881–911.
- [49] Sinno T, Brown RA. Modeling Microdefect Formation in Czochralski Silicon. *Journal of The Electrochemical Society*. 1999;146(6):2300–2312.
- [50] Szabo G. Thermal Strain during Czochralski Crystal Growth. *J Cryst Growth*. 1985;73:131–141.
- [51] Lan CW. Recent progress of crystal growth modeling and growth control. *Chemical Engineering Science*. 2004;59(7):1437 – 1457.
- [52] Derby J, Brown R. Thermal-capillary analysis of Czochralski and Liquid Encapsulated Czochralski Crystal Growth. I. Simulation. *J Cryst Growth*. 1986;74:605–624.

- [53] Derby J, Brown R. Thermal-capillary analysis of Czochralski and Liquid Encapsulated Czochralski Crystal Growth. II. Processing Strategies. *J Cryst Growth*. 1986;75:227–240.
- [54] Derby J, Brown R. On the Dynamics of Czochralski Crystal Growth. *J Cryst Growth*. 1987;83:137–151.
- [55] Marsden J, Hughes T. *Mathematical Foundations of Elasticity*. New York, U.S.A.: Dover Publications. 1983.
- [56] Chorin AJ, Marsden JE. *A Mathematical Introduction to Fluid Mechanics 3rd Ed*. New York, U.S.A.: Springer. 1983.
- [57] Savaré G. Parabolic problems with mixed variable lateral conditions: An abstract approach. *Journal de Mathématiques Pures et Appliqués*. 1997; 76(4):321 – 351.
- [58] Bonaccorsi S, Guatteri G. A Variational Approach to Evolution Problems with Variable Domains. *Journal of Differential Equations*. 2001;175(1):51 – 70.
- [59] Lederman C, Wolanski N, Vazquez JL. A mixed semilinear parabolic problem in a noncylindrical space-time domain. *Differential Integral Equations*. 2001;14(4):385–404.
- [60] Lumer G, Schnaubelt R. Time-dependent parabolic problems on non-cylindrical domains with inhomogeneous boundary conditions. *Journal of Evolution Equations*. 2001;1:291–309.
- [61] Burdzy C, Chen ZQ, Sylvester J. The heat equation in time dependent domains with insulated boundaries. *Journal of Mathematical Analysis and Applications*. 2004;294(2):581 – 595.

- [62] Da Prato G, Kunstmann PC, Weis L, Lasiecka I, Lunardi A, Schnaubelt R, Lunardi A. An Introduction to Parabolic Moving Boundary Problems. In: *Functional Analytic Methods for Evolution Equations*, vol. 1855 of *Lecture Notes in Mathematics*, pp. 23–31. Springer Berlin / Heidelberg. 2004;.
- [63] Baconneau O, Lunardi A. Smooth Solutions to a Class of Free Boundary Parabolic Problems. *Transactions of the American Mathematical Society*. 2004;356(3):pp. 987–1005.
- [64] Kloeden P, Marn-Rubio P, Real J. Pullback attractors for a semilinear heat equation in a non-cylindrical domain. *Journal of Differential Equations*. 2008;244(8):2062 – 2090.
- [65] Kloeden PE, Real J, Sun C. Pullback attractors for a semilinear heat equation on time-varying domains. *Journal of Differential Equations*. 2009;246(12):4702 – 4730.
- [66] Armaou A, Christofides PD. Nonlinear feedback control of parabolic partial differential equation systems with time-dependent spatial domains. *Journal of mathematical analysis and applications*. 1999;239(1):124–157.
- [67] Armaou A, Christofides PD. Robust control of parabolic PDE systems with time-dependent spatial domains. *Automatica*. 2001;37(1):61–69.
- [68] Hinze M, Ziegenbalg S. Optimal control of the free boundary in a two-phase Stefan problem. *Journal of Computational Physics*. 2007;223(2):657 – 684.

- [69] Dunbar W, Petit N, Rouchon P, Martin P. Boundary control of a nonlinear Stefan problem. In: *Decision and Control, 2003. Proceedings. 42nd IEEE Conference on*, vol. 2. 2003; pp. 1309 – 1314 Vol.2.
- [70] Wang PKC. Stabilization and Control of Distributed Systems with Time-Dependent Spatial Domains. *J Optim Theor & Appl.* 1990;65:331–362.
- [71] Wang PKC. Feedback Control of a Heat Diffusion System with Time-Dependent Spatial Domains. *Optim Contr Appl & Meth.* 1995;16:305–320.
- [72] Prato GD, Zolésio J. An optimal control problem for a parabolic equation in non-cylindrical domains. *Systems & Control Letters.* 1988;11(1):73 – 77.

Chapter 2

Boundary control synthesis for a lithium-ion battery thermal regulation problem

The material presented in this chapter has been accepted in whole as the following:

[1] J. Ng and S. Djurjic, “Boundary control synthesis for a lithium-ion battery thermal regulation problem,” *AIChE Journal*, 2013

2.1 Introduction

The development of Lithium-ion (Li-ion) battery technology is one of the most important fields in the emerging global market for advanced energy storage devices, and there continues to be an intensive research effort within this area to meet the current and future demands of consumers and industry which utilize this technology. Presently, Li-ion battery technology has been widely

adopted for use in personal electronics, and is also the most promising candidate for use in electric vehicles (EVs) and hybrid electric vehicles (HEVs), because of their advantageous characteristics in terms of energy density, capacity, voltage, charge retention, low self-discharge rate, and stability, compared to other rechargeable types such as lead-acid, nickel-metal hydride, or zinc-halogen batteries [2]. One of the key issues in the application of the technology to high-performance electronic devices, HEVs, and EVs, is battery thermal management. At high-discharge rates, Li-ion batteries generate a significant amount of heat which can detrimentally affect the overall performance of the devices. Excessive heat and uneven temperature distributions prolonged over time can cause damage to the battery resulting in decreases in capacity, charge retention, battery lifespan, and physical deformations of the battery itself. Under more extreme conditions, the battery can undergo thermal runaway, which may result in the rupture of the battery casing, explosion, and ignition of the flammable electrolytes [3, 4].

There is a large amount of literature focused on the thermal analysis of Li-ion batteries which employ experimental and computation techniques to model the complex electrochemical reactions responsible for heat generation under a variety of operating conditions [5, 6, 7]. In conjunction with these studies, there are complementary works discussing various approaches in the thermal management of Li-ion batteries [2, 8]. The primary means of temperature regulation are typically through exclusive and combinations of passive and active control strategies each involving air for heating/cooling, liquid for heating/cooling, and also the use of phase change materials (PCMs). The implementation of any of the aforementioned control methods are dependent on a number of factors including the battery system setup (e.g. single cell, battery pack, shape, etc.) which affects the feasibility of heating/cooling system

design. In all cases, model based control design has the potential of enhancing these existing methodologies by improving controller performance.

Control design based on lumped-parameter models of systems has been widely adopted in industry and successfully applied to many chemical and materials engineering processes. On the other hand, control design methods based on PDE models, while less popular, are advantageous for processes such as the regulation of the temperature distribution in Li-ion batteries in which the distribution of the state is a critical factor. There are several approaches to the PDE model based control design such as modal analysis and early lumping methods [9], proper orthogonal decomposition [10], backstepping methods [11, 12], and other methods including the use of infinite-dimensional systems theory [13, 14, 15, 16, 17]. While each differ in the abstract representation of the physical system, all of the approaches face similar challenges in terms of fundamental control concepts such as stabilization, optimality, state measurement and observer design. These mathematical issues must be reconciled with practical considerations such as the placement of actuators and sensors, despite the added complexity even in considering simplified linear PDEs models in higher spatial dimensions.

In this work, we focus on the model based control design for a Lithium-ion battery thermal regulation problem. The dynamics of the battery temperature distribution are modelled by a linear non-homogeneous parabolic PDE on a 2-dimensional spatial domain given as a disk region with radial and angular coordinates. We consider the case in which controller action is restricted to a portion of the boundary which reflects more realistic thermal management system design considerations where physical limitations prohibit the placement of internal actuators in the battery cell itself, or along the entire boundary. The non-radially symmetric temperature distribution due to

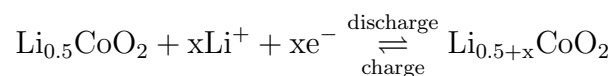
the application of the control input along a portion of the spatial domain boundary also provides a clearer picture of the heat transfer phenomena for the thermal regulation problem. The approach to the controller design is based on the infinite-dimensional system representation of the PDE boundary control problem [18, 19, 16, 20, 21]. There are several key challenges in this context with regards to the model and system setup considered in this work. First, time-varying state (temperature) dependent and state independent heat generation terms, due to the underlying exothermic electrochemical reactions, are present in the model and are sources of instability which must be properly regulated by the controller. Second, the restriction of the input to a portion of the boundary represents a boundary control problem and requires the reformulation of the system for the purpose of controller design. The third primary challenge is the state measurement problem. In practice, the temperature distribution of the whole system is not directly known and must be estimated by measurements taken at the boundary of the system, and/or measurements by sensors located at points within the domain from which the temperature field can then be approximated. We provide the observer based control formulation for the boundary control problem and demonstrate that the stability of the closed loop system is achieved by the optimal design of the controller and observer gain operators using the separation principle for the boundary control system. As an alternative approach, we also provide the output feedback control design based on the combined use of static measurements and interpolation of the temperature field which provides a robust and physically realizable pragmatic method for the realization of the Li-ion battery thermal regulation boundary control problem.

This chapter is organized as follows: Section 2.2 provides an overview of the PDE model of the battery temperature dynamics. Section 2.3 deals with

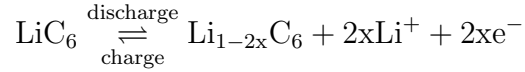
the infinite-dimensional system representation of the boundary control problem which yields a suitable form for the state estimation and output feedback controller design in Section 2.4. The Section 2.5 provides numerical simulation results for a set of case studies carried out to compare the controller formulation under different tuning parameters and the overall behaviour of the closed loop feedback system.

2.2 Model description

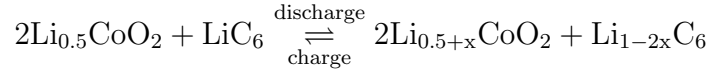
Li-ion batteries consist of three primary active components: a carbon anode, a metal oxide cathode, and a lithium salt in an organic solvent which serves as the electrolyte, and a nonactive current collection component. The anode and the cathode are separated by a thin sheet of micro-perforated plastic which prevents contact between the positive and negative electrodes while allowing ions to pass through. During the charging of the battery, lithium ions move from the cathode to the anode, and vice versa during the discharging of the battery, electrons travel through an external circuit which produces an electrical current through the collection layer, and heat within the battery enclosure is generated by the combination of this flow of electrons along with entropy changes of each of the reactive species. The electrochemical reactions during the charging and discharging of the battery are described by a set of half-reactions which occur at the cathode and anode. For a Li-ion battery which uses lithium-nickel-manganese-cobalt-oxide ($\text{LiNiMn}_2\text{CoO}_2$) as the cathode material, the cathode half reaction is:



The anode half reaction is:



The overall reaction is given by:



The entropy changes of each of LiNiMnCoO_2 , LiC_6 , and LiCoO_2 have been experimentally determined as functions of the battery cell state of charge (SOC), and the current i , and are dependent on time according to the known battery rate of discharge [22, 23, 24]. The SOC refers to the chemical oxidation state of the active materials in the battery system which is measured as a fraction of the maximum capacity. The SOC decreases as the battery is discharged, and increases during charging. The rate of discharge relative to the maximum capacity is measured in terms of the C-rate. During thermal testing, batteries are discharged at various C-rates, and the surface temperatures are measured to determine the entropy changes, $S_\Delta(t)$, in terms of the SOC with respect to the rate at which the battery is discharged.¹ The model of the battery temperature dynamics in this section are given in [25] and references therein. In particular, $S_\Delta(t)$ is obtained from experimental studies, cited in that paper, of the particular battery system at a specified discharge rate which provide *a priori* knowledge of the time-dependent heat generation terms of the PDE model such that no online estimation of the associated entropy changes are required in the controller design considered in this work. On the

¹For example, a 1C rate implies that the chosen discharge current will deplete the battery charge in 1 hour. A battery with a 100 Amp-hr capacity rating is discharged at a current of 100 Amps (i.e. at a 1C discharge rate), such that the SOC at the 30 minute mark is 0.5.

other hand, online estimates of the rate of heat release can easily be combined with the approach taken in this current chapter. The model and subsequent controller design are also appropriate for use in describing the temperature dynamics during discharge-recharge cycling by extension of the experimental results to provide $S_{\Delta}(t)$ for the battery discharge-recharge cycle. However, this current chapter will only focus on the thermal regulation problem for the discharge part of the cycle.

The energy balance model for the transient temperature $Z(\xi, t)$ in a spatial region $\Omega \in \mathbb{R}^N$ with points ξ , and boundary $\partial\Omega$, is described by the parabolic PDE [25]:

$$\begin{aligned} \rho C_p \frac{\partial Z}{\partial t} &= \nabla \cdot (K_0 \nabla Z) + \dot{Q}(Z, \xi, t), & \text{for } \xi \in \Omega, \quad t \in (0, T] \\ -K_0 \frac{\partial Z}{\partial n} &= h(Z - Z_a), & \text{for } \xi \in \partial\Omega, \quad t \in (0, T] \end{aligned} \quad (2.2.1)$$

where ∇ is the gradient operator. The index T denotes the time at which the battery is depleted (SOC = 0). The heat generation term \dot{Q} is given by:

$$\dot{Q} = \frac{i^2}{\sigma_{\text{con}}} - Z S_{\Delta}(t) \frac{i}{n_R F_c}, \quad \text{for } S_{\Delta}(t) = \sum_k S_{\Delta,k}(t) \quad (2.2.2)$$

where $S_{\Delta,k}(t)$ is the entropy change for the k^{th} species shown in the Fig.2.1 [25].

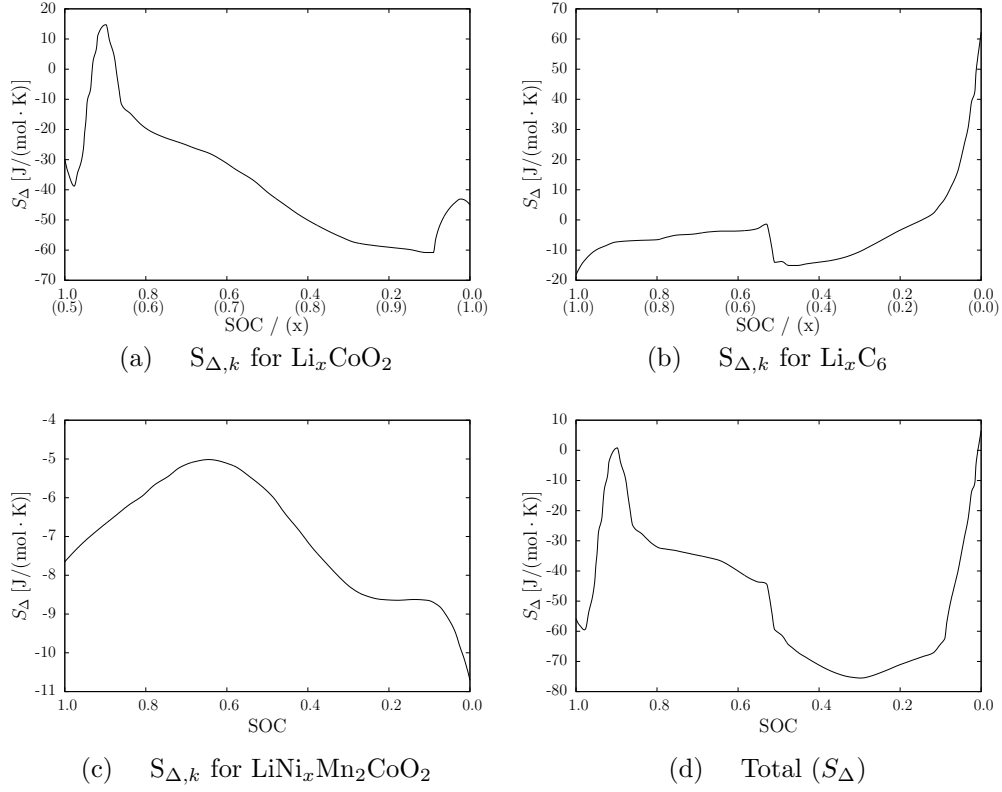


Figure 2.1: Entropy changes for 2.1(a) LiCoO_2 , LiC_6 , $\text{LiNiMn}_2\text{CoO}_2$, and the total entropy change S_{Δ} , as functions of the state of charge (SOC) [25].

It will be convenient to work with the dimensionless form of the problem for the remainder of this work. Normalization with $\tilde{t} = t\kappa/|\xi|^2$, $\tilde{\xi} = \xi/|\xi|$, $z(\xi, t) = (Z - Z_a)/Z_a$, and dropping the tildes yields the dimensionless form of the PDE:

$$\begin{aligned} \frac{\partial z}{\partial t} &= \nabla^2 z + g(t)z + q(t) & \text{for } \xi \in \Omega, \quad t \in (0, T] \\ -\beta \nabla z &= z & \text{for } \xi \in \partial\Omega, \quad t \in (0, T] \end{aligned} \quad (2.2.3)$$

where $\kappa = K_0/\rho C_p$, $g(t) = -S_{\Delta}(t)iVZ_a^2/n_R F_c K_0$, $q(t) = Z_a V i^2 / K_0 \sigma_{\text{con}} - S_{\Delta}(t)Z_a^2 V i / n_R F_c K_0$, and $\beta = K_0/hZ_a^2$.

Li-ion battery units are manufactured in a variety of configurations with various geometries including rectangular parallel-piped and cylindrical forms. Batteries with cylindrical geometry are constructed with thin layers of the cathode, separator, current collector, and anode, which are spirally-wound and inserted into a cylindrical can. The battery geometry considered for the remainder of this work is the unit disk depicted in Fig.2.2 where $\xi = (r, \theta)$, $0 \leq r \leq 1$, $-\pi \leq \theta \leq \pi$, and $\Omega := (0, 1) \times (-\pi, \pi)$ where the spirally wound layers make up the homogeneous disk region. The physical properties of the battery are taken according to the proportion of each component present in the battery, see Table 2.4. Although the disk itself is taken to be radially symmetric, we do not assume the temperature distribution of the disk to be radially symmetric. The PDE system is then given by:

$$\begin{aligned} \frac{\partial z}{\partial t} &= A(r, \theta, t)z + q(t), & (r, \theta) \in \Omega, & \quad t \in (0, T] \\ z(r, \theta, 0) &= z_0(r, \theta), & (r, \theta) \in \Omega, & \quad t = 0 \end{aligned} \tag{2.2.4}$$

where z_0 is the initial condition and the 2-D spatial operator $A(r, \theta, t)$ is defined as:

$$A(r, \theta, t) = \frac{1}{r} \frac{\partial}{\partial r} \left(r \frac{\partial}{\partial r} \right) + \frac{1}{r^2} \frac{\partial^2}{\partial \theta^2} + g(t) \tag{2.2.5}$$

The boundary conditions are given by:

$$\begin{aligned} z(r, -\pi, t) &= z(r, \pi, t), & 0 < r < 1, & \quad t \in (0, T] \\ \frac{\partial z}{\partial \theta}(r, -\pi, t) &= \frac{\partial z}{\partial \theta}(r, \pi, t), & 0 < r < 1, & \quad t \in (0, T] \\ \frac{\partial z}{\partial r}(0, \theta, t) &= 0, & -\pi < \theta < \pi, & \quad t \in (0, T] \\ \beta \frac{\partial z}{\partial r}(1, \theta, t) + z(1, \theta, t) &= b_{\text{ctr}}(\theta)u(t), & -\pi < \theta < \pi, & \quad t \in (0, T] \end{aligned} \tag{2.2.6}$$

where $z(r, \theta, t)$ is bounded at the origin $r = 0$, i.e. $|z(0, \theta, t)| < \infty$. As previously mentioned, in many applications, physical limitations may prohibit the input from being applied to the entire domain boundary. To reflect this restriction, we consider the case in which the input is applied at $r = 1$ over a region of the boundary $\epsilon \in (-\pi, \pi)$ and centred at θ_{ctr} such that:

$$b_{\text{ctr}}(\theta)u(t) = \begin{cases} u(t) & \text{for } \theta \in [\theta_{\text{ctr}} - \epsilon/2, \theta_{\text{ctr}} + \epsilon/2] \\ 0 & \text{for } \theta \notin [\theta_{\text{ctr}} - \epsilon/2, \theta_{\text{ctr}} + \epsilon/2] \end{cases} \quad (2.2.7)$$

In this form, the function $b_{\text{ctr}}(\theta) = H(\theta - (\theta_{\text{ctr}} - \epsilon/2)) - H(\theta - (\theta_{\text{ctr}} + \epsilon/2))$, where $H(\theta)$ is the heaviside step function, and has discontinuities at $\theta = \theta_{\text{ctr}} - \epsilon/2$ and $\theta = \theta_{\text{ctr}} + \epsilon/2$. In practice, it is usually not possible for the input to be uniformly applied over the interval. Also $dH(\theta)/d\theta = \delta(\theta)$ where $\delta(\theta)$ is the delta function is not differentiable which introduces some mathematical technicalities. In particular, the formulation of the control problem will require a continuous second order derivative of $b(\theta)$. A more realistic assumption which remedies both the practical and technical issues which is utilized in this work is where $b_{\text{ctr}}(\theta)u(t)$ is given by:

$$b_{\text{ctr}}(\theta)u(t) = \begin{cases} \hat{b}_{\text{ctr}}(\theta)u(t) & \text{for } \theta \in [\theta_{\text{ctr}} - \epsilon/2, \theta_{\text{ctr}} + \epsilon/2] \\ 0 & \text{for } \theta \notin [\theta_{\text{ctr}} - \epsilon/2, \theta_{\text{ctr}} + \epsilon/2] \end{cases} \quad (2.2.8)$$

where:

$$\hat{b}_{\text{ctr}}(\theta) = \frac{1}{1 + e^{-2K_1(\theta - \theta_{\text{ctr}} + \epsilon/2)}} - \frac{1}{1 + e^{-2K_1(\theta - \theta_{\text{ctr}} - \epsilon/2)}} \quad (2.2.9)$$

The functions in Eq.2.2.8 approximating the heaviside functions are referred to as logistic functions where the parameter K_1 affects how steeply the function increases and decreases, and have continuous second order derivatives. One

can view $b_{\text{ctr}}(\theta)$ as a type of shaping function which determines the range and “shape” by which the input is applied on the boundary.

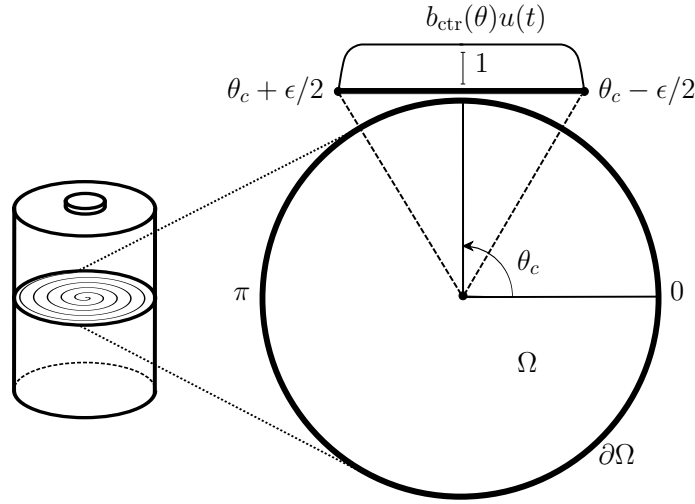


Figure 2.2: Battery system schematic with boundary actuation.

2.3 Boundary control and infinite-dimensional system representation

The PDE system in Eqs.2.2.4-2.2.6 represents a boundary control problem where the input appears as an inhomogeneous term in the boundary condition. In this section, the problem is reformulated by means of a state transformation such that the resulting system has homogeneous boundary conditions. The corresponding infinite-dimensional system representation of the problem as an abstract evolution system on a Hilbert space is then provided. Consider the transformation by defining the new variable:

$$v(r, \theta, t) = z - b(r, \theta)u(t), \quad \text{where} \quad b(r, \theta) = b_{\text{ctr}}(\theta) \frac{r^2}{2\beta + 1} \quad (2.3.1)$$

such that $b(r, \theta)u(t)$ satisfies the radial boundary conditions. The initial and boundary control problem in Eqs.2.2.4-2.2.6 is transformed to the PDE system in terms of v with homogeneous boundary conditions:

$$\begin{aligned} \frac{\partial v}{\partial t} &= A(r, \theta, t)v - b(r, \theta)\dot{u}(t) + A(r, \theta, t)b(r, \theta)u(t) + q(t) \\ v(r, \theta, 0) &= v_0(r, \theta) \\ v(r, -\pi, t) &= v(r, \pi, t), \quad \frac{\partial v}{\partial \theta}(r, -\pi, t) = \frac{\partial v}{\partial \theta}(r, \pi, t) \\ \frac{\partial v}{\partial r}(0, \theta) &= 0, \quad \beta \frac{\partial v}{\partial r}(1, \theta) + v(1, \theta) = 0 \end{aligned} \tag{2.3.2}$$

where the operator $A(r, \theta, t)$ is given in Eq.2.2.5 and:

$$\begin{aligned} A(r, \theta, t)b(r, \theta)u(t) &= \frac{b_{\text{ctr}}(\theta)}{2\beta + 1}(4 + \mu(\theta) + r^2g(t))u(t), \\ &\text{with} \\ \mu(\theta) &= b_{\text{ctr}}^{-1}(\theta) \frac{d^2 b_{\text{ctr}}}{d\theta^2} \end{aligned} \tag{2.3.3}$$

One can note that for $\theta \notin [\theta_{\text{ctr}} - \epsilon/2, \theta_{\text{ctr}} + \epsilon/2]$, the function determining boundary region on which the input is applied becomes $b_{\text{ctr}}(\theta) = 0$, so that $v(r, \theta, t) = z(r, \theta, t)$, which corresponds to the PDE system in Eqs.2.2.4-2.2.6.

The Fourier-Bessel expansion of the initial data $v_0(r, \theta)$ is given in terms of the double set of eigenfunctions $\phi_{mn}^{(1)}$ and $\phi_{mn}^{(2)}$ of $A(r, \theta, t)$ where:

$$v(r, \theta, 0) = \sum_{m=0, n=1}^{\infty} (A_{mn}\phi_{mn}^{(1)} + B_{mn}\phi_{mn}^{(2)}) = v_0(r, \theta) \tag{2.3.4}$$

The eigenfunctions obtained from the nontrivial eigenvalue problem for $A(r, \theta, t)$

are expressed as the combination of Bessel functions and trigonometric functions where $J_m(\alpha_{m,n}r)$, $m = 0, 1, 2, \dots$, $n = 1, 2, \dots$ are Bessel functions of the first kind of order m , where $\phi_{mn}^{(1)}$ and $\phi_{mn}^{(2)}$ are given by:

$$\begin{aligned}\phi_{mn}^{(1)} &= \sqrt{\frac{2}{\pi}} \frac{J_m(\alpha_{m,n}r)}{|J_{m+1}(\alpha_{m,n})|} \cos(m\theta) \\ \phi_{mn}^{(2)} &= \sqrt{\frac{2}{\pi}} \frac{J_m(\alpha_{m,n}r)}{|J_{m+1}(\alpha_{m,n})|} \sin(m\theta)\end{aligned}\tag{2.3.5}$$

The zeros of the Bessel functions denoted by $\alpha_{m,n}$ determined from the transcendental equation:

$$\frac{\beta}{2} (J_{m-1}(\alpha_{m,n}) - J_{m+1}(\alpha_{m,n})) + J_m(\alpha_{m,n}) = 0\tag{2.3.6}$$

The coefficients A_{mn} and B_{mn} are determined using orthogonality relations with:

$$\begin{aligned}A_{mn} &= \sqrt{\frac{2}{\pi}} \frac{1}{|J_{m+1}(\alpha_{m,n})|} \int_{\Omega} v_0(r, \theta) J_m(\alpha_{m,n}r) r \cos(m\theta) d\theta dr = \langle v_0, \psi_{mn}^{(1)} \rangle \\ B_{mn} &= \sqrt{\frac{2}{\pi}} \frac{1}{|J_{m+1}(\alpha_{m,n})|} \int_{\Omega} v_0(r, \theta) J_m(\alpha_{m,n}r) r \sin(m\theta) d\theta dr = \langle v_0, \psi_{mn}^{(2)} \rangle\end{aligned}\tag{2.3.7}$$

The adjoints $\psi_{mn}^{(i)}$, $i = 1, 2$ are orthonormal to the respective $\phi_{mn}^{(i)}$, $i = 1, 2$ in the Eq.2.3.5, i.e: for $m, k \geq 0$ and $n, l \geq 1$

$$\langle \phi_{mn}^{(i)}, \psi_{kl}^{(i)} \rangle = \delta_{mk} \delta_{nl}\tag{2.3.8}$$

The zeros of the Bessel function $\alpha_{m,n} > 0$ for $m = 0, n \geq 1$ are simple and correspond to radially symmetric eigenfunctions, while $\alpha_{m,n} > 0$ for $m \geq 1, n \geq 1$

form a double set and correspond to a double of linearly independent eigenfunctions with dependence on the angular variable. Together, the eigenfunctions $\phi_{mn}^{(i)}$ and $\psi_{mn}^{(i)}$ form an orthonormal basis of the Hilbert space $L^2(\Omega)$ on which any $z(r, \theta, t) \in L^2(\Omega)$ can be represented by an infinite Fourier-Bessel series expansion.

2.3.1 Infinite-dimensional system representation

The thermal regulation problem, specifically the PDE model of the battery temperature dynamics, can be represented as an abstract initial value problem on an infinite-dimensional state space of functions which is analogous to the representation of ordinary differential equations on a finite-dimensional vector space. Moreover, this type of representation provides a convenient form to study the dynamics of the system and also to consider the output feedback controller design problem. Let us briefly depart from the battery thermal regulation problem and introduce the function space setting in which the infinite-dimensional system representation of the boundary control problem is considered.

Let Ω be a spatial domain in \mathbb{R}^N with points ξ , volume element dv , and boundary $\partial\Omega$. The letters $s, t \in [0, T]$ will denote the time indices where $0 \leq s \leq t \leq T < \infty$. General Banach spaces will be denoted by the calligraphic letters, e.g. \mathcal{Z} with norm $\|\cdot\|$. The set of bounded linear operators $F : \mathcal{Z} \rightarrow \mathcal{Y}$ is denoted $\mathcal{L}(\mathcal{Z}, \mathcal{Y})$, and $F : \mathcal{Z} \rightarrow \mathcal{Z}$ as $\mathcal{L}(\mathcal{Z})$. For functions $z \in \mathcal{Z}$ we denote $C([0, T]; \mathcal{Z})$ as the class of all continuously differentiable functions defined for $t \in [0, T]$ and taking values in \mathcal{Z} . The space $L^2(\Omega)$ is the standard space of square integrable functions, and is a Hilbert space with the inner product $\langle u, v \rangle = \int_{\Omega} u(\xi)v(\xi)dv$ [19]. For time-dependent functions, we denote

$L^2([0, T]; \mathcal{Z})$ as the set of all functions z taking values in \mathcal{Z} and $\|z(\xi, t)\|_{\mathcal{Z}}^2$ square integrable in $[0, T]$ with the norm $\|z\|_{L^2([0, T]; \mathcal{Z})} = \left(\int_0^T \|z(\xi, t)\|_{\mathcal{Z}}^2 dt \right)^{1/2}$. Unless specified otherwise, we denote $\|\cdot\|$ as the $L^2(\Omega)$ norm.

Parabolic PDEs can be represented in this function space setting as general abstract initial value problems in the form:

$$\dot{z}(t) = A(t)z(t), \quad z(0) = z_0 \tag{2.3.9}$$

where the nonautonomous operator $A(t)$ is associated with the PDE spatial operator and a domain $D(A(t))$ densely defined in the state space \mathcal{Z} , which is usually a Hilbert space [18, 20]. The solution of initial value problems with nonautonomous operators as in the Eq.2.3.9 are expressed in terms of two-parameter semigroups which determine the evolution of the state on \mathcal{Z} . Formally, we define this operator as follows [18, Theorem, 6.1, Chapter 5.6].

Definition 2.3.1. A two-parameter semigroup $U(t, s)$, $0 \leq s \leq t \leq T$ is a family of bounded linear operators on \mathcal{Z} which satisfies: (i) $\|U(t, s)\| \leq C$ where C is a positive constant; (ii) $(t, s) \rightarrow U(t, s)$ is continuous in the uniform operator topology; and (iii) for $0 \leq s \leq \tau \leq t \leq T$, we have $U(t, t) = I$, $U(t, s) = U(t, \tau)U(\tau, s)$, and:

$$\frac{\partial U(t, s)}{\partial t} = A(t)U(t, s), \quad \frac{\partial U(t, s)}{\partial s} = -U(t, s)A(s);$$

The two-parameter semigroup $U(t, s)$ is often referred to as an evolution operator due to the property (iii) in Definition 3.4.1. The solution of the initial value problem in Eq.2.3.9 is expressed in terms of this operator:

$$z(t) = U(t, s)z_s, \quad z(s) = z_s \quad 0 \leq s \leq t \leq T \tag{2.3.10}$$

Remark 2.3.2. As a brief example, consider the distributed control problem for the 1-D heat equation on the domain $\Omega := [0, 1]$:

$$\begin{aligned} \frac{\partial z}{\partial t} &= \alpha(t) \frac{\partial^2 z}{\partial \xi^2} + u(\xi, t), & z(\xi, 0) &= z_0(\xi) \\ \frac{\partial z}{\partial \xi}(0, t) &= 0, & \frac{\partial z}{\partial \xi}(1, t) &= 0 \end{aligned} \tag{2.3.11}$$

where $u(\xi, t)$ is the input distributed over Ω . The time-dependent coefficient $\alpha(t)$ describes processes in which the conductivity or diffusivity changes over time, for example, where catalyst activation/deactivation is present [26], and in models of moisture sorption in composite materials [27]. Assume first that $u(\xi, t) = 0$. The solution $z(\xi, t)$ is given by:

$$z(\xi, t) = U(t, 0)z_0 = \sum_{n=0}^{\infty} e^{\int_0^t \lambda_n(\tau) d\tau} \langle z_0(\xi), \phi_n(\xi) \rangle \phi_n(\xi) \tag{2.3.12}$$

where $\phi_n(\xi) = \sqrt{2} \cos(n\pi\xi)$ are the eigenfunctions and $\lambda_n(t) = -\alpha(t)(n\pi)^2$ are the eigenvalues. The PDE in Eq.2.3.11 can also be represented as the evolution system $\dot{z}(t) = A(t)z(t) + Bu(t)$ on the state space $\mathcal{Z} = L^2([0, 1])$ where $A(t)z = \alpha(t)(\partial^2 z / \partial \xi^2)$ and $B = I$. Note that the eigenfunctions form an orthonormal basis of \mathcal{Z} . Defining the state $z(t) := [z(\xi)](t)$, the solution of Eq.2.3.11 is expressed as:

$$z(t) = U(t, 0)z_0 + \int_0^t U(t, \tau)u(\tau) d\tau$$

where the operator $U(t, s)$, $0 \leq s \leq t \leq T$ is the two-parameter semigroup which describes the state evolution on \mathcal{Z} from any initial state $z_s \in L^2(\Omega)$ and

is given by (cf. Eq.2.3.12):

$$U(t, s)z_s = \sum_{n=0}^{\infty} e^{\int_s^t \lambda_n(\tau) d\tau} \langle z_s, \phi_n \rangle \phi_n \quad (2.3.13)$$

One can verify that the operator in Eq.2.3.13 satisfies the properties in Definition 2.3.1.

The following section deals with the representation of the battery thermal regulation problem within this infinite-dimensional systems framework. The use of boundary actuation to control the temperature requires some modification to the above procedure. Specifically, one considers the transformation of $z(r, \theta, t)$ in the original PDE system in terms of $v(r, \theta, t)$ given in Eq.2.3.1.

2.3.2 Boundary control formulation as an infinite-dimensional system

Consider the boundary control problem on the state space $\mathcal{Z} = L^2(\Omega)$ with states $z(t) = [z(r, \theta)](t)$ such that the system in Eqs.2.2.4-2.2.6 is represented as the initial value problem:

$$\dot{z}(t) = \mathfrak{A}(t)z(t) + q(t), \quad z(0) = z_0, \quad \mathfrak{B}z(t) = b_{\text{ctr}}u(t) \quad (2.3.14)$$

with nonautonomous differential operator $\mathfrak{A}(t) = A(r, \theta, t)$:

$$\mathfrak{A}(t) := \frac{1}{r} \frac{\partial}{\partial r} \left(r \frac{\partial}{\partial r} \right) + \frac{1}{r^2} \frac{\partial^2}{\partial \theta^2} + g(t) \quad (2.3.15)$$

The domain $D(\mathfrak{A}(t)) \subset \mathcal{Z}$ is defined as:

$$D(\mathfrak{A}(t)) = \left\{ z \in \mathcal{Z} \left| \begin{array}{l} z, \frac{\partial z}{\partial r}, \frac{\partial z}{\partial \theta} \text{ are a.c.}, \\ \frac{\partial^2 z}{\partial r^2}, \frac{\partial^2 z}{\partial \theta^2} \in \mathcal{Z}, \text{ and } \frac{\partial z}{\partial r}(0, \theta, t) = 0 \end{array} \right. \right\} \quad (2.3.16)$$

The boundary operator $\mathfrak{B} : \mathcal{Z} \rightarrow \mathbb{R}$ is defined as:

$$\mathfrak{B}z = \beta \frac{\partial z}{\partial r}(1, \theta, t) + z(1, \theta, t), \quad D(\mathfrak{A}(t)) \subset D(\mathfrak{B}) \quad (2.3.17)$$

Let us define the associated operator $A(t)$ on \mathcal{Z} with domain $D(A(t)) = D(\mathfrak{A}) \cap \ker \mathfrak{B} = \{z \in D(\mathfrak{A}(t)) / \mathfrak{B}z = 0\}$ given by:

$$D(A(t)) = \left\{ z \in \mathcal{Z} \left| \begin{array}{l} z, \frac{\partial z}{\partial r}, \frac{\partial z}{\partial \theta} \text{ are a.c.}, \frac{\partial^2 z}{\partial r^2}, \frac{\partial^2 z}{\partial \theta^2} \in \mathcal{Z}, \\ \text{and } \frac{\partial z}{\partial r}(0, \theta, t) = 0, \beta \frac{\partial z}{\partial r}(1, \theta, t) + z(1, \theta, t) = 0 \end{array} \right. \right\} \quad (2.3.18)$$

with $A(t)z(t) = \mathfrak{A}(t)z(t)$ in $D(A(t))$. Let $B = [b(r, \theta)] = b_{\text{ctr}}(\theta)r^2/(2\beta + 1)$ where $B \in L^2(\Omega)$ is continuous and bounded for all $r, \theta \in \Omega$ and satisfies:

$$\mathfrak{B}(Bu(t)) = b_{\text{ctr}}(\theta)u(t), \quad \text{for all } u(t) \in \mathbb{R} \quad (2.3.19)$$

Using the transformation in Eq.2.3.1 with $v(t) = z(t) - Bu(t)$, the boundary control problem for the PDE system in the Eq.2.3.2 is represented as the nonautonomous infinite-dimensional system with state $v(t) = [v(r, \theta)](t)$:

$$\dot{v}(t) = A(t)v(t) - B\dot{u}(t) + \mathfrak{A}(t)Bu(t) + q(t) \quad (2.3.20)$$

The operator $A(t)$, $0 \leq s < t \leq T$, is given by:

$$A(t)v(t) = \sum_{m=0, n=1}^{\infty} \lambda_{mn}(t) \langle v(t), \psi_{mn} \rangle \phi_{mn}$$

where

$$\lambda_{mn}(t) = -\alpha_{m,n}^2 + g(t), \tag{2.3.21}$$

$$\psi_{mn} = \begin{pmatrix} \psi_{mn}^{(1)} \\ \psi_{mn}^{(2)} \end{pmatrix} \quad \text{and} \quad \phi_{mn} = \begin{pmatrix} \phi_{mn}^{(1)} \\ \phi_{mn}^{(2)} \end{pmatrix}$$

The operator $A(t)$ generates the two-parameter semigroup $U(t, s)$, $0 \leq s \leq t \leq T$ given by:

$$U(t, s)v(s) = \sum_{m=0, n=1}^{\infty} \exp \left\{ \int_s^t \lambda_{mn}(\tau) d\tau \right\} \langle v(s), \psi_{mn} \rangle \phi_{mn} \tag{2.3.22}$$

The analytic form of the two-parameter semigroup generated by the nonautonomous operator $A(t)$ resembles the form of the standard one-parameter semigroups generated by analogous autonomous operators on a Hilbert space [16]. One can note that for each $t \in [0, T]$, the operator $A(t)$ is the infinitesimal generator of an analytic semigroup $S_t(s)$, $s \geq 0$ [18]. For all $t \in 0 \leq s \leq t \leq T$, the operator $U(t, s)$ determines the state evolution according to the previous definition.

Proposition 1. The operator $U(t, s)$ in Eq.2.3.22 satisfies (i)-(iii) of Definition 2.3.1.

The solution of the initial value problem corresponding to the transformed system in Eq.2.3.20 is expressed as:

$$\begin{aligned}
 v(t) = & U(t, s)v_s - \int_s^t U(t, \tau)B\dot{u}(\tau)d\tau \\
 & + \int_s^t U(t, \tau)\mathfrak{A}(\tau)Bu(\tau)d\tau + \int_s^t U(t, \tau)q(\tau)d\tau
 \end{aligned} \tag{2.3.23}$$

Then, the solution of the original system is given by:

$$\begin{aligned}
 z(t) = & Bu(t) - U(t, 0)Bu(0) + U(t, 0)z_0 - \int_0^t U(t, \tau)B\dot{u}(\tau)d\tau \\
 & + \int_0^t U(t, \tau)\mathfrak{A}(\tau)Bu(\tau)d\tau + \int_0^t U(t, \tau)q(\tau)d\tau
 \end{aligned} \tag{2.3.24}$$

The Eq.2.3.24 is provided in terms of the boundary input $u(t)$ as well as its derivative $\dot{u}(t)$. Problems of this type have been considered by extension of the state space to include the input space \mathcal{U} , i.e. on the extended state space $\mathcal{Z}^e := L^2(\Omega) \oplus \mathbb{R}$. In this way, the controller design is based on the extended system which is driven by integral action via the derivative of the input $\dot{u}(t)$, and the input $u(t)$ is then determined by integration [16]. On the other hand, the controller can be designed based on the input itself provided that the system is well defined for $u(t) \in \mathcal{U}$ (in practice, the input space is typically defined as $\mathcal{U} = \mathbb{R}$), and square integrable over $t \in [0, T]$. This condition is formally stated by the following Proposition which will be utilized in the following sections in which the state estimation and controller design problems will be considered.

Proposition 2. The solution of the boundary control problem expressed in Eq.2.3.24 is well defined for every input $u(t) \in L^2([0, T]; \mathcal{U})$.

Let us briefly summarize the procedure thus far before proceeding to the following sections. We have considered the PDE system in Eqs.2.2.4-2.2.6 which has two distinguishing features: First, the presence of time-dependent generation terms, and second, the input is applied over a portion of the boundary. The transformation in Eq.2.3.1 was utilized to convert the problem to a PDE system in Eq.2.3.2 with homogeneous boundary conditions. Next, the infinite-dimensional system representation of the boundary control problem was considered on the state space $\mathcal{Z} = L^2(\Omega)$. The formal definition yielded the representation of the PDE in Eq.2.3.2 as the nonautonomous infinite-dimensional system in Eq.2.3.20. Utilizing the two-parameter semigroup given in Eq.2.3.22, the solution of the nonautonomous infinite-dimensional system is given in Eq.2.3.23. Finally, the solution of the original system is provided in the Eq.2.3.24. The following sections deal with the state estimation and output feedback control problem for the determination of the input.

Remark 2.3.3. One can notice that the time-dependence of the operator $A(t)$ is due to the generation term $g(t)$ associated with the state. For $g(t) = g$ (constant), the operator in Eq.2.3.21 becomes:

$$Av(t) = \sum_{m=0, n=1}^{\infty} \lambda_{mn} \langle v(t), \psi_{mn} \rangle \phi_{mn}, \quad \text{where} \quad \lambda_{mn} = -\alpha_{m,n}^2 + g, \quad (2.3.25)$$

which generates the analytic semigroup $S(t)$, $t \geq 0$:

$$S(t-s)v(s) = \sum_{m=0, n=1}^{\infty} e^{\lambda_{mn}(t-s)} \langle v(s), \psi_{mn} \rangle \phi_{mn} \quad (2.3.26)$$

2.4 State estimation and output feedback control

The measurement of the battery temperature is a critical factor in the state estimation problem, the design of the control law, and the overall performance of the closed loop system. The true state (temperature distribution) must be estimated from a finite-number of sensors collecting information about the partial state of the system, e.g. combinations of point, regional, boundary and in-domain temperature measurements.

Methods utilized to approximate the state must take into consideration physical design and practical limitations. From a battery engineering perspective, an ideal situation would be where the temperature measurements are noninvasive of the actual functional parts of the battery, i.e. realized by placement of thermocouples which measure the temperature only on points or regions of the boundary. In some lumped parameter models of the battery system, this approach is utilized [28]. However, as in the present context in which the temperature is assumed to be distributed, the restriction to boundary measurements represents a complex problem. From a mathematical control perspective, the approach to the state estimation and controller design problem is the construction of an observer. The case in which only boundary measurements are available inherits two primary challenges: First, the temperature of the system throughout of the domain must be reconstructed from the measured temperature available only on a portion(s) of the boundary, and therefore requires the determination of a relationship between the two. Second, the relationship between the boundary and domain temperatures can only be developed from the state estimates of the system (along with state estimates

or measured states available on the boundary) since the temperature of the actual system is not known *a priori*. Although there are some works on the recovery of the system state from boundary measurements, compensator design remains an active area research in distributed parameter systems [29, 30].

A less restrictive set of problems exist for cases in which measurements of the temperature field are assumed to be available from embedded sensors. Usually, the sensor measurements are taken to be point or averaged readings over small increments, from which the partial state of the system is ascertained. This idea naturally leads to important questions pertaining to the number and optimal placement of sensors required to ensure that the system is (approximately) observable, detectable, stabilizable, etc., by checking rank conditions dependent on the sensor locations, definition of the measurement functions. From a control engineering perspective, one alternative to the state estimation problem is the use of point or regional sensors to reconstruct the temperature field by interpolation. An advantage of this approach is that it circumvents the need to design an observer, by using the reconstructed temperature field to obtain the state of the system which is then directly utilized in the controller design. This convenience comes at a cost of introducing computational overhead necessary to interpolate the temperature field from measurements, but this cost is offset since the method does not require an observer system to be run concurrent to the process. Moreover, the controller performance based directly on the measured states may be an improvement over the use of an observer system which requires the careful design of the observer gain such that the states converge to those of the actual system in a reasonable time to ensure the stability of the closed loop system. While the direct use of the measured states provides a more robust method for the feedback design problem, the accuracy of the estimation and state reconstruction also

depends on the number and placement of the measurement locations. These ideas along with comparative cases will be discussed in further detail within later sections. In this section, we restrict our discussion and focus on first, the observer design method to demonstrate the dynamical properties of the closed loop output feedback system. Secondly, we consider the direct use of the state measurements for the state reconstruction via interpolation which will enable the practical realization of the output feedback boundary controlled battery temperature regulation problem.

2.4.1 Observer design

In practice, sensors are used to measure the temperature at points or regions which contain only partial information about the entire state of the system. Generally, for the cases where sensors are placed within the domain, the output of the system $y(t)$ is represented as:

$$y(t) = Cz(t) := \int_{\Omega} c(r, \theta) z(r, \theta, t) dr d\theta \quad (2.4.1)$$

where $c(r, \theta)$ is a distributed measurement function of (r, θ) which is defined on all of the domain, or at specific points or regions within the domain. In the cases for which measurements are taken at points within the domain, the function $c(r, \theta)$ is approximated by the shape function around the measurement points $(r_i, \theta_i) \in \Omega$, $i = 1, 2, \dots, n_{\text{msr}}$ with $c(r, \theta)$ given by:

$$c(r, \theta) = \frac{1}{4\zeta_1\zeta_2} \delta_{[r_i-\zeta_1, r_i+\zeta_1]}(r) \delta_{[\theta_i-\zeta_2, \theta_i+\zeta_2]}(\theta) \quad (2.4.2)$$

where $\delta_{[r_i-\zeta_1, r_i+\zeta_1]}(r) = 1$ for $r_i - \zeta_1 \leq r \leq r_i + \zeta_1$, and 0 otherwise (similarly, $\delta_{[\theta_i-\zeta_2, \theta_i+\zeta_2]}(\theta)$ is defined). In the case of a single temperature measurement,

for example, C is a bounded linear operator $C \in \mathcal{L}(\mathcal{Z}, \mathcal{Y})$ with the norm $1/(2\sqrt{\zeta_1\zeta_2})$ and $\mathcal{Y} = \mathbb{R}$. Measurements on the boundary at $r = 1$ and θ_j , $j = 1, 2, \dots, m_{\text{msr}}$ can be approximated by the functions $c(1, \theta) = \delta_{[\theta_j - \zeta_2, \theta_j + \zeta_2]}(\theta)$, or analogous to the input function as in Eq.2.2.8, taken from a region of the boundary $\eta \in (-\pi, \pi)$ centred at θ_{msr} . In the case of point measurements where $c(r, \theta)$ is given in Eq.2.4.2, the compensator design problem for the boundary control system, as in Eq.2.3.20, is given by:

$$\dot{v}(t) = A(t)v(t) + \mathfrak{A}(t)Bu(t) - B\dot{u}(t) + q(t), \quad y(t) = Cv(t) \quad (2.4.3)$$

Recall from Proposition 2 that the solution of Eq.2.4.3 is well defined for every $u(t) \in L^2([0, T]; \mathcal{U})$ such that the control law can be determined based on the input, rather than its derivative, and denote this system by $\Sigma(A(t), \mathfrak{A}(t)B, C)$ which is assumed to be exponentially detectable. Consider a Luenberger observer for the system in Eq.2.4.3 given by:

$$\dot{\hat{v}}(t) = A(t)\hat{v}(t) + \mathfrak{A}(t)Bu(t) - B\dot{u}(t) + q(t) - L(y(t) - \hat{y}(t)), \quad \hat{y}(t) = C\hat{v}(t) \quad (2.4.4)$$

where $\hat{v}(t)$ denotes the state estimates with initial condition $\hat{v}(0) = \hat{v}_0$ and $L \in \mathcal{L}(\mathcal{Y}, \mathcal{Z})$ is the observer gain operator. The dynamics of the error $\varepsilon(t) = v(t) - \hat{v}(t)$ between the states $v(t)$ and the estimates $\hat{v}(t)$ are governed by the system:

$$\dot{\varepsilon}(t) = (A(t) + LC)\varepsilon(t) \quad (2.4.5)$$

Note that the entropy related generation term $g(t) \in C([0, T], \mathcal{Z})$ is bounded (see Fig.2.1) such that $\|g(t)\| \leq k_g = \sup\{\|g(t)\| : t \in [0, T]\}$, and that the operator $A(t)$ in Eq.2.3.18 can be seen as a perturbation of an autonomous

operator A which is the infinitesimal generator of a strongly continuous semigroup $S_A(t)$, $t \geq 0$. That is,

$$A(t) = A + g(t), \quad \text{where} \quad g(t)v \in C([0, T]; \mathcal{Z}) \quad (2.4.6)$$

The semigroup $S_A(t)$ is exponentially stable:

$$\|S(t)\| \leq Me^{\omega t}, \quad \omega_0 := \sup_{m \geq 0, n \geq 1} (-\alpha_{mn}^2) \leq \omega \quad (2.4.7)$$

where M is a generic positive constant, and $\omega < 0$. By choosing the observer gain such that $k_g + \|LC\| = \gamma < 0$, the operator $A(t) + LC$ generates the exponentially stable two-parameter semigroup $U_{LC}(t, s)$:

$$\|U_{LC}(t, s)\| \leq Me^{(\omega+\gamma)(t-s)} \quad (2.4.8)$$

Then, the solution of Eq.2.4.5 is expressed as:

$$\varepsilon(t) = U_{LC}(t, s)\varepsilon_0 \quad (2.4.9)$$

where $\varepsilon_0 = v_0 - \hat{v}_0$. Since $U_{LC}(t, s)$ is exponentially stable, the error $\varepsilon(t)$ converges to zero as $t \rightarrow \infty$. Now, suppose for the moment that the nonhomogeneous generation term, independent of the state, is zero, i.e. $q(t) = 0$. Consider the input $u(t) = F\hat{v}(t)$ where $F \in \mathcal{L}(\mathcal{Z}, \mathcal{U})$. The closed loop system for Eqs.2.4.3-2.4.4 can be written together on the extended state space $\mathcal{Z}^e = \mathcal{Z} \oplus \mathcal{Z}$ as:

$$\dot{v}^e(t) = A^e(t)v^e(t), \quad \text{where} \quad v^e(t) = \begin{pmatrix} v(t) \\ \hat{v}(t) \end{pmatrix} \quad (2.4.10)$$

and the operator $A^e(t)$ is defined as:

$$A^e(t) = \begin{pmatrix} A(t) + BF(I + BF)^{-1}LC & \mathfrak{A}(t)BF - BF(I + BF)^{-1}(A(t) + LC + \mathfrak{A}(t)BF) \\ -(I + BF)^{-1}LC & (I + BF)^{-1}(A(t) + LC + \mathfrak{A}(t)BF) \end{pmatrix}$$

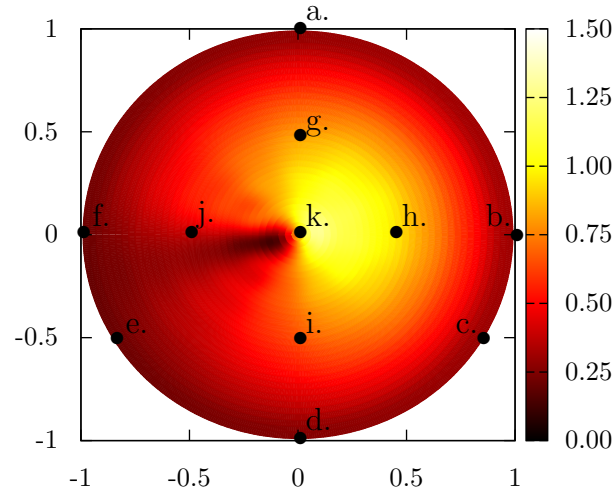
Utilizing the operator matrices $I_1 = \begin{pmatrix} I & -I \\ 0 & I \end{pmatrix}$ and $I_2 = \begin{pmatrix} I & I \\ 0 & I \end{pmatrix}$ the extended operator $A^e(t)$ is transformed to the following form:

$$I_1 A^e(t) I_2 = \begin{pmatrix} A(t) + LC & 0 \\ -(I + BF)^{-1}LC & (I + BF)^{-1}(A(t) + \mathfrak{A}(t)BF) \end{pmatrix} \quad (2.4.11)$$

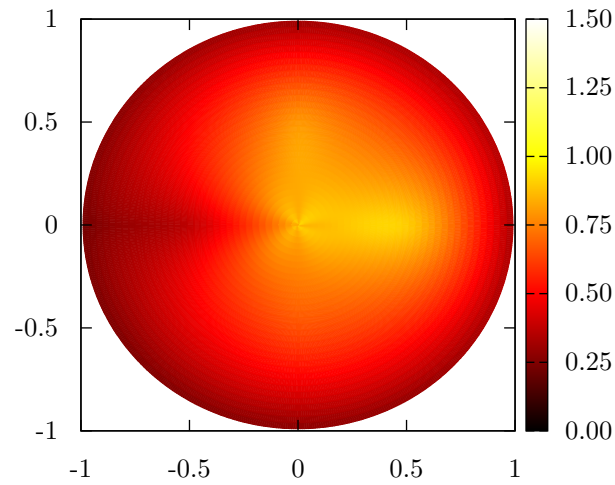
The closed loop behaviour of the output feedback system can be understood from the Eq.2.4.11 where the eigenspectrum of the closed loop system is given by $\sigma(A(t) + LC) \cup \sigma(A(t) + \mathfrak{A}(t)BF)$. One can see that if L is chosen such that $A(t) + LC$ generates a stable two-parameter semigroup, then the choice of F such that $A(t) + \mathfrak{A}(t)B$ generates an exponentially stable two-parameter semigroup also stabilizes the closed loop system. Each of the gain operators L and F can be designed optimally by considering the appropriate minimization problems [16, 31]. One can note that the inclusion of the nonhomogeneous generation term $q(t)$ does not change the structure of the Eq.2.4.11, but appears as additional terms in the Eq.2.4.10 which are all independent of the state. An alternative approach to the stabilizing regulator design is by the conversion of the nonhomogeneous state equation in Eq.2.4.3 into a homogeneous state equation via transformation. The associated optimization problem for the resulting homogeneous system given in terms of the transformed state can then be considered [31, Chapter 7.2, Part 4].

2.4.2 Interpolation based output feedback controller design

Another approach towards the output feedback controller design is by directly utilizing the set of point or regional sensor measurements to reconstruct the entire temperature field by interpolation. That is, by utilizing the set of measurement points (r_i, θ_i) (and also (r_j, θ_j)), the temperature is approximated for all $(r, \theta) \in \Omega$ and $t \in [0, T]$ as $z(r, \theta, t) \approx \hat{z}(r, \theta, t)$, such that the output is given by $y(t) \approx \hat{z}(t) = \langle \hat{z}(r, \theta), \psi_{mn} \rangle$. One advantage of utilizing the temperature readings to interpolate the entire temperature field is that the output contains more information about the system than from individual temperature measurements, provided that the sensors are reasonably placed to capture the distribution. The logical choices of sensor locations in the present context of the battery control problem should reflect the axial symmetry of the domain and the expected dynamical behaviour of the temperature evolution. For example, the temperature distribution in Fig.2.3(a) is reconstructed in Fig.2.3(b) by utilizing a total number of 9 measurement locations, where $\{a, b, d, f\}$ are point measurements along the boundary, $\{g, h, i, j\}$ are taken along an intermediate ring at the interior of the domain, and the sensor $\{k\}$ is located at the centre of the disk. Although the initial temperature distribution is not axisymmetric, one can note from modal analysis that the dominant mode is associated with the eigenfunction $\phi_{01}^{(1)} > 0$, Eq.2.3.5, which is radially symmetric. This implies that non-radially symmetric initial temperature distributions eventually tend to exhibit radial symmetry, and this dynamical behaviour is reflected in the configuration of sensor placement shown in Fig.2.3(a).



(a) Temperature distribution $z(r, \theta, 0) = z_0(r, \theta)$ and sensor locations $\{a., b., \dots, k.\}$



(b) Temperature distribution $\hat{z}(r, \theta, 0) = \hat{z}_0(r, \theta)$ reconstructed using sensor locations $\{a., b., d., f., g., h., i., j., k.\}$.

Figure 2.3: Initial battery temperature distribution $z(r, \theta, 0) = z_0(r, \theta)$ and temperature distribution reconstructed by Delaunay triangulation interpolation method [32].

In terms of the output feedback control problem, the controller design is then considered for the system $\Sigma(A(t), \mathfrak{A}(t)B, I)$. The determination of the input $u(t)$ has two components: First, the stabilization of the state related generation term $g(t)$, and second, the stabilization of the non-state related generation term $q(t)$. For the state related component, one may consider the finite-time horizon quadratic minimization of the cost functional [31]:

$$J(v_0; 0, T, u) = \int_0^T (|v(\tau)|^2 + |Ru(\tau)|^2) d\tau + \langle v(T), Qv(T) \rangle \quad (2.4.12)$$

The operator $Q \in \mathcal{L}(\mathcal{Z})$ is self-adjoint and nonnegative and $R \in \mathcal{U}$ is coercive. The associated solution is determined in terms of the operator $\Pi(t) \in \mathcal{L}(\mathcal{Z})$ which is the strongly continuous, self adjoint, nonnegative solution of the differential Riccati equation [31]:

$$\begin{aligned} \dot{\Pi}(t) + (A(t))^* \Pi(t) + \Pi(t) A(t) \\ - \Pi(t) (\mathfrak{A}(t)B) R^{-1} (\mathfrak{A}(t)B)^* \Pi(t) + I = 0 \end{aligned} \quad (2.4.13)$$

with final time condition $\Pi(T) = Q$. The non-state related generation term is accounted for by considering the auxiliary differential equation in terms of $\Gamma(t)$:

$$\dot{\Gamma}(t) = [(A(t))^* - \Pi(t) (\mathfrak{A}(t)B) (\mathfrak{A}(t)B)^*] \Gamma(t) + \Pi(t) q(t), \quad \Gamma(T) = 0 \quad (2.4.14)$$

Together, the finite time optimization problem has the minimizing solution related by the feedback formula:

$$u_{\min}(t) = -R^{-1} (\mathfrak{A}(t)B)^* (\Pi(t)v(t)) - (\mathfrak{A}(t)B)^* \Gamma(t) \quad (2.4.15)$$

Given that the interpolated temperature field provides a good approximation to the actual one, the state $\hat{v}(t) \approx v(t)$ can be utilized in the feedback formula in Eq.2.4.15 to stabilize the system.

There are two important issues to be discussed before proceeding to the realization of the battery control problem in the following section. First, one can note that the generation terms $g(t)$ and $q(t)$ which are the sources of instability in the system effect all of the modes (m, n) of the system. For the state related generation term $g(t)$, this instability can be seen directly from the Eq.2.3.21 where $\lambda_{mn}(t) = -\alpha_{m,n}^2 + g(t)$. Since $g(t)$ is bounded, there exists a finite-set of modes which are unstable, i.e. the set (m_u, n_u) such that $\lambda_{m_u, n_u} > 0$. Then, a finite-dimensional controller in terms of $\Pi(t)$ in Eqs.2.4.13-2.4.15 of order $m_u + n_u$ can be designed to stabilize these modes. However, the non-state related generation term $q(t)$, while also bounded and only dominant in the first few modes, contributes to all of (m, n) . Consequently, it is not feasible to obtain a finite-dimensional controller in terms of $\Gamma(t)$ from Eq.2.4.14 such that the control law in Eq.2.4.15 which will completely negate the contribution of the non-state related generation term. However, in the following section, we will demonstrate that it is possible to mitigate the growth in temperature by using a low order finite-dimensional controller based on the infinite-dimensional system representation of the battery control problem with boundary input.

Remark 2.4.1. The choices of actuator and sensor placement is a further design consideration which have the potential to impact controller performance, and is beyond the scope of this present work. There is a large amount of literature dedicated to these types of issues, see e.g. [33, 34]. In the application considered in this present work, the choice of sensor locations reflects

the geometric symmetry of the battery model. The sensor locations depicted in Fig.2.3(a) should be selected to capture the non-axisymmetric temperature distribution of the battery cell. One can note that the geometry of the system enables one to reduce the number of sensors by taking advantage of the prescribed boundary conditions. That is, the temperature measurements at the locations $\{b, c, d, e, f\}$ are taken along the boundary of the system and satisfy the same boundary condition. One can then choose any of these locations to serve as a pseudo temperature reading instead of any or all of the other sensor locations for use in the interpolation scheme for state reconstruction. However, a temperature measurement should be taken within the region of the boundary where the input is applied which differs from the measurements outside of the region of boundary input.

2.5 Numerical Simulation and Case Studies

This section deals with the application of the closed loop output feedback controller design based on the infinite-dimensional systems representation of the Li-ion battery boundary controlled thermal regulation problem. A set of case studies will be considered to demonstrate the effect of controller tuning on the overall behaviour of the temperature dynamics in the closed loop system. The general approach will be to utilize a plant model, and employ a finite-dimensional output feedback controller based on the formulation presented in Section 2.4.2. We consider a battery system with a 1.5 Amp hour capacity discharged at a rate of 1C where the dynamics of the plant model is based on the modal decomposition of the PDE system in Eqs.2.2.4-2.2.6 with parameters listed in Table 2.4. The open loop dimensionless temperature distribution $z(r, \theta, t)$ of the battery at select time instances is shown in Fig.2.4 starting

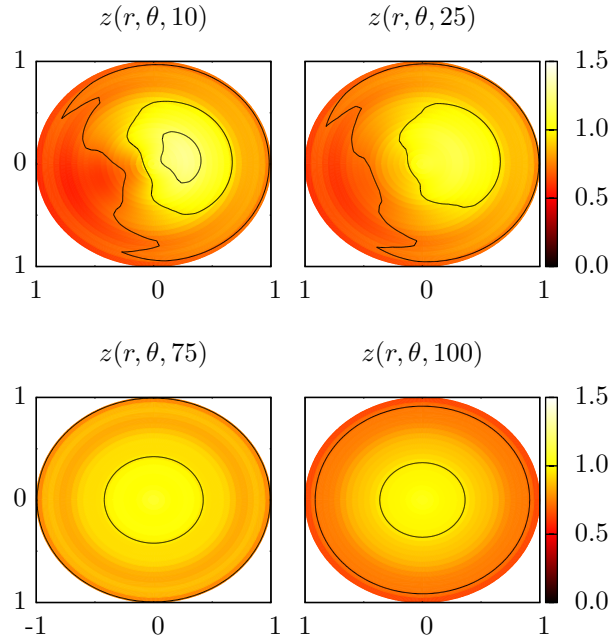


Figure 2.4: Open loop temperature distributions.

from the initial distribution shown in Fig.2.3(a). One can see the effect on the battery temperature due to the generation terms $g(t)$ and $q(t)$ which are dependent on the total entropy change, Fig.2.1(d), as the battery is discharged.

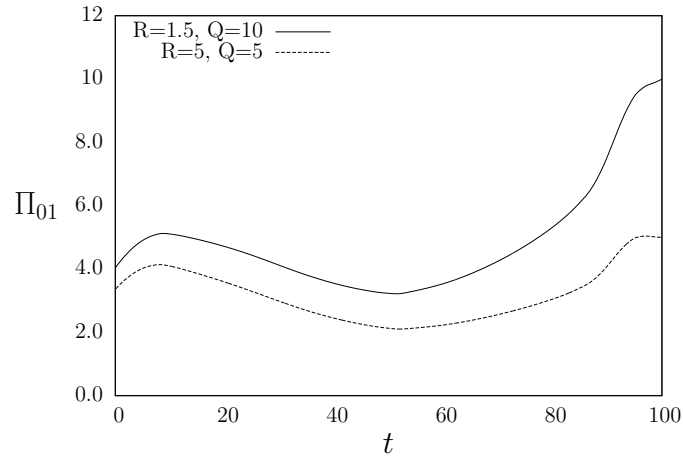
The output feedback controller design is based on the method proposed in Section 2.4.2. First the temperature measurement locations shown in Fig.2.3(a) are used to reconstruct the temperature distribution $\hat{z}(r, \theta, t)$ by interpolation as in Fig.2.3(b). The first order control law corresponds to the single unstable mode of the system at $m = 0, n = 1$, i.e. $\lambda(t)_{01} > 0$ and $\lambda(t)_{mn} < 0$ for all $m \geq 1, n \geq 2, t \in [0, T]$. The quadratic minimization problem given in Eqs.2.4.12-2.4.14 is solved to obtain the feedback formula in Eq.2.4.15, and is

explicitly given by:

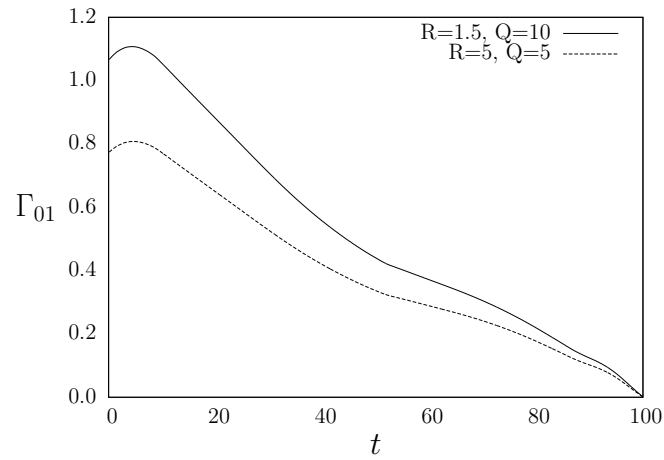
$$\begin{aligned}
u_{\min}(t) &= -R^{-1}\Pi_{01}(t)\langle(\mathfrak{A}(t)B)\hat{v}, \psi_{01}\rangle\phi_{01} - \Gamma_{01}(t)\langle(\mathfrak{A}(t)Bv), \psi_{01}\rangle\phi_{01} \\
&= -D^{-1} \left[\Pi_{01}(t) \left(\int_{-\pi}^{\pi} \int_0^1 (\mathfrak{A}(t)B)\hat{z}\psi_{01} dr d\theta \right) \phi_{01} \right. \\
&\quad \left. + \Gamma_{01}(t) \left(\int_{-\pi}^{\pi} \int_0^1 (\mathfrak{A}(t)B)\psi_{01} dr d\theta \right) \phi_{01} \right]
\end{aligned} \tag{2.5.1}$$

where $D = R - \Pi_{01} \left(\int_{-\pi}^{\pi} \int_0^1 (\mathfrak{A}(t)B)B\psi_{01} dr d\theta \right) \phi_{01}$. The solutions $\Pi_{01}(t)$ and $\Gamma_{01}(t)$ of the differential Riccati and auxiliary equations are dependent on the controller tuning parameters $Q \in \mathbb{R}$ and $R \in \mathbb{R}$ and are shown in Fig.2.5(a) and Fig.2.5(b), respectively.

The following case studies are considered to examine the effect of sensor placement, number of sensors, and controller tuning parameters on the closed loop feedback system. Cases 1 and 2 use the same sensor number and placement, while the controller used in Case 1 is relatively more aggressive controller than the controller used in Case 2. The second set of cases Cases 3 and 4 use a reduced number of sensors in a different configuration than Cases 1 and 2.



(a) Solution $\Pi_{01}(t)$ of the differential Riccati equation for $R = 1.5, Q = 10$ and $R = 5, Q = 5$.



(b) Solution $\Gamma_{01}(t)$ of the auxiliary equation for $R = 1.5, Q = 10$ and $R = 5, Q = 5$.

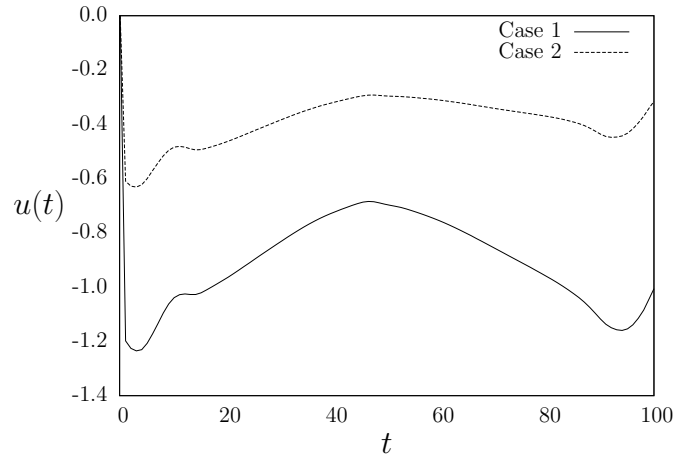
Figure 2.5: Solutions $\Pi_{01}(t)$ and $\Gamma_{01}(t)$ under controller tuning parameters.

2.5.1 Case 1 and Case 2

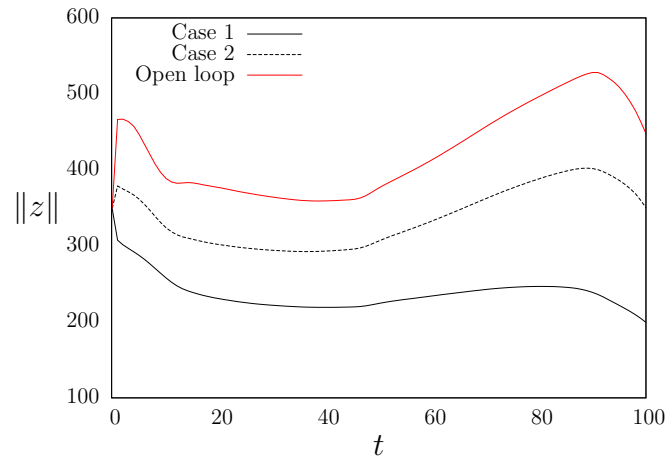
Table 2.1: Case 1 and Case 2: measurement and control parameters

Parameter	Setting
Number of sensors	9
Sensor locations	a,b,d,f,g,h,i,j,k
Centre of input	$\theta_c = \pi/2$
Boundary input region	$r = 1, \theta \in (\pi/4, 3\pi/4)$
Shape parameter	$K_1 = 20$
Case 1: Controller tuning	$R = 1.5, Q = 10$
Case 2: Controller tuning	$R = 5, Q = 5$

The closed loop feedback systems for Case 1 and Case 2 were simulated using the sensor and tuning parameters in Table 2.1. The boundary input profiles for each set of tuning parameters is shown in Fig.2.6(a). As expected, the tuning parameters used in the control design for Case 1 resulted in a relatively more aggressive input profile compared to the input profile used in the control design for Case 2. The battery temperature distribution and the reconstructed temperature distribution at select time instances for Case 1 is shown in Fig.2.8(a) (cf. Fig.2.4) where the influence of the input over the region of the boundary centred at $\pi/2$ on the whole distribution can be clearly seen. The overall temperature distribution and dynamical behaviour is captured by the interpolation scheme using the number and configuration of sensors. The total system energy $E = \|z(r, \theta, t)\|^2$ profiles for Case 1, Case 2, and for the open system, are shown in Fig.2.6(b). One can see the growth in overall system energy in the open loop system due to the exothermic heat generation and the energy profiles of the closed loop systems each show a lower total system energy profile. At the end of the discharge cycle, $E \approx 200$ for the controller designed using the parameters in Case 1, compared to $E \approx 450$ for



(a) Input profiles for Case 1 and Case 2.



(b) System energy profiles for Case 1, Case 2, and the open loop system.

Figure 2.6: Input and energy profiles for Case 1 and Case 2.

the open loop system. While the controller is not able to completely dissipate the heat generated by the exothermic chemical reactions producing the current in the battery, the maximum temperature and overall temperature variance is reduced by use of the output feedback controller with boundary actuation. As previously discussed, it is not possible to completely negate the influence of

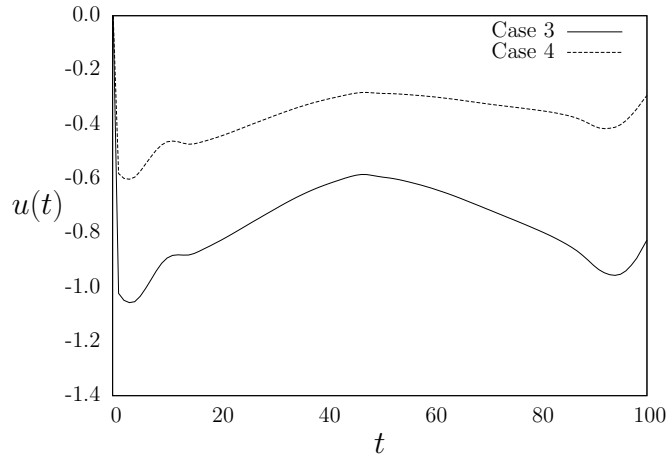
the non-state generation term $q(t)$ since it affects and infinite-number modes. However, increasing the order of the controller will further mitigate the effect of this generation term.

2.5.2 Case 3 and Case 4

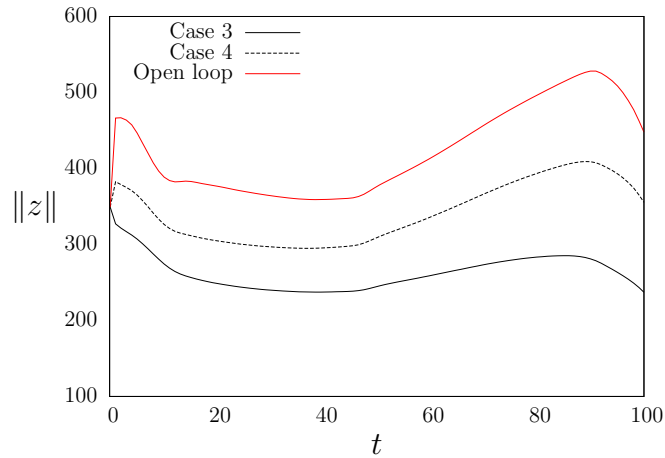
Table 2.2: Case 3 and Case 4: measurement and control parameters

Parameter	Setting
Number of sensors	4
Sensor locations	a,c,e,k
Centre of input	$\theta_c = \pi/2$
Boundary input region	$r = 1, \theta \in (\pi/4, 3\pi/4)$
Shape parameter	$K_1 = 20$
Case 3: Controller tuning	$R = 1.5, Q = 10$
Case 4: Controller tuning	$R = 5, Q = 5$

In Case 3 and Case 4, the number of sensors were reduced relative to the number used in Case 1 and Case 2, and the placement of the sensors was also altered (cf. Fig.2.3(a)). The sensor and tuning parameters for each case are listed Table 2.2, the boundary input profiles are shown in Fig.2.7(a), energy profiles are shown in Fig.2.7(b), and the battery temperature distribution and the reconstructed temperature distribution at select time instances for Case 3 is shown in Fig.2.8(b). Once again, the input and energy profiles reflect the difference in tuning parameters for each of the controllers corresponding to Case 1 and Case 2. Comparing the temperature distributions in Fig.2.8(a) and Fig.2.8(b) illustrates how changing the number of and the configuration of sensors influences the reconstruction of the temperature distribution. The sensor placements, measurements taken, and the resulting interpolation in Case 1 is better able to capture the non-symmetric temperature distribution of the



(a) Input profiles for Case 3 and Case 4.



(b) System energy profiles for Case 3, Case 4, and the open loop system.

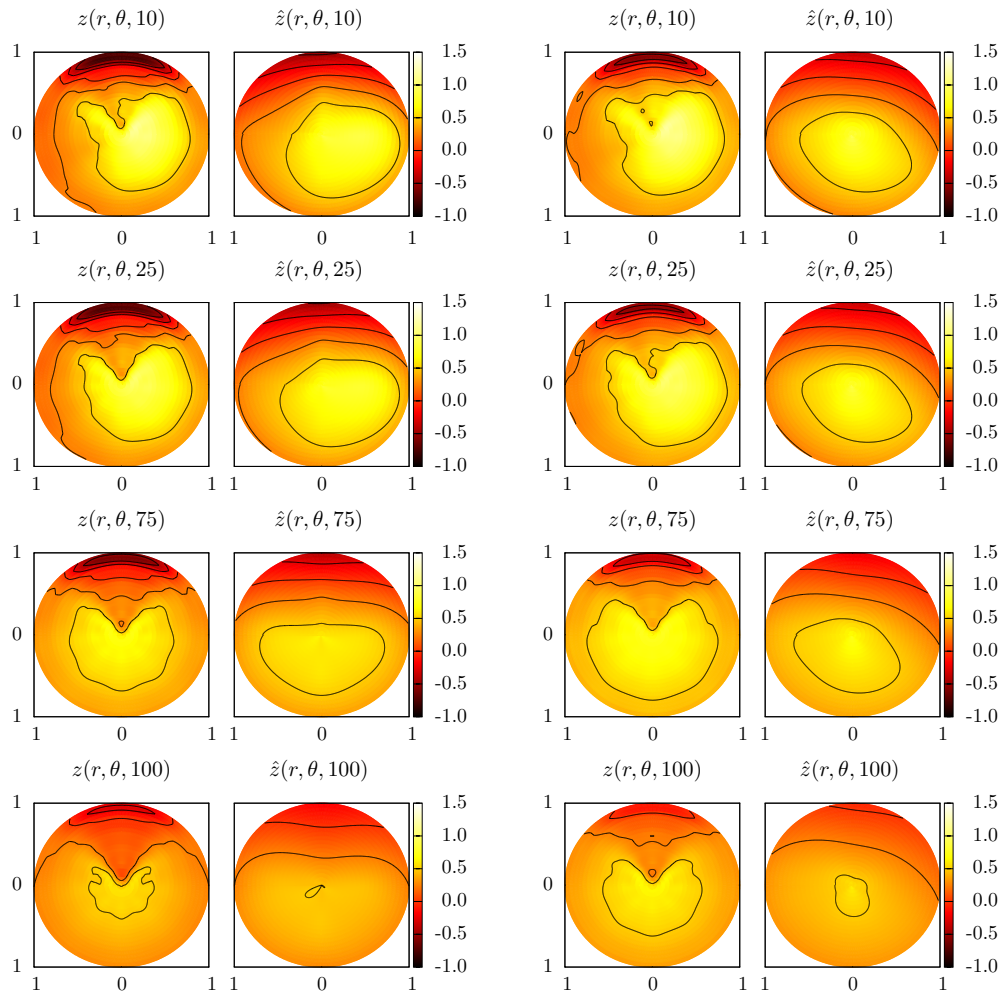
Figure 2.7: Input and energy profiles for Case 3 and Case 4.

disk compared to the interpolation based on the sensor locations in Case 3. As previously mentioned, the temperature tends to an axi-symmetric distribution over time as the battery is discharged, and the reconstructed distributions for Case 1 and Case 3 become more similar.

One can notice that the input and energy profiles for Case 2 and Case 4, having the same tuning parameters, are closely aligned. On the other hand,

the input and the resulting energy profiles for Case 1 and Case 3 show a greater difference. At the end of the discharge cycle, the energy $E \approx 225$ for the controller designed using the parameters in Case 3 (compared to $E \approx 200$ for Case 1), and $E \approx 350$ for each of the controllers corresponding to Case 2 and Case 4. This suggests that there may be a relationship between aggressive controller tuning and the number and/or placement of sensors. In other words, the input to the system generated by the controller is influenced by the number and the placement of sensors (and subsequently, the accuracy of the temperature distribution reconstruction), but this influence is diminished for less aggressive control designs.

Remark 2.5.1. One of the controller performance metrics employed in the case studies provided is the measurement of the total system energy profiles under the different combinations of controller tunings and sensor locations. Another potential set of metrics of interest would be the comparison of the total system energy profiles of the current model based controller design, and also the variation in temperature profiles, versus other control schemes, e.g. PI and PID control.



(a) Closed loop temperature distributions for Case 1 (b) Closed loop temperature distributions for Case 3

Figure 2.8: Closed loop temperature distributions for Case 1 and Case 3. (Left column) Actual temperature $z(r, \theta, t)$. (Right column) Reconstructed temperature $\hat{z}(r, \theta, t)$.

2.6 Summary

This chapter considered the thermal regulation problem for a Li-ion battery by output feedback control and boundary control actuation. The model of the battery temperature dynamics was given by a non-homogeneous parabolic partial differential equation (PDE) on a 2-dimensional spatial domain with angular and radial coordinates. The heat generation during battery discharge is attributed the underlying exothermic electrochemical reactions which appear as state related and non-state related generation terms in the model. Several key challenges in the output feedback model based controller design were addressed in this work: First, the dependence of the state on time-varying system parameters yielded a nonautonomous infinite-dimensional system with time-varying nonhomogeneous generation term. Second, the restriction of the input along a portion of the battery domain boundary required the reformulation of the boundary control problem into a suitable form. Third, the compensator design problem was considered and the closed loop system for the observer based optimal boundary control system was demonstrated to be stable under appropriate design of the observer and controller gain operators using the separation principle. Finally, the outback feedback control problem based on state measurement and interpolation of the temperature field was provided and the numerical simulation results for several case studies were presented.

Table 2.3: Nomenclature

Symbol	Description
C_p	Specific heat capacity ($\text{J}\cdot\text{kg}^{-1}\text{K}^{-1}$)
F_c	Faraday constant ($96,485\text{C}\cdot\text{mol}^{-1}$)
h	Heat transfer coefficient ($\text{W}\cdot\text{m}^{-1}\text{K}^{-1}$)
i	Current ($\text{Amps}\cdot\text{m}^{-2}$)
K_0	Thermal conductivity ($\text{W}\cdot\text{m}^{-1}\text{K}^{-1}$)
n_R	Reaction charge number
\dot{Q}	Heat generation ($\text{W}\cdot\text{m}^{-3}$)
S_Δ	Entropy change ($\text{J}\cdot\text{mol}^{-1}\cdot\text{K}^{-1}$)
V	Volume (m^3)
x	Electrode averaged ion concentration
Z	Temperature (K)
Z_a	Ambient temperature (K)
ρ	Density ($\text{kg}\cdot\text{m}^{-3}$)
σ_{con}	Electrical conductivity ($S\cdot\text{m}^{-1}$)

Table 2.4: Physical properties

Component	Thickness (μm)	Proportion				
		$p^{(i)}$ (%)	$p^{(i)}\rho^{(i)}$	$p^{(i)}K_0^{(i)}$	$p^{(i)}C_p^{(i)}$	$p^{(i)}\sigma_{\text{con}}^{(i)}$
LiCoO ₂	92	0.42	962	0.78	0.49	0.000042
LiC ₆	87	0.39	1962	1.95	0.27	0.000039
Al	10	0.045	122	9.0	0.039	1.71
Cu	10	0.045	405	17.1	0.017	2.70
Separator	22	0.10	120	0.10	0.7	-
Total	221	1.00	3571	29.93	1.522	4.4100081

2.7 Proof of Proposition 1

It is standard to prove (i) and (ii), and for brevity we only provide an outline of the procedure (e.g. see, [31]).

The entropy related generation term $g(t)$ is bounded by definition $\|g(t)\| \leq k_g = \sup\{\|g(t)\| : t \in [0, T]\}$, and the operator $A(t)$ in Eq.2.3.18 can be seen as a perturbation of an autonomous operator $A(t) = A + g(t)$, where $g(t)v \in C([0, T]; \mathcal{Z})$. The semigroup $S_A(t)$ generated by A is exponentially stable, $\|S_A(t)\| \leq M e^{\omega t}$, $\omega_0 := \sup_{m \geq 0, n \geq 1} (-\alpha_{mn}^2) \leq \omega$ where M is a generic positive constant, $\omega > 0$. Then for $z \in \mathcal{Z}$, $z(t) = S(t)z_0 + \int_0^t S(t-\tau) (g(\tau)z(\tau)) d\tau$ and application of Gronwall's lemma yields the bound on the evolution operator

$$\|U(t, s)\| \leq M e^{(\omega + k_g)(t-s)}$$

The uniform continuity in the operator topology can be demonstrated considering the approximation $U_k(t, s)$, and application of the Contraction Mapping Principle (method of successive approximations), one can show that for any $z \in \mathcal{Z}$, $\lim_{k \rightarrow \infty} U_k(t, s)z = U(t, s)z$ uniformly.

(iii): The first identity $U(t, t) = I$ is easily seen by inspection. The second identity can directly verified where for $0 \leq s \leq r \leq t \leq T$:

$$\begin{aligned}
U(t, r)U(r, s)v &= \sum_{m=0, n=1}^{\infty} e^{\int_r^t \lambda_{mn}(\tau) d\tau} \left\langle \sum_{k, l=0}^{\infty} e^{\int_s^r \lambda_{kl}(\tau) d\tau} \langle v, \psi_{kl} \rangle \phi_{mn}, \psi_{mn} \right\rangle \phi_{mn} \\
&= \sum_{m=0, n=1}^{\infty} e^{\int_r^t \lambda_{mn}(\tau) d\tau} \\
&\quad \times \left(\int_{\Omega} \sum_{k, l=0}^{\infty} e^{\int_s^r \lambda_{kl}(\tau) d\tau} \left(\langle v, \psi_{kl}^{(1)} \rangle \phi_{kl}^{(1)} + \langle v, \psi_{kl}^{(2)} \rangle \phi_{kl}^{(2)} \right) \begin{pmatrix} \psi_{mn}^{(1)} \\ \psi_{mn}^{(2)} \end{pmatrix} d\theta dr \right) \phi_{mn} \\
&= \sum_{m=0, n=1}^{\infty} e^{\int_r^t \lambda_{mn}(\tau) d\tau} \\
&\quad \times \left(\int_{\Omega} \sum_{k, l=0}^{\infty} e^{\int_s^r \lambda_{kl}(\tau) d\tau} \begin{pmatrix} \langle v, \psi_{kl}^{(1)} \rangle \phi_{kl}^{(1)} \psi_{mn}^{(1)} + \langle v, \psi_{kl}^{(2)} \rangle \phi_{kl}^{(2)} \psi_{mn}^{(1)} \\ \langle v, \psi_{kl}^{(1)} \rangle \phi_{kl}^{(1)} \psi_{mn}^{(2)} + \langle v, \psi_{kl}^{(2)} \rangle \phi_{kl}^{(2)} \psi_{mn}^{(2)} \end{pmatrix} d\theta dr \right) \phi_{mn}
\end{aligned}$$

Note that double series terms within the inner product are equal to zero for all $k \neq m$ and $l \neq n$, and equal to 1 for each $k = m$ and $l = n$, due to the orthogonality of the eigenfunctions. Also, for every $k, m = 0, 1, 2, \dots, l, n = 1, 2, 3, \dots$, the inner product of the cross terms $\int_{\Omega} \langle v, \psi_{kl}^{(2)} \rangle \phi_{kl}^{(2)} \psi_{mn}^{(1)} dr d\theta = 0$ and $\int_{\Omega} \langle v, \psi_{kl}^{(1)} \rangle \phi_{kl}^{(1)} \psi_{mn}^{(2)} dr d\theta = 0$, such that:

$$\begin{aligned}
U(t, r)U(r, s)v &= \sum_{m=0, n=1}^{\infty} e^{\int_r^t \lambda_{mn}(\tau) d\tau + \int_s^r \lambda_{mn}(\tau) d\tau} \begin{pmatrix} \langle v, \psi_{mn}^{(1)} \rangle \\ \langle v, \psi_{mn}^{(2)} \rangle \end{pmatrix} \phi_{mn} \\
&= \sum_{m=0, n=1}^{\infty} e^{\int_s^t \lambda_{mn}(\tau) d\tau} \left\langle v, \begin{pmatrix} \psi_{mn}^{(1)} \\ \psi_{mn}^{(2)} \end{pmatrix} \right\rangle \phi_{mn} \\
&= U(t, s)v
\end{aligned}$$

The second identity in (iii) can also be directly verified as follows:

$$\begin{aligned}
\frac{\partial U(t, s)}{\partial t} &= \frac{\partial}{\partial t} \sum_{m=0, n=1}^{\infty} e^{\int_s^t \lambda_{mn}(\tau) d\tau} \langle v, \psi_{mn} \rangle \phi_{mn} \\
&= - \sum_{m=0, n=1}^{\infty} (\alpha_{m,n}^2 - g(t)) e^{\int_s^t \lambda_{mn}(\tau) d\tau} \langle v, \psi_{mn} \rangle \phi_{mn} \\
&= \sum_{m=0, n=1}^{\infty} \lambda_{mn}(t) e^{\int_s^t \lambda_{mn}(\tau) d\tau} \langle v, \psi_{mn} \rangle \phi_{mn} \\
&= A(t)U(t, s)
\end{aligned}$$

From the other side we have:

$$\begin{aligned}
&A(t)U(t, s) \\
&= \sum_{m=0, n=1}^{\infty} \lambda_{mn}(t) \left\langle \sum_{k,l=0}^{\infty} e^{\int_r^t \lambda_{kl}(\tau) d\tau} \langle \cdot, \psi_{kl} \rangle \phi_{mn}, \psi_{mn} \right\rangle \phi_{mn} \\
&= \sum_{m=0, n=1}^{\infty} \lambda_{mn}(t) \\
&\quad \times \left(\int_{\Omega} \sum_{k,l=0}^{\infty} e^{\int_r^t \lambda_{kl}(\tau) d\tau} \left(\langle \cdot, \psi_{kl}^{(1)} \rangle \phi_{kl}^{(1)} + \langle \cdot, \psi_{kl}^{(2)} \rangle \phi_{kl}^{(2)} \right) \begin{pmatrix} \psi_{mn}^{(1)} \\ \psi_{mn}^{(2)} \end{pmatrix} d\theta dr \right) \phi_{mn}
\end{aligned}$$

Similar as in the previous case, we have that:

$$\begin{aligned}
A(t)U(t, s) &= \sum_{m=0, n=1}^{\infty} \lambda_{mn}(t) \left\langle \sum_{k,l=0}^{\infty} e^{\int_r^t \lambda_{kl}(\tau) d\tau} \langle \cdot, \psi_{kl} \rangle \phi_{mn}, \psi_{mn} \right\rangle \phi_{mn} \\
&= \sum_{m=0, n=1}^{\infty} \lambda_{mn}(t) e^{\int_s^t \lambda_{mn}(\tau) d\tau} \langle \cdot, \psi_{mn} \rangle \phi_{mn} \\
&= \frac{\partial}{\partial t} U(t, s)
\end{aligned}$$

2.8 Proof of Proposition 2

From the definition of the operator in Eqs.2.3.21-2.3.22, we have that:

$$\begin{aligned}
Bu &= \sum_{m=0, n=1}^{\infty} \langle B, \psi_{mn} \rangle \phi_{mn} u \\
U(t, s)Bu &= \sum_{m=0, n=1}^{\infty} e^{\int_s^t \lambda_{mn}(\eta) d\eta} \langle B, \psi_{mn} \rangle \phi_{mn} u \\
U(t, s)z &= \sum_{m=0, n=1}^{\infty} e^{\int_0^t \lambda_{mn}(\eta) d\eta} \langle z, \psi_{mn} \rangle \phi_{mn} \\
U(t, s)\mathfrak{A}Bu &= \sum_{m=0, n=1}^{\infty} e^{\int_s^t \lambda_{mn}(\eta) d\eta} \langle \mathfrak{A}(s)B, \psi_{mn} \rangle \phi_{mn} u
\end{aligned}$$

The term involving the derivative of the input is expanded as:

$$\begin{aligned}
\int_0^t U(t, \tau)B\dot{u}(\tau)d\tau &= \int_0^t \sum_{m=0, n=1}^{\infty} e^{\int_{\tau}^t \lambda_{mn}(\eta) d\eta} \langle B, \psi_{mn} \rangle \phi_{mn} \dot{u}(\tau) d\tau \\
&= \sum_{m=0, n=1}^{\infty} \left(\int_0^t e^{-\alpha_{mn}^2(t-\tau)+G(t)-G(\tau)} \langle B, \psi_{mn} \rangle \dot{u}(\tau) d\tau \right) \phi_{mn} \\
&= \sum_{m=0, n=1}^{\infty} \left(e^{-\alpha_{mn}^2 t + G(t)} \int_0^t e^{\alpha_{mn}^2 \tau - G(\tau)} \dot{u}(\tau) d\tau \right) \langle B, \psi_{mn} \rangle \phi_{mn} \\
&= \sum_{m=0, n=1}^{\infty} \left[\left(u(t) - u(0) e^{\int_0^t \lambda_{mn}(\eta) d\eta} \right) \right. \\
&\quad \left. + \int_0^t \lambda_{mn}(\tau) e^{\int_{\tau}^t g(\eta) d\eta} u(\tau) d\tau \right] \langle B, \psi_{mn} \rangle \phi_{mn}
\end{aligned}$$

Combining Eqs.2.3.24 and the expression above, the mild solution is given by:

$$\begin{aligned}
z(t) &= \sum_{m=0, n=1}^{\infty} \left(u(t) - u(0) e^{\int_0^t \lambda_{mn}(\eta) d\eta} \right) \langle B, \psi_{mn} \rangle \phi_{mn} \\
&+ \sum_{m=0, n=1}^{\infty} e^{\int_0^t \lambda_{mn}(\eta) d\eta} \langle z_0, \psi_{mn} \rangle \phi_{mn} \\
&- \sum_{m=0, n=1}^{\infty} \left[\left(u(t) - u(0) e^{\int_0^t \lambda_{mn}(\eta) d\eta} \right) + \right. \\
&\quad \left. \int_0^t \lambda_{mn}(\tau) e^{\int_{\tau}^t g(\eta) d\eta} u(\tau) d\tau \right] \langle B, \psi_{mn} \rangle \phi_{mn} \\
&+ \int_0^t \sum_{m=0, n=1}^{\infty} e^{\int_{\tau}^t \lambda_{mn}(\eta) d\eta} \langle \mathfrak{A}(\tau) B, \psi_{mn} \rangle \phi_{mn} u(\tau) d\tau \\
&+ \int_0^t U(t, \tau) q(\tau) d\tau
\end{aligned}$$

Rearranging terms gives that:

$$\begin{aligned}
z(t) &= U(t, 0) z_0 + \int_0^t U(t, \tau) q(\tau) d\tau \\
&+ \sum_{m=0, n=1}^{\infty} \int_0^t e^{\int_{\tau}^t \lambda_{mn}(\eta) d\eta} u(\tau) \left[\langle \mathfrak{A}(\tau) B, \psi_{mn} \rangle - \lambda_{mn}(\tau) \langle B, \psi_{mn} \rangle \right] \phi_{mn} d\tau
\end{aligned}$$

To demonstrate that the above equation is well defined for every $u(t) \in L^2([0, T]; \mathcal{U})$, recall that $g(t), q(t) \in L^2([0, T]; \mathcal{Z})$, $B \in L^2(\Omega)$, $D(\mathfrak{A}(t)) \subset L^2(\Omega)$. Moreover, from Fig.2.1(d), the generation term $g(t) \leq g(0) + Mt$ for all $0 \leq \tau \leq s \leq T < \infty$ where M is a finite positive constant and $g(0)$ is the initial generation. Note that the operator $\mathfrak{A}(t)$ defined in Eq.2.3.15 can be represented as $\mathfrak{A}(t) = \mathfrak{A} + g(t)$ such that $\mathfrak{A}B = b_{\text{ctr}}(\theta)(4 + \mu(\theta))/(2\beta + 1)$ and $g(t)B = g(t)b_{\text{ctr}}(\theta)r^2/(2\beta + 1)$, from Eq.2.3.3, and $\lambda_{mn}(t) = -\alpha_{mn}^2 + g(t)$, from

Eq.2.3.21. Then by substituting these terms into the above equation yields:

$$z(t) = U(t, 0)z_0 + \int_0^t U(t, \tau)q(\tau)d\tau + \sum_{m=0, n=1}^{\infty} \int_0^t e^{\int_{\tau}^t \lambda_{mn}(\eta)d\eta} u(\tau) [\langle \mathfrak{A}B, \psi_{mn} \rangle + \alpha_{mn}^2 \langle B, \psi_{mn} \rangle] \phi_{mn} d\tau$$

Integrating over $t \in [0, T]$ and appealing to the Hölder inequality, we have that:

$$\left| \int_0^t e^{\int_{\tau}^t \lambda(\eta)d\eta} u(\tau) d\tau \right|^2 \leq \frac{1}{2} \sqrt{\frac{\pi}{M}} \exp \left\{ \frac{(-\alpha_{mn}^2 + g(0) + Mt)^2}{M} \right\} \times \left[\operatorname{erf} \left(\frac{\alpha_{mn}^2 - g(0)}{\sqrt{M}} \right) + \operatorname{erf} \left(\frac{-\alpha_{mn}^2 + g(0) + Mt}{\sqrt{M}} \right) \right] \int_0^t |u(\tau)|^2 d\tau$$

where $\operatorname{erf}(x) = 2/\sqrt{\pi} \int_0^x \exp(-\xi^2) d\xi$ is the error function. Since $-1 \leq \operatorname{erf} x \leq 1$ for all $x \in \mathbb{R}$, then we have that:

$$\left| \int_0^t e^{\int_{\tau}^t \lambda(\eta)d\eta} u(\tau) d\tau \right|^2 \leq \frac{1}{2} \sqrt{\frac{\pi}{M}} \exp \left\{ \frac{(-\alpha_{mn}^2 + g(0) + MT)^2}{M} \right\} \int_0^t |u(\tau)|^2 d\tau$$

for all $0 \leq \tau \leq t \leq T$, and therefore $z(t)$ is well defined for every $u(t) \in L^2([0, T]; \mathcal{U})$.

Bibliography

- [1] Ng J, Dubljevic S. Boundary control synthesis for a lithium-ion battery thermal regulation problem. *AIChE Journal*. 2013;
- [2] Lu L, Han X, Li J, Hua J, Ouyang M. A review on the key issues for lithium-ion battery management in electric vehicles. *Journal of Power Sources*. 2013;226(0):272 – 288.
- [3] Balakrishnan P, Ramesh R, Kumar TP. Safety mechanisms in lithium-ion batteries. *Journal of Power Sources*. 2006;155(2):401 – 414.
- [4] Wang Q, Ping P, Zhao X, Chu G, Sun J, Chen C. Thermal runaway caused fire and explosion of lithium ion battery. *Journal of Power Sources*. 2012; 208(0):210 – 224.
- [5] Gu W, Wang C. Thermal-Electrochemical Modeling of Battery Systems. *Journal of The Electrochemical Society*. 2000;147(8):2910–2922.
- [6] Chen S, Wan C, Wang Y. Thermal analysis of lithium-ion batteries. *Journal of Power Sources*. 2005;140(1):111 – 124.
- [7] Bandhauer T, Garimella S, Fuller T. A Critical Review of Thermal Issues in Lithium-Ion Batteries. *Journal of the Electrochemical Society*. 2011; 158(3):R1–R25.
- [8] Rao Z, Wang S. A review of power battery thermal energy management. *Renewable and Sustainable Energy Reviews*. 2011;15(9):4554 – 4571.
- [9] Ray WH. *Advanced Process Control*. New York: McGraw-Hill. 1981.

- [10] Atwell JA, King BB. Proper Orthogonal Decomposition for Reduced Basis Feedback Controllers for Parabolic equations. *Mathematical and Computer Modeling*. 2001;33:1–19.
- [11] Smyshlyaev A, Krstic M. Explicit formulae for boundary control of parabolic PDEs. *Lecture Notes In Control & Information Sciences*. 2004; 301:231–249.
- [12] Krstic M. *Boundary Control of PDEs: A Course on Backstepping Designs*. Philadelphia, PA, USA: Society for Industrial and Applied Mathematics. 2008.
- [13] Christofides PD, Daoutidis P. Finite-dimensional control of parabolic PDE systems using approximate inertial manifolds. *J Math Anal Appl*. 1997;216:398–420.
- [14] Christofides PD. *Nonlinear and Robust Control of PDE Systems: Methods and Applications to Transport-Reaction Processes*. Boston: Birkhäuser. 2001.
- [15] Orlov Y, Utkin V. Sliding mode control in indefinite-dimensional systems. *Automatica*. 1987;23(6):753 – 757.
- [16] Curtain RF, Zwart H. *An introduction to infinite-dimensional linear systems theory*. New York, NY, USA: Springer-Verlag New York, Inc. 1995.
- [17] Garcia MR, Vilas C, Banga JR, Alonso AA. Exponential observers for distributed tubular (bio)reactors. *AIChE Journal*. 2008;54(11):2943–2956.
- [18] Pazy A. *Semigroups of Linear Operators and Applications to Partial Differential Equations*. New York, U.S.A.: Springer-Verlag. 1983.

- [19] McOwen R. *Partial differential equations: methods and applications, 2nd ed.* USA: Prentice Hall. 2002.
- [20] Tanabe H. *Functional analytic methods for partial differential equations.* New York: Marcel Dekker Inc. 1997.
- [21] Evans L. *Partial differential equations.* USA: American Mathematical Society. 1998.
- [22] Williford RE, Viswanathan VV, Zhang JG. Effects of entropy changes in anodes and cathodes on the thermal behavior of lithium ion batteries. *Journal of Power Sources.* 2009;189(1):101 – 107.
- [23] Reynier Y, Graetz J, Swan-Wood T, Rez P, Yazami R, Fultz B. Entropy of Li intercalation in Li_xCoO_2 . *Phys Rev B.* 2004;70:174304.
- [24] Reynier Y, Yazami R, Fultz B. Thermodynamics of lithium intercalation into graphites and disordered carbons. *Journal of The Electrochemical Society.* 2004;151(3):A422–A426.
- [25] Jeon DH, Baek SM. Thermal modeling of cylindrical lithium ion battery during discharge cycle. *Energy Conversion and Management.* 2011; 52(89):2973 – 2981.
- [26] Delmon D, Froment G. *Catalyst Deactivation.* Amsterdam, Netherlands: Elsevier Science Publishers. 1987.
- [27] Weitsman Y. Diffusion with time-varying diffusivity, with application to moisture-sorption in composites. *Journal of Composite Materials.* 1976; 10(3):193–204.

- [28] Forgez C, Do DV, Friedrich G, Morcrette M, Delacourt C. Thermal modeling of a cylindrical LiFePO₄/graphite lithium-ion battery. *Journal of Power Sources*. 2010;195(9):2961 – 2968.
- [29] Smyshlyaev A, Krstic M. Backstepping observers for a class of parabolic PDEs. *Systems & Control Letters*. 2005;54(7):613 – 625.
- [30] Ramdani K, Tucsnak M, Weiss G. Recovering the initial state of an infinite-dimensional system using observers. *Automatica*. 2010; 46(10):1616 – 1625.
- [31] Bensoussan A, Prato GD, Delfour M, Mitter S. *Representation and Control of Infinite Dimensional Systems*. Boston: Birkhäuser. 2007.
- [32] Berg Md, Cheong O, Kreveld Mv, Overmars M. *Computational Geometry: Algorithms and Applications*. Santa Clara, CA, USA: Springer-Verlag, 3rd ed. 2008.
- [33] Ichikawa A, Ryan E. Sensor and controller location problems for distributed parameter systems. *Automatica*. 1979;15(3):347 – 352.
- [34] Kubrusly C, Malebranche H. Sensors and controllers location in distributed systems - A survey. *Automatica*. 1985;21(2):117 – 128.

Chapter 3

Control of parabolic PDEs with time-varying spatial domain: Czochralski crystal growth process

The material presented in this chapter is partially published in [1, 2], and has been accepted in whole as the following:

[3] J. Ng, Ilyasse Aksikas and S. Dubljevic, “Control of parabolic PDEs with time-varying spatial domain: Czochralski crystal growth process,” *International Journal of Control*, 2013

3.1 Introduction

Many important industrial processes such as tubular reactors, metal casting, annealing, and crystal growth involve chemical reactions, phase transitions and deformations in the synthesis and treatment of the materials. The changes in

the state and/or shape of the material during its processing regime, or other time-dependent property of the system, introduce complexities in the modelling of the transport phenomena using partial differential equations (PDEs). Within this broad collection of systems is a class of free boundary problem which includes the well-known two-phase Stefan problem that is used to describe the melting or solidification of a material [4, 5], and the problems arising in the study of thermal combustion and the general dynamics of flames [6]. In these cases the changes in the domain boundary at the solid-liquid or solid-gas interface are due to the interphase dynamics between the two complementary regions.

In contrast to the aforementioned types of free boundary problems, another class of moving boundary problem arises in processes where the domain boundary changes according to some extraneous force acting on the material. One can consider an annealing process as a prototypical example whereby a solid slab is drawn from or pushed into a liquid medium, so that the spatial domain boundary at the solid-liquid interface changes according to the force applied by the mechanical actuator. The models of the temperature or concentration dynamics for this class of moving boundary problems are derived from first-principles continuum mechanics via the Transport Theorem for spatial domains with moving boundaries, and energy balance relations [7]. This approach to the model development yields a general class of convection-diffusion-reaction PDE defined on time-dependent spatial domain which is characterized by the presence of the boundary velocity as a time-dependent coefficient associated with first-order convective-transport terms. As a result, the temperature or concentration dynamics are unidirectionally coupled with the spatial domain boundary motion.

It has been noted that PDE systems defined on time-dependent spatial domains are inherently non-autonomous even if the PDEs do not contain time-dependent coefficients [8]. On the other hand, the class of PDE considered in this work also contains the time-dependent boundary velocity term which contributes to the overall system dynamics, and which subsequently vanish if the boundary motion ceases. There are many works which consider nonautonomous parabolic systems arising from PDEs with fixed spatial domains [9, 10, 11, 12]. In general, the solutions of nonautonomous systems are expressed in terms of two-parameter semigroups which inherit many of the properties of the standard one-parameter semigroups generated by time-invariant parabolic operators. The results have been extended to distributed and boundary control problems including linear quadratic regulator synthesis for general nonautonomous parabolic systems [13, 14]. There are a few number of recent works which have been dedicated to the study of parabolic PDEs on time-dependent spatial domains. In these studies, a variety of approaches have been taken to establish existence and regularity properties of solutions including the utilization of transformations which map the system onto a new fixed spatial domain [15, 16, 17], while others have described the time evolution of the spatial domain via continuously differentiable diffeomorphisms [8, 18]. Methods employed in several other works utilize variational and approximation methods to obtain results on the existence, uniqueness and regularity of solutions [19, 20], while providing a general function space setting in which to study the PDE operators in the context of infinite-dimensional systems theory. Several other works have considered the control problem based on parabolic PDE models with time-dependent spatial domains, using nonlinear and robust control methods. However, only relatively few works have considered the control problem for PDEs defined on time-dependent spatial domains [21, 22, 23].

In this work, we consider the optimal control of a general class of convection-diffusion-reaction parabolic PDEs defined on a time-varying spatial domain, which is characterized by the unidirectional coupling of the underlying spatial domain boundary motion to the temperature or concentration dynamics. The functional analytic description of the PDE with time-dependent coefficients, which is defined on the time-dependent spatial domain with moving boundary, yields the associated representation as an abstract linear nonautonomous parabolic evolution system on an appropriately defined infinite-dimensional function space. The analysis of the parabolic evolution operator enables the representation of solutions to the linear system from the perspective of operator semigroups so that the optimal control problem can be handled by using the tools of time-varying infinite-dimensional systems theory. The optimal control problem is considered in the context of the Czochralski (CZ) crystal growth process which is utilized for the production of semiconductor materials for the microelectronics industry [24, 25, 26]. In this process large boules of single crystals are growth from a melt via solidification at the crystal-melt interface. The product quality is affected by fluctuations in the crystal temperature around a desired nominal distribution. To the authors knowledge, the optimal control of the crystal temperature in the context provided in this present work has not been studied.

This chapter is organized as follows: In Section 3.2 the function space setting which reflects the domain's time-varying nature is introduced. The class of parabolic PDEs defined on the time-dependent spatial domain is introduced in the Section 3.3 along with the CZ crystal temperature model. The functional analytic description of the parabolic PDE and representation as a nonautonomous parabolic evolution system is provided in Section 3.4. The

optimal control problem is considered in the Section 3.5. Numerical simulation results are provided in Section 3.6 and demonstrate the effectiveness of the regulator in the optimal stabilization of the temperature distribution in the crystal domain with moving boundary. Finally, Section 3.7 concludes this work with a brief summary of results.

3.2 Preliminaries

This section provides a brief description of the function space setting in which the class of parabolic PDE defined on a time-varying spatial domain will be considered [27, 19, 20, 28, 29].

Let $\{\Omega_t\}$ be a family of continuous open bounded subsets of \mathbb{R}^m where Ω_t varies in time $t \in [0, T]$ according to the motion of the boundary $\partial\Omega_t$. The variation of the sets is assumed to be C^2 -continuous in time and regular such that the domain is never divided or penetrated. For Ω and Γ defined as:

$$\Omega = \bigcup_{t \in [0, T]} \Omega_t \times \{t\}, \quad \Gamma = \bigcup_{t \in [0, T]} \partial\Omega_t \times \{t\} \quad (3.2.1)$$

let $\mathbf{\Omega}$ denote a fixed open set in \mathbb{R}^m with smooth boundary $\partial\mathbf{\Omega}$ where $\Omega_t \subset \mathbf{\Omega}$ for all $t \in [0, T]$, and such that the cylinder $\mathbf{\Omega} \times [0 \times T]$ contains Ω . For each $t \in [0, T]$, the set of all k -times continuously differentiable functions in $\Omega_t = \{\xi \in \mathbb{R}^m : (\xi, t) \in \Omega\}$, is denoted by $C^k(\Omega_t)$, where k a non-negative integer. The m-tuple of nonnegative integers $\alpha = (\alpha_1, \dots, \alpha_m)$ is a multi-index, $|\alpha| = \alpha_1 + \dots + \alpha_m$ and $D^\alpha = \partial^{|\alpha|} / (\partial \xi_1^{\alpha_1} \dots \partial \xi_m^{\alpha_m})$ is the distributional partial derivative. For $f \in C^k(\Omega_t)$ the functional $\|\cdot\|_{k,p}$, $1 \leq p < \infty$ is defined

as:

$$\|f\|_{k,p} = \left(\int_{\Omega_t} \sum_{|\alpha| \leq k} |D^\alpha f|^p d\xi \right)^{1/p} \quad (3.2.2)$$

The Banach space $H^{k,p}(\Omega_t)$ is the completion of $\{f \in C^k(\Omega_t) : \|f\|_{k,p} < \infty\}$ with respect to the norm in Eq.3.2.2. The Hilbert space $H^{0,2}(\Omega_t) = L^2(\Omega_t)$ is equipped with the inner product:

$$\langle f, g \rangle = \int_{\Omega_t} fg d\xi \quad \text{for } f, g \in L^2(\Omega_t), \quad (3.2.3)$$

Let $\{\phi(t)\}$ denote a family of functions defined on the subdomains Ω_t for every $t \in [0, T]$ which form an orthonormal basis of $L^2(\Omega_t)$ for every $t \in [0, T]$, and define the complement $\Omega_t^c := \{\xi \in \mathbb{R}^m : \xi \in \Omega \setminus \Omega_t\}$ such that:

$$\phi(\xi, t) = \begin{cases} \phi(\xi) & \text{for } \xi \in \Omega_t \\ 0 & \text{for } \xi \in \Omega_t^c \end{cases} \quad (3.2.4)$$

In this way, the family of Hilbert spaces $L^2(\Omega_t)$ are precompact in $L^2(\Omega)$, generalized as $L^2(\Omega_t) \subset L^2(\Omega)$, and enables the use of the inner product function on $L^2(\Omega)$ where:

$$\langle \phi(t), \phi(t) \rangle_{L^2(\Omega)} = \int_{\Omega} \phi(\xi, t) \phi(\xi, t) d\xi = \int_{\Omega} \phi(\xi) \phi(\xi) d\xi + \int_{\Omega_t^c} 0 d\xi = \langle \phi, \phi \rangle_{L^2(\Omega_t)}$$

Spaces involving functions of time $0 \leq s \leq t \leq T$ and taking values in a Banach space \mathcal{Z} are denoted as: $C^k([s, t], \mathcal{Z}) := \{f : [s, t] \rightarrow \mathcal{Z} \mid f \text{ is } C^k\text{-continuous}\}$, and $L^2([s, t], \mathcal{Z}) := \{f : [s, t] \rightarrow \mathcal{Z} \mid f \text{ is measurable and, } (\int_s^t \|f(t)\|^2 dt)^{1/2} < \infty\}$. The Banach space of bounded linear operators from \mathcal{Z} to \mathcal{Y} is denoted $\mathcal{L}(\mathcal{Z}, \mathcal{Y})$ where $\mathcal{L}(\mathcal{Z}, \mathcal{Z}) = \mathcal{L}(\mathcal{Z})$.

3.3 Parabolic PDE on time-dependent spatial domain

The class of parabolic PDE on time-dependent spatial domains considered in this work arises from the continuum mechanics approach to the model formulation via the *Transport Theorem* together with standard balance principles [7], and yields a class of convection-diffusion-reaction PDE characterized by the presence of the boundary velocity in the PDE expression, which is associated with a first order convective transport term. The model formulation is provided in the following section [17].

3.3.1 Model formulation

Let Ω be a simple body in \mathbb{R}^3 (i.e. $m = 3$) with material points, $X = \{X_1, X_2, X_3\} \in \Omega$, volume element dX and smooth boundary $\partial\Omega$, spatial points $\xi = \{\xi_1, \xi_2, \xi_3\} \in \mathbb{R}^3$ and volume element $d\xi$. Let Ω_0 be the initial configuration and $\Omega_t \subset \mathbb{R}^3$ be the configuration at time $t \in [0, T]$, so that simple motion (material velocity motion-deformation) from one body configuration to another one can be described by introducing the following well defined mapping.

Definition 3.3.1. The regular motion of Ω is determined by the continuous mapping $\varphi_t : \Omega \rightarrow \mathbb{R}^3$ such that $\xi = \varphi_t(X)$ and $\Omega_t = \varphi_t(\Omega)$, with continuous inverse, $\varphi_t^{-1} : \varphi_t(\Omega) \rightarrow \Omega$. The material velocity of the motion $\mathbf{V} : \Omega \rightarrow \mathbb{R}^3$ is defined by

$$\mathbf{V}(X, t) = \mathbf{V}_t(X) = \frac{\partial \varphi}{\partial t}(X, t) = \frac{d}{dt} \varphi_X(t) \quad (3.3.1)$$

The spatial velocity of motion $\mathbf{v} : \varphi_t(\Omega) \rightarrow \mathbb{R}^3$ defines the spatial velocity field $\mathbf{v}(\xi, t)$ with relation $\mathbf{v}(\xi, t) = \mathbf{V}_t \circ \varphi_t^{-1}$.

The regularity of the motion defined in Definition 3.3.1 presumes that Ω is never divided or penetrated. Moreover, Definition 3.3.1 gives that the evolution of Ω is described by the semi-flow ($t \geq 0$) property. In other words, there is a collection of maps $\varphi_{t,s}$ such that for each s and z , the integral curve of flow $t \mapsto \varphi_{t,s}(X)$ is given by $\varphi_{t,s} \circ \varphi_{s,r} = \varphi_{t+r}$ for all r, s, t , such that the configuration Ω_t at time $t \in [0, T]$ can be described in terms of a fixed configuration by change of variables [7]. Utilizing these general results, the *Transport Theorem* for a time-dependent spatial domain is given as follows.

Proposition 3. Let $z(\xi, t)$ be the bounded and continuous function on Ω for all $t \in [0, T]$, and continuous on $\partial\Omega_t$, which represents the temperature. The rate of change of $z : \Omega_t \times [0, T] \rightarrow \mathbb{R}$ with respect to time in Ω_t is expressed as

$$C_p \frac{d}{dt} \int_{\Omega_t} \rho(\xi, t) z(\xi, t) d\xi = C_p \int_{\Omega_t} \rho(\xi, t) \left(\frac{\partial z}{\partial t}(\xi, t) + \mathbf{v}(\xi, t) \cdot \nabla z(\xi, t) \right) d\xi \quad (3.3.2)$$

where the density $\rho : \Omega_t \times [0, T] \rightarrow \mathbb{R}$ is bounded $C^1(\Omega_t)$ and satisfies $\frac{\partial \rho}{\partial t}(\xi, t) + \nabla \cdot \rho(\xi, t) \mathbf{v}(\xi, t) = 0$, (conservation of mass), and the specific heat capacity C_p is constant.

Proof. The Jacobian of $\varphi_t(X)$ is the determinant of the deformation gradient, i.e. $J(X, t) = \det \left(\frac{\partial \varphi}{\partial X}(X, t) \right)$ and $\frac{\partial J}{\partial t}(X, t) = \nabla \cdot \mathbf{v}(\xi, t) J(X, t)$. Under the assumption that mass is conserved in Ω_t then $\frac{D\rho}{Dt}(\xi, t) + \rho(z, t) \nabla \cdot \mathbf{v}(\xi, t) = 0$ where $\frac{D(\cdot)}{Dt} = \partial_t(\cdot) + \mathbf{v} \cdot \nabla(\cdot)$ is the material derivative operator, and by change

of variables

$$\begin{aligned}
\frac{d}{dt} \int_{\varphi_t(\Omega)} \rho(\xi, t) z(\xi, t) dv &= \frac{d}{dt} \int_{\Omega} \rho(\varphi_t, t) z(\varphi_t, t) J(X, t) dX \\
&= \int_{\Omega} \left(\frac{D\rho}{Dt}(\varphi_t, t) z(\varphi_t, t) J(X, t) + \right. \\
&\quad \left. \rho(\varphi_t, t) \frac{Dz}{Dt}(\varphi_t, t) J(X, t) + \rho(\varphi_t, t) z(\varphi_t, t) \frac{\partial J}{\partial t}(X, t) \right) dX \\
&= \int_{\Omega} \rho(\varphi_t, t) \left(\frac{\partial z}{\partial t}(\varphi_t, t) + \mathbf{v}(\varphi_t, t) \cdot \nabla z(\varphi_t, t) \right) J(X, t) dX
\end{aligned}$$

where Ω is fixed such that the differentiation and integration operations may be interchanged. Changing the variables back to ξ gives the result in Eq.3.3.2. \square

Recall that the *Conservation Law* describes the total heat balance in Ω_t as

$$C_p \frac{d}{dt} \int_{\Omega_t} \rho z d\xi = \int_{\partial\Omega_t} \kappa \nabla z \cdot \nu ds + \int_{\Omega_t} g z d\xi$$

where ν is the normal component of the surface element $ds \in \partial\Omega_t$, κ is the thermal conductivity of the material, and $g : \Omega \times t \rightarrow \mathbb{R}$ is a continuous function which represents the linearized internal reaction-generation factor. Substituting the expression in Eq.3.3.2 to the L.H.S. and the application of the *Divergence theorem* for the integral over $\partial\Omega_t$ yields

$$C_p \int_{\Omega_t} \rho \left(\frac{\partial z}{\partial t} + \mathbf{v} \cdot \nabla z \right) d\xi = \int_{\Omega_t} \nabla \cdot (\kappa \nabla z) d\xi + \int_{\Omega_t} g z d\xi \quad (3.3.3)$$

One can note that $\kappa \nabla z$ relates the flux over the boundary to the difference between z and the bulk temperature z_B , which gives the generalized boundary

condition on $\partial\Omega_t$

$$\int_{\partial\Omega_t} \kappa \nabla z \, ds = C_p \int_{\partial\Omega_t} \rho \mathbf{v} \cdot (z - z_B) \, ds \quad (3.3.4)$$

From Eqs.3.3.3-3.3.4, the initial and boundary value problem describing the dynamics of the temperature distribution in a region Ω_t undergoing deformation along a velocity field $\mathbf{v}(\xi, t)$ is given by

$$\begin{aligned} C_p \rho \frac{\partial z}{\partial t} &= \nabla \cdot (\kappa \nabla z) - C_p \rho \mathbf{v} \cdot \nabla z + gz & \text{in } \Omega \\ \kappa \nabla z &= C_p \rho \mathbf{v} \cdot (z - z_B) & \text{on } \Gamma \\ z &= z_0 & \text{in } \Omega_0 \end{aligned} \quad (3.3.5)$$

where $z(\xi, 0) = z_0(\xi)$ is the initial temperature distribution of the body Ω_0 . One can note in Eq.3.3.5 that the convective transport phenomena given by

$$\mathbf{v} \cdot \nabla z = \frac{d\xi_i}{dt} \frac{\partial z_i}{\partial \xi_j}, \quad i, j = \{1, 2, 3\}$$

arises from the domain deformation [7], and vanishes if the motion of Ω is isochronic, i.e. Ω_t is constant for all $t \in [0, T]$. For the case in which the material coordinates are fixed and only boundary undergoes motion, the velocity field along which the boundary moves is a function of time $\mathbf{v} = \mathbf{v}(t)$ or a constant $\mathbf{v} = v$ when the boundary velocity does not change. In the case when the boundary is time invariant, $\mathbf{v} = 0$, Ω_t is fixed for all $t \in [0, T]$, and the above expression leads to the well known reaction-diffusion parabolic PDE system with fixed domain since neither internal material points nor the boundary undergo motion. In the remainder of the chapter, we consider the boundary motion as function of time, i.e. $\mathbf{v} = \mathbf{v}(t)$.

The previous assumption of conservation of mass which has been included in the model derivation has another physical interpretation which is that the density of the material entering (or leaving) the body is equal to the density of the material present in the body (or across its boundary). In this case, one can consider the density as a constant term in the expression of the Transport Theorem in the Eq.3.3.2 and the subsequent initial and boundary value problem in the Eq.3.3.5. In the remainder of the chapter, we will follow this interpretation and consider the material density as a constant.

In general, one needs to introduce the most general type of boundary conditions in the form provided in Eq.3.3.5 in order to account for the transport of heat or concentration across the boundary interface which impacts the temperature or concentration inside the material region. Also, one might consider a combination of boundary conditions which reflect the process setup. However, in this work, we relax this restriction and consider the boundary conditions to be of homogeneous Neumann type which represent zero-flux across the boundary interfaces.

3.3.2 General class of PDE

The general class of initial and boundary value problem in the Eq.3.3.5 with natural boundary conditions given as homogeneous Neumann boundary conditions is formally given by:

$$\begin{aligned}
 \frac{\partial z(\xi, t)}{\partial t} + A(\xi, t)z(\xi, t) &= f(\xi, t) && \text{in } \Omega \\
 \frac{\partial z(\xi, t)}{\partial \nu} &= 0, && \text{on } \Gamma \\
 z(\xi, 0) &= z_0(\xi) && \text{in } \Omega_0
 \end{aligned} \tag{3.3.6}$$

where $z : \Omega_t \times [0, T] \rightarrow \mathbb{R}$ represents the temperature within the region Ω_t with initial value $z_0 \in L^2(\Omega_0)$, ν is the outward normal vector to $\xi \in \Gamma$, and $f \in C^r([0, T], L^2(\Omega))$, $r \geq 0$, is a prescribed non-homogeneous term. The operator $A(\xi, t)$ is defined as:

$$A(\xi, t)z := - \sum_{i,j=1}^m \frac{\partial}{\partial \xi_i} \left(a^{ij}(\xi, t) \frac{\partial z}{\partial \xi_j} \right) + \sum_{i=1}^m v^i(t) \frac{\partial z}{\partial \xi_i} + g(\xi, t)z \quad (3.3.7)$$

The coefficients $a(\xi, t) \in L^2(\Omega)$, $\mathbf{v}(t) \in \mathbb{R}^m$, and $g(\xi, t) \in L^2(\Omega)$ describe the heterogeneous thermal conductivity or diffusivity of the material, boundary velocity, and linearized reactionary generation or consumption, respectively.

We assume that the operator in the Eq.3.3.7 satisfies the following:

- E1. The operator $A(\xi, t)$ is uniformly elliptic, i.e. there exists $\varepsilon > 0$ such that $\forall (\xi, t) \in \Omega$:

$$\sum_{i,j=1}^m a^{ij}(\xi, t) \boldsymbol{\eta}_i \boldsymbol{\eta}_j \geq \varepsilon |\boldsymbol{\eta}|^2, \quad \forall \boldsymbol{\eta} \in \mathbb{R}^m \quad (3.3.8)$$

- E2. The coefficients $\alpha^{ij} = \{a^{ij}(\xi, t), v^i(t), c(\xi, t)\}$ are further assumed to be sufficiently Hölder continuous in time, i.e. for $s, t \in [0, T]$, and constants $L > 0$ and $\beta \in (0, 1]$:

$$|\alpha^{ij}(\xi, t) - \alpha^{ij}(\xi, s)| \leq L |t - s|^\beta \quad (3.3.9)$$

The first-order terms $\partial/\partial \xi_i$ gives the vector field along which $\partial\Omega_t$ flows such that $\mathbf{v}(t) \cdot \nabla z = \sum_{i=1}^m v^i(t) \partial z / \partial \xi_i$ represents the convective transport which is due to the motion of the domain boundary. This first-order term characterizes the class of operators in the Eq.3.3.7 and arises from the Transport Theorem

on time-dependent spatial domains given in the Eq.3.3.2.

3.3.3 CZ crystal temperature model

The class of PDE defined in the Eq.3.3.6 defined on time-dependent spatial domain includes the PDE utilized to describe crystal temperature distribution of the CZ crystal growth process depicted in Fig.3.1 [25, 26]. For simplicity, we consider the 1-dimensional model on the time-dependent spatial domain $\Omega_t = (0, l(t))$:

$$\text{Pe} \frac{\partial z}{\partial t} = \nabla \cdot \kappa_r \nabla z - \text{Pe} v(t) \frac{\partial z}{\partial \xi} + b(\xi, t) u(t) \quad (3.3.10)$$

where $z(\xi, t)$ is the crystal temperature, and the control term $b(\xi, t)u(t)$ represents the heat input along the crystal length. The Peclet number $\text{Pe} =$

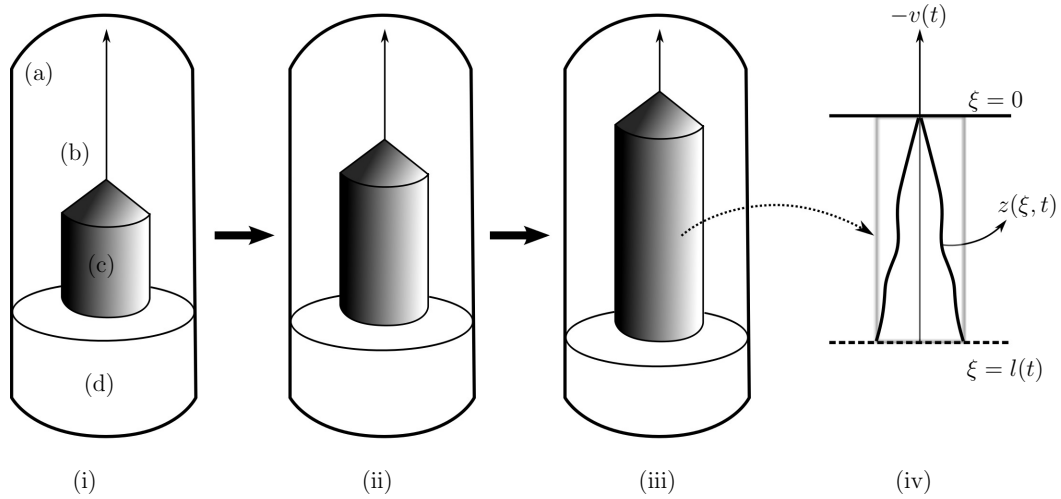


Figure 3.1: CZ crystal growth process with components (a) furnace, (b) pulling arm, (c) crystal, and (d) melt. Subfigures (i)-(iii) depict the crystal growth over different time instances inside of the furnace. Subfigure (iv) depicts the crystal temperature distribution $z(\xi, t)$ on the interval $\xi \in [0, l(t)]$. The boundary velocity $v(t)$ at $\xi = l(t)$ is in the opposite direction of the crystal pulling.

$\rho C_p v_0 R_c / \kappa_s$ is a dimensionless positive constant, with ρ , C_p , v_0 , R_c and κ_s denoting the crystal density, heat capacity, nominal growth rate, crucible radius, and thermal conductivity, respectively, and $\kappa_r = \kappa_c / \kappa_s$ is the scaled thermal conductivity ratio with κ_c denoting the crystal conductivity. The model in the Eq.3.3.10 is similar to the crystal temperature model used in [25] and [26] with the exception that $\kappa_r(z) = \kappa_r$ is taken as a constant in this work as it is assumed that the thermal effects on the crystal conductivity are negligible due to the high crystal purity. The evolution of the crystal length $l(t)$ is determined by the action of a mechanical pulling arm which draws the crystal from a pool of melt. The dynamics of the mechanical actuator are governed, see for example [21], by the second order ordinary differential equation:

$$M(t) \frac{d^2 \hat{l}(t)}{dt^2} + c \frac{d\hat{l}(t)}{dt} + a\hat{l}(t) = f_{\text{mec}}(t) \quad (3.3.11)$$

where $l(t) = \hat{l}(t) + \varepsilon$, $\varepsilon > 0$, $l(t) \in (0, l_{\text{max}})$, $M(t)$ is the crystal mass which increases as the crystal grows, $a, c > 0$ are the finite coefficients of elasticity and dampening of the rigid body system, and the input to this mechanical subsystem is the finite and continuous force $f_{\text{mec}}(t)$ applied by the actuator. The crystal pull rate at the side of the pulling arm at $\xi = 0$ determines the velocity of the boundary at the side of the melt at $\xi = l(t)$ such that $v(t) = -dl(t)/dt$.

One can then note that the PDE in the Eq.3.3.10 is unidirectionally coupled through the boundary velocity $v(t)$ to the mechanical actuator drawing the crystal from the melt, i.e. the crystal temperature dynamics does not determine the rate of pulling such that the Eq.3.3.10 is a linear PDE with the time-dependent coefficient.

Remark 3.3.2. The 1-dimensional PDE model is a simplification of the 3-dimensional physical system and provides for the controller synthesis to focus on the stabilization of the temperature gradient along the crystal length from the side of the melt at $\xi = l(t)$ to the side of the pulling arm at $\xi = 0$. Utilizing this simplification also enables the system to be represented as a distributed control problem, with input along the crystal length, rather than having to consider the boundary control problem which introduces several complexities related to having the input applied along the radius of the crystal.

3.4 Infinite-dimensional system representation

The initial and boundary value problem in the Eq.3.3.6 defined on the time-dependent spatial domain is represented as an abstract nonautonomous evolution system in the following way. Consider the strongly elliptic operator $A(\xi, t)$ in the Eq.3.3.7 which is associated with the family of linear operators $A(t)$, $t \in [0, T]$, with the domain:

$$D(A(t)) := H^{1,2}(\Omega) \cap H^{2,2}(\Omega) \quad (3.4.1)$$

For $z(t) \in D(A(t))$ we define:

$$A(t)z := A(\xi, t)z \quad (3.4.2)$$

The initial and boundary value problem in the Eq.3.3.6 is represented as a nonautonomous evolution system on the state space $L^2(\Omega)$:

$$\frac{dz(t)}{dt} = A(t)z(t) + f(t), \quad z(0) = z_0 \quad (3.4.3)$$

where $z_0 \in L^2(\Omega_0)$ denotes the initial state. In the case where the operator $A(t) = A$ is time-invariant, the solution of the nonhomogeneous initial value problem in the Eq.3.4.3 is expressed in terms of the one-parameter semigroup $\mathcal{S}(t), t \geq 0$ of bounded linear operators on $L^2(\Omega)$ which is generated by the operator $A : D(A) \rightarrow L^2(\Omega)$. In contrast to the autonomous case, the expression of the solution of the Eq.3.4.3 is given in terms of a two-parameter semigroup $U(t, s), 0 \leq s \leq t \leq T$. First we note that for each $t \in [0, T]$, the domain $D(A(t)) := H^{1,2}(\Omega_t) \cap H^{2,2}(\Omega_t)$ is dense in $L^2(\Omega_t) \subset L^2(\Omega)$. It is demonstrated in [30] that the assumptions E1 and E2 of the operator $A(\xi, t)$ yield the following properties of the associated operator $A(t)$:

P1. For every $t \in [0, T]$, the resolvent $R(\lambda, A(t)) = (\lambda - A(t))^{-1}$ exists for all λ in the resolvent set $\rho(A(t)) \supset S_\delta := \{\lambda \in \mathbb{C} \mid \arg \lambda < \delta, \delta \in (\pi/2, \pi]\} \cup \{0\}$ with $\operatorname{Re} \lambda \leq 0$, and there exists a positive constants L_1 and C such that:

$$\|R(\lambda, A(t))\| \leq \frac{L_1}{|\lambda| + C} \quad (3.4.4)$$

P2. For every $s, t, \tau \in [0, T]$ there exist constants $L_2 > 0$ and $\alpha \in (0, 1]$ such that:

$$\|(A(t) - A(s))A(\tau)^{-1}\| \leq L_2|t - s|^\alpha \quad (3.4.5)$$

By [30, Chapter 5.6, Theorem 6.1,], there exists a unique solution to the nonautonomous parabolic evolution equation in the Eq.3.4.3 which is expressed in terms of a two-parameter semigroup of operators.

Definition 3.4.1. A two-parameter semigroup $U(t, s)$, $0 \leq s \leq t \leq T$ is a family of bounded linear operators on $L^2(\Omega)$ which satisfies:

- i) $\|U(t, s)\| \leq C$ where C is a positive constant;
- ii) $(t, s) \rightarrow U(t, s)$ is continuous in the uniform operator topology for $0 \leq s \leq t \leq T$;
- iii) For $0 \leq s \leq r \leq t \leq T$:

$$U(t, t) = I, \quad U(t, s) = U(t, r)U(r, s);$$

and for $0 \leq s \leq t \leq T$:

$$\frac{\partial U(t, s)}{\partial t} = A(t)U(t, s), \quad \frac{\partial U(t, s)}{\partial s} = -U(t, s)A(s);$$

The two-parameter semigroup $U(t, s)$ is often referred to as an evolution operator due to the property *iii*) in Definition 3.4.1. The solution of the nonhomogeneous Cauchy problem in the Eq.3.4.3 is then expressed as:

$$z(t) = U(t, s)z(s) + \int_s^t U(t, \tau)f(\tau)d\tau \quad (3.4.6)$$

for all $0 \leq s \leq t \leq T$ and $z(s) \in L^2(\Omega_s)$.

Having the above properties and system representation, let us now consider PDE model of the CZ crystal temperature dynamics given in the Eq.3.3.10. In particular, the abstract properties P1 and P2 can be verified so that the optimal control problem can be considered in the following section. We consider that the boundary conditions imposed on the Eq.3.3.10 are homogenous

Neumann boundary conditions:

$$\frac{\partial z}{\partial \xi}(0, t) = 0, \quad \frac{\partial z}{\partial \xi}(l(t), t) = 0 \quad (3.4.7)$$

We recall that the model corresponds to the class of PDE system given in the Eq.3.3.6 with the second-order term of the operator $A(\xi, t)$ given by $\kappa_0(\partial^2/\partial \xi^2)$, where $\kappa_0 = \kappa_r/\text{Pe}$. The solution of $\det(\kappa_0 - \hat{\varepsilon}) = 0$ is $\hat{\varepsilon} = \kappa_0 > 0$, such that the operator $A(\xi, t)$ of the Eq.3.3.10 satisfies the strong ellipticity condition E1. Moreover, the time-varying term is given by the boundary velocity and governed by the second order ODE given in the Eq.3.3.11 such that $v(t) \in C^1([0, T])$ and satisfies E2. The operator $A(\xi, t)$ is associated with the family of operators:

$$A(t)z := \kappa_0 \frac{d^2 z}{d\xi^2} - v(t) \frac{dz}{d\xi} \quad (3.4.8)$$

with domain:

$$D(A(t)) = \left\{ z \in L^2(\Omega) : z, \frac{dz}{d\xi} \in L^2(\Omega) \text{ are a.c.}, \right. \\ \left. \frac{d^2 z}{d\xi^2} \in L^2(\Omega) \text{ and } \frac{dz}{d\xi}(0) = 0, \frac{dz}{d\xi}(l(t)) = 0 \right\} \quad (3.4.9)$$

where a.c. means absolutely continuous. Utilizing the standard transformation found in [31] and [32] the operator $A(t)$ is rewritten as:

$$A_S(t)z = \frac{1}{r(\xi, t)} \frac{d}{d\xi} \left(p(\xi, t) \frac{dz}{d\xi} \right) + q(\xi, t)z \quad (3.4.10)$$

where:

$$r(\xi, t) := \exp\left(-\frac{v(t)}{\kappa_0}\xi\right), \quad p(\xi, t) = \kappa_0 r(\xi, t), \quad q(\xi, t) = 0 \quad (3.4.11)$$

One can observe that for each $t \in [0, T]$ the operator $A_S(t) = A(t)$ in the Eq.3.4.8 is the negative of a Sturm-Liouville operator which implies the following.

Proposition 4. For each $t \in [0, T]$, the operator $A(t)$ in the Eq.3.4.8 is the infinitesimal generator of a C_0 -semigroup of bounded linear operators $A(t) : D(A(t)) \subset L^2(\Omega_t) \rightarrow L^2(\Omega_t)$.

The eigenvalues of $A(t)$ in the Eq.3.3.10 and the adjoint operator $A^*(t) = \kappa_0(d^2/d\xi^2) + v(t)(d/d\xi)$ are determined for each $t \in [0, T]$ as:

$$\lambda_n(t) = -\kappa_0 \left(\frac{n\pi}{l(t)} \right)^2 - \frac{1}{2\kappa_0} \frac{v(t)^2}{2} \quad (3.4.12)$$

For each $t \in [0, T]$, the eigenvalues in the Eq.3.4.12 are real, simple and discrete, such that the spectrum $\sigma(A(t))$ consists of isolated eigenvalues $\{\lambda_n(t)\}_{n=1}^{\infty}$ with finite multiplicity and no finite accumulation points, $\lambda(t) < 0$ and $\{0\} \notin \sigma(A(t))$. The corresponding eigenfunctions of $A(t)$ are determined as:

$$\begin{aligned} \phi_n(\xi, t) = \\ A_n(t) \exp\left(\frac{v(t)}{2\kappa_0}\xi\right) \left(\cos\left(\frac{n\pi}{l(t)}\xi\right) - \frac{v(t)}{2\kappa_0(n\pi/l(t))} \sin\left(\frac{n\pi}{l(t)}\xi\right) \right) \end{aligned} \quad (3.4.13)$$

The coefficients:

$$A_n(t) = \sqrt{\frac{2}{l(t)}} \left(1 + \left(\frac{v(t)}{2\kappa_0(n\pi/l(t))} \right)^2 \right)^{-\frac{1}{2}} \quad (3.4.14)$$

orthonormalize $\phi_n(\xi, t) = \{\phi_n(t)\}_{t \in [0, T]}$ with respect to the family of adjoint eigenfunctions $\psi_n(\xi, t) = \{\psi_n(t)\}_{t \in [0, T]}$ determined as:

$$\psi_n(\xi) = \exp\left(-\frac{v(t)}{\kappa_0}\xi\right) \phi_n(\xi, t) \quad (3.4.15)$$

For each $t \in [0, T]$, the eigenfunctions $\{\phi_n(t)\}_{t \in [0, T]}$ and $\{\psi_n(t)\}_{t \in [0, T]}$ form a *Riesz basis* of $L^2(\Omega_t)$, continuously satisfy the boundary conditions given in the Eq.3.4.7, and each forms a one dimensional eigenspace. By [33] for each $t \in [0, T]$ the operator $A(t)$ is the infinitesimal generator of a C_0 -semigroup denoted here as $\mathcal{S}_t(s)$, $s \geq 0$, such that $A(t)$ is closed and densely defined on $L^2(\Omega_t)$ for each $t \in [0, T]$ and the resolvent $R_\mu(A(t), \mu) = (A(t) - \mu)^{-1}$ is compact for $\mu \in \rho(A(t))$ where the resolvent set is defined as $\rho(A(t)) := \{\lambda(t) \in \mathbb{C} : (A(t) - \lambda(t)) \text{ is one to one } (A(t) - \lambda(t))^{-1} : D(A(t)) \rightarrow D(A(t)) \text{ is bounded}\}$. Furthermore, $\mathcal{S}_t(s)$ is injective, i.e. for $z \in L^2(\Omega_t)$, $\mathcal{S}_t(s)z = 0$ implies that $z = 0$ which means that $\mathcal{S}_t(s)$ is invertible and $A(t)^{-1}$ exists [34]. One can observe from the expression in the Eq.3.4.12 that the eigenvalues are negative for each $s \in [0, T]$, $v(t) \neq 0$ such that:

$$\|\mathcal{S}_t(s)\| \leq Ce^{\omega s}, \quad \omega = \sup_{\substack{n \geq 1 \\ s \in [0, T]}} \text{Re}(\lambda_n(s)) < 0 \quad (3.4.16)$$

for constant $C \geq 0$, which implies the system is stable for every $0 \leq s \leq t \leq T$.

Remark 3.4.2. One can notice that the moving boundary is manifested in the expression of the eigenvalues in Eq.3.4.12 which are associated with the dynamics of the system. In particular, the domain length $l(t)$ and $v(t)$ each appear as time-varying terms in the expression and it is interesting to notice the contribution of the term $v(t)^2/2$ which resembles the kinetic energy expression. In the case that the domain motion ceases, i.e. $l(t) = l$ and

$v(t) = 0$ the eigenvalues in the Eq.3.4.12 and the associated eigenfunctions in the Eq.3.4.13, each simplify to the respective expressions of eigenvalues and eigenfunctions which correspond to the Laplacian operator given by the Eq.3.4.8 with $v(t) = 0$. That is, $\lambda_n = (n\pi/l)^2$, $\phi_n = \psi_n = \sqrt{2/l} \cos(n\pi\xi/l)$, and $A(t) = A$ is the infinitesimal generator of the one-parameter semigroup:

$$\mathcal{S}(t-s)z(s) = \sum_{n=1}^{\infty} e^{-\kappa_0(n\pi/l)^2(t-s)} \langle z(s), \phi_n \rangle \phi_n \quad (3.4.17)$$

where $\mathcal{S}(t)$, $t \geq 0$ is the C_0 -semigroup of operators on $L^2(\Omega)$ which is associated with the standard heat equation.

Proposition 5. For all $t \in [0, T]$ the operator $A(t)$ in the Eq.3.4.8 satisfies the properties P1 and P2.

Let the projection on the n^{th} eigenfunction at time t be denoted as $E_n(\cdot) = \langle \cdot, \psi(t) \rangle \phi_n(t)$. For each $t \in [0, T]$ and $z \in D(A(t))$:

$$\begin{aligned} R_\mu(A(t), \mu)z &= (A(t) - \mu)^{-1}z \\ &= \sum_n (\lambda_n(t) - \mu)^{-1} E_n(z) \\ &\leq \max_{t \in [0, T]} (\lambda_n(t) - \mu)^{-1} \sum_n E_n(z) \\ &= \max_{t \in [0, T]} (\lambda_n(t) - \mu)^{-1} z \end{aligned} \quad (3.4.18)$$

Then there exist positive constants L and k such that:

$$\|(A(t) - \mu)^{-1}\| \leq L(\mu - k)^{-1} \quad (3.4.19)$$

which verifies the property P1. It follows that there exists a sector:

$$S_\omega = \{\lambda \in \mathbb{C} : |\arg \lambda| < \frac{\pi}{2} + \omega\} \setminus \{0\}, \quad \omega \in (0, \pi/2] \quad (3.4.20)$$

contained in $\rho(A(t))$ such that $\sigma(A(t)) \subset \mathbb{C} \setminus S_\omega$, which means that $A(t)$ is a *sectorial operator* for every $t \in [0, T]$. Then for all $t \in [0, T]$, $A(t)$ infinitesimal generator of a family of analytic semigroups on $L^2(\Omega)$ [12].

The property P2 is verified by again noting that $\{0\} \notin \sigma(A(t))$, and that $A(t)$ has bounded inverse for all $t \in [0, T]$, i.e. $A(\tau)^{-1} \leq L_1$ with constant $L_1 > 0$. Since $v(t) \in C^1([0, T])$, direct calculation yields:

$$\begin{aligned} \|(A(t) - A(s))A(\tau)^{-1}z\|_{0,2} &\leq L_1\|(v(s) - v(t))\nabla z\|_{0,2} \\ &\leq L_2|t - s|^\beta\|\nabla z\|_{0,2} \\ &\leq L_3|t - s|^\beta\|z\|_{1,2} \end{aligned} \quad (3.4.21)$$

which demonstrates that the property P2 is satisfied. Furthermore, it is clear that $\lim_{t \rightarrow T} \|(A(t) - A(T))A(0)^{-1}\| = 0$. Then by [30, Chapter 5.8, Theorem 8.1,], the operator $U(t, s)$ also satisfies:

$$\|U(t, s)\| \leq Ce^{-\sigma(t-s)} \quad (3.4.22)$$

for constants $C \geq 0$ and $\sigma > 0$.

Finally, the infinite-dimensional system representation of parabolic PDE model of the CZ crystal temperature regulation problem in the Eq.3.3.10 is given by:

$$\frac{dz}{dt} = A(t)z + B(t)u, \quad z(0) = z_0 \quad (3.4.23)$$

where $A(t)$ is the nonautonomous linear operator defined in the Eq.3.4.8 on the state space $\mathcal{Z} = L^2(\Omega)$. We assume that the space of inputs is a separable Hilbert space denoted as \mathcal{U} and assume that $u(t) \in L^2([0, T], \mathcal{U})$ and denote the operator $B(t) \in C([0, T], \mathcal{L}(\mathcal{U}, \mathcal{Z}))$ associated with $b(\xi, t) \in L^2(\Omega_t)$ for every $t \in [0, T]$. By Proposition 5 and by [30, Chapter 5.6, Theorem 6.1], there exists a unique two-parameter semigroup $U(t, s)$, $0 \leq s \leq t \leq T$ defined in Definition 3.4.1 which is associated with the operator $A(t)$ defined in the Eq.3.4.8. Then the solution of the nonautonomous linear system in the Eq.3.4.23 is expressed as:

$$z(t) = U(t, s)z_s + \int_s^t U(t, \tau)B(\tau)u(\tau)d\tau \quad (3.4.24)$$

In the following section we utilize the above abstract results as foundation for the optimal control synthesis with the application to the CZ crystal temperature regulation problem.

Remark 3.4.3. One can consider the more general case of the boundary conditions for the CZ crystal temperature problem:

$$\kappa \frac{\partial z}{\partial \xi}(0, t) = 0, \quad \kappa_0 \frac{\partial z}{\partial \xi}(l(t), t) - v(t)z(l(t), t) = 0 \quad (3.4.25)$$

In this case, for each $t \in [0, T]$, the eigenvalues are determined as solutions μ_n of the transcendental equation:

$$\tan(\mu_n l(t)) = \frac{4\kappa_0 \mu_n v(t)}{v(t)^2 - 4\kappa_0^2 \mu_n^2} \quad (3.4.26)$$

which for each $t \in [0, T]$ yields a discrete eigenspectrum with corresponding eigenfunctions similar to the expression in the Eq.3.4.13. The coefficient $v(t)$ in the Eq.3.4.25 implies that $D(A(t))$ is time-dependent not only with

respect to the domain motion at $\xi = l(t)$, but also with respect to the coefficients present at the boundary, i.e. $D(A(t)) = \{z \in L^2(\Omega), z \text{ and } dz/d\xi \in L^2(\Omega) \text{ are a.c., and } (dz/d\xi)(0) = 0, \kappa_0(dz/d\xi)(l(t)) - v(t)z(l(t)) = 0\}$. The case of time-dependent operator domain $D(A(t))$ with respect to time-dependent coefficients present in the imposed boundary conditions is studied in [12], and requires the satisfaction of properties additional to the properties P1 and P2 (Section 3.4) in order to prove the existence of the two-parameter semigroup associated with general nonautonomous parabolic operators [12, Chapter 6, and references therein].

3.5 The optimal control problem

The finite-time horizon optimal control problem associated with the Eq.3.4.23 is given as the minimization of the cost functional:

$$J(z_0; 0, T, u) = \int_0^T (|C(\tau)z(\tau)|^2 + |Ru(\tau)|^2) d\tau + \langle z(T), Qz(T) \rangle \quad (3.5.1)$$

over all inputs $u \in L^2([0, T], \mathcal{U})$ subject to the Eq.3.4.23. The operator $Q \in \mathcal{L}(\mathcal{Z})$ is self-adjoint and nonnegative and $R \in \mathcal{U}$ is coercive. The output measurements $y(t) = C(t)z(t)$ are related to the states via the operator $C(t) \in C([0, T], \mathcal{L}(\mathcal{Z}, \mathcal{Y}))$ where \mathcal{Y} is a separable Hilbert space. The optimization problem has the unique minimizing solution $u^{\min}(t)$ such that the optimal pair $u^{\min}(t) \in C([0, T]; \mathcal{U})$ and $z^{\min}(t) \in C^1([0, T]; \mathcal{Z}) \cap C([0, T]; D(A(t)))$ are related by the feedback formula:

$$u_{t \in [0, T]}^{\min}(t) = -R^{-1}B^*(t)\Pi(t)z_{\min}(t) \quad (3.5.2)$$

with the optimal cost related to the initial state as $J(z_0; 0, T, u^{\min}) = \langle \Pi(0)z_0, z_0 \rangle$.

The operator $\Pi(t) \in \mathcal{L}(\mathcal{Z})$ is the strongly continuous, self adjoint, nonnegative solution of the differential Riccati equation:

$$\begin{aligned} \frac{d}{dt}\Pi(t) + A^*(t)\Pi(t) + \Pi(t)A(t) \\ - \Pi(t)B(t)R^{-1}B^*(t)\Pi(t) + C^*(t)C(t) = 0 \end{aligned} \quad (3.5.3)$$

with final condition $\Pi(T) = Q$ [35]. The mild form expression of the Eq.3.5.3 is given in terms of $U(t, s)$ as:

$$\begin{aligned} \Pi(t)z = & U^*(T, t)QU(T, t)z_0 + \int_t^T U^*(\tau, t)C^*(\tau)C(\tau)U(\tau, t)z d\tau \\ & - \int_t^T U^*(\tau, t)\Pi(\tau)B(\tau)R^{-1}B^*(\tau)\Pi(\tau)U(\tau, t)z d\tau \end{aligned} \quad (3.5.4)$$

Having the above expressions for the operator $\Pi(t)$, we consider the optimal control problem for the CZ crystal temperature regulation problem in this context. First, one can note that the operator $A(t)$ in the Eq.3.4.8 is non-self adjoint for $v(t) \neq 0$. The eigenfunctions $\phi_n(t), n \in \mathbb{N}$ in the Eq.3.4.13 is the set of eigenfunctions of $A(t)$ which form an orthonormal basis of $L^2(\Omega_t)$ for each $t \in [0, T]$, and correspond to the family of eigenvalues $\lambda_n(t)$ in the Eq.3.4.12. Similarly, the eigenfunctions of the adjoint $A^*(t)$ are denoted $\psi_n(t), n \in \mathbb{N}$, and are related to $\phi(t)$ by the weight function $r(\xi, t)$ such that $\phi(t) = r(\xi, t)\psi(t)$ and $\langle \phi_n(t), \psi_m(t) \rangle_r = \int_{\Omega_t} r(\xi, t)\phi_n(t)\phi_m(t)d\xi = \delta_{nm}$ where $\delta_{nm} = 1$ if $n = m$ and $\delta_{nm} = 0$ otherwise, for each $t \in [0, T]$. We consider the differential Riccati

equation in the Eq.3.5.3 in the inner product form:

$$\begin{aligned} & \frac{d}{dt} \langle \phi_n(t), \Pi(t) \phi_m(t) \rangle_r + \langle A(t) \phi_n(t), \Pi(t) \phi_m(t) \rangle_r \\ & + \langle \phi_n(t), \Pi(t) A(t) \phi_m(t) \rangle_r + \langle C(t) \phi_n(t), C(t) \phi_m(t) \rangle_r \\ & - \langle \Pi(t) B(t) R^{-1} B^*(t) \Pi(t) \phi_n(t), \phi_m(t) \rangle_r = 0 \end{aligned} \quad (3.5.5)$$

with $\langle \phi_n(T), \Pi(T) \phi_m(T) \rangle_r = \langle \phi_n(T), Q \phi_m(T) \rangle_r$. For simplicity, let $R = I$, $B(t) = I$ and $C(t) = I$, so the Eq.3.5.5 becomes the system of infinitely many quadratic, nonlinear and nonautonomous ordinary differential equations:

$$\dot{\Pi}_{nn}(t) + 2\lambda_n(t)\Pi_{nn}(t) - \Pi_{nn}^2(t) + 1 = 0 \quad (3.5.6)$$

with final value $\Pi_{nn}(T) = Q_{nn}$. In order to solve the nonlinear ODE in the Eq.3.5.6, we first reorder the time index by taking $\tau = T - t$ so that the Eq.3.5.6 becomes an initial value problem with the initial value $\Pi_{nn}(0) = Q$, and secondly apply Radon's Lemma [36] which yields the time-varying linear system:

$$\frac{d}{dt} \begin{pmatrix} V \\ W \end{pmatrix} = \begin{pmatrix} -\lambda_n(\tau) & 1 \\ 1 & \lambda_n(\tau) \end{pmatrix} \begin{pmatrix} V \\ W \end{pmatrix} \quad (3.5.7)$$

with initial values $V(0) = 1$ and $W(0) = Q_{nn}$. If $(V \ W)^T$ is a solution of the Eq.3.5.7 then $WV^{-1} = \Pi_{nn}(t)$ is a solution of the Eq.3.5.6. There is a large number of works on the existence and properties of solutions to the general differential Riccati equation in Eq.3.5.3 and in the form of the Eq.3.5.7 [36, see, for example,]. An explicit solution for $\Pi_{nn}(t)$ can be readily determined for the Eqs.3.5.6-3.5.7 in the case of autonomous systems [34]. In contrast, the present nonautonomous case does not admit such an analytic solution which

is due to the time-dependence of the eigenvalues $\lambda_n(t)$ of the operator $A(t)$ which appear in the Eqs.3.5.6-3.5.7. However, one can notice that each of the time-varying terms for the domain length $l(t)$ and the boundary velocity $v(t)$ appear in the expression of $\lambda(t)$ in the Eq.3.4.12, and because the solution operator $\Pi(t)$ is determined from the Eqs.3.5.6-3.5.7 which are dependent on the eigenvalues $\lambda_n(t)$, then the optimal control law in the Eq.3.5.2 is influenced by the underlying spatial domain motion itself.

Remark 3.5.1. One can consider a different type of control problem for the PDE system in the Eq.3.3.6 in which the distributed control within the domain is replaced by boundary actuation. That is, the boundary condition imposed on the PDE in the Eq.3.3.6 is given by:

$$\frac{\partial z}{\partial \nu} = u(\xi, t) \quad \text{on } \Gamma \quad (3.5.8)$$

which corresponds to the Neumann boundary control problem with input function $u(\xi, t)$ applied at $\partial\Omega$ of the time-dependent spatial domain. Several works including [10, 13] have considered this type of control formulation and the associated optimal control problem for nonautonomous parabolic systems on fixed spatial domains [14, 35, see, for example,]. The boundary control setup introduces several complexities arising from the definition of the input on the time-varying boundary. Additional regularity assumptions are required of the PDE system, operator coefficients, and the spatial domain itself [14]. The reconciliation of these results towards the present formulation of the PDE on time-dependent spatial domain and associated nonautonomous evolution system representation is omitted in this work.

3.6 Numerical results

In order to demonstrate the application of the regulator formulation for the CZ crystal temperature control problem, we consider a situation in which there exists a perturbation of the crystal temperature around a desired distribution. The control objective is to stabilize the temperature at the nominal zero distribution by utilizing the optimal control law determined in the previous sections. The crystal pulling is realized by standard finite-dimensional optimal control synthesis applied to the system in the Eq.3.3.11, with $M = 1.95$, $c = 2.5$ and $a = 2$. The crystal is being drawn from a melt at a velocity $v(t)$ such that spatial domain change is due to the motion of the boundary at the melt side, $\xi = l(t)$. The evolution of the domain length $l(t)$ and the boundary velocity $v(t)$ is depicted in Fig.3.2 with simulation time interval taken as $t \in [0, 100]$ which represents 10 minutes of processing time. The initial crystal length at $t = 0$ is 15.84 cm with a dimensionless value of $l(0) = 2.64$ units. The total change in the crystal length during the simulation time interval is 0.16 units or 0.96 cm, such that at $t = 100$ the final length of the crystal is $l(100) = 2.8$ units or 16.8 cm, which gives an average growth rate of 5.76 cm per hour during the simulation time [25].

The Galerkin method is implemented in the modal decomposition of the PDE system in the Eq.3.3.10 utilizing a finite set of $N = 10$ basis functions chosen as the time-dependent set of eigenfunctions in the Eqs.3.4.13-3.4.15 [21]. Increasing N did not result in a significant change in the system dynamics. The Peclet number and scaled thermal conductivity ratio in the Eq.3.3.10 are given by $Pe = 0.1$ and $\kappa_r = 0.175$, respectively [24]. The input operator $B(t) = B \in \mathcal{L}(\mathbb{R}, L^2(0, l(t)))$ is parameterized by the function $b(\xi) = (1/2\varepsilon)\hat{\delta}_{[\xi_c-\varepsilon, \xi_c+\varepsilon]}$ where $\hat{\delta}_{[a,b]} = 1$ for $a < \xi < b$ and $\hat{\delta}_{[a,b]} = 0$ otherwise [34]. The fixed input

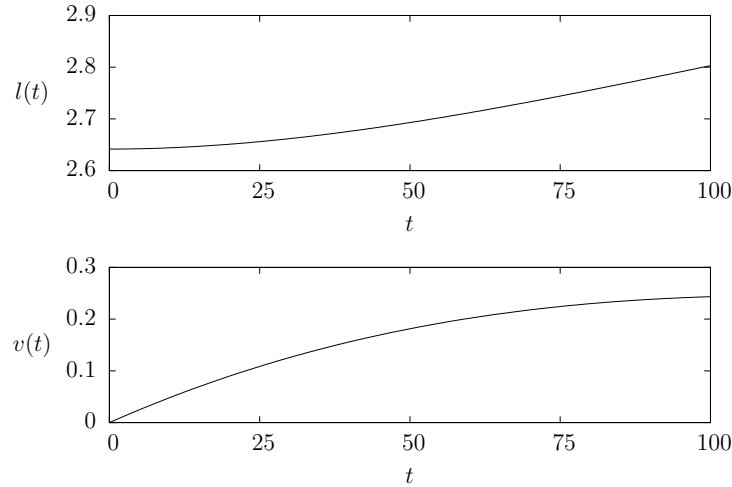


Figure 3.2: Crystal length $l(t)$ and boundary velocity $v(t)$.

location is taken at $\xi_c = 0.875$. Similarly, the output operator $C(t) = C \in \mathcal{L}(L^2(0, l(t)), \mathbb{R})$ is parameterized by a similar function $c(\xi)$ and the output measurements are taken at $\xi_o = 2.00$. The optimal input in the Eq.3.5.2 is calculated from the solution of the Eq.3.5.3 with parameters $Q = 75 I_{N_c \times N_c}$ and $R = 0.05$. The first $N_c = 3$ modes were utilized in the calculation in order to synthesize a low-dimensional controller and prevent the occurrence of the peaking phenomenon due to high-gain feedback [37]. The crystal temperature evolution $z(\xi, t)$ is shown in the Fig.3.4 with stationary boundary at $\xi = 0$ and moving boundary at $\xi = l(t)$ having the profile shown in the Fig.3.2.

The initial temperature distribution at $t = 0$ shows a gradient along the crystal length with a higher temperature on the side of the melt at $\xi = l(t)$ relative to the side at $\xi = 0$. One can see from the Fig.3.4 the influence of the input around the input location at $\xi_c = 0.875$ on the temperature distribution throughout the domain. The calculated input profile $u(t)$ decreases for all $t \in [1, 100]$ as shown in the Fig.3.3, and one can observe that the input to

the system converges towards zero as the temperature along the crystal length is stabilized around the nominal zero distribution of $z(\xi, t) = 0$. The total energy profiles of the open and closed loop systems is shown in the Fig.3.4 and illustrates the effect of the input on the total system energy evolution relative to the open-loop system with no heat input.

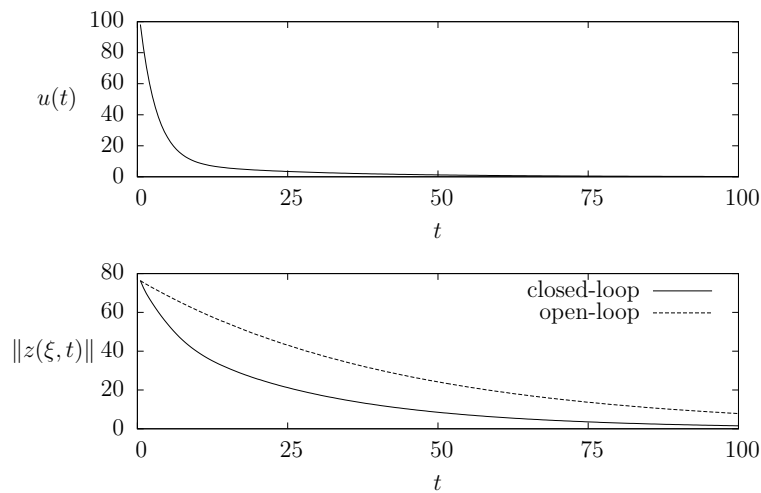


Figure 3.3: (Top) Optimal input applied to the crystal at $\xi_c = 0.875$. (Bottom) Total open and closed loop system energy.

3.7 Summary

In this chapter we have considered the optimal control formulation for a class of PDEs defined on time-dependent spatial domains where the boundary motion is unidirectionally coupled to the dynamics of the convection-diffusion-reaction process. The results presented in this work include the introduction of a function-space framework for time-dependent spatial domains, and the PDE

properties which enable the representation of the control problem as an abstract nonautonomous parabolic evolution system. The analysis of the nonautonomous parabolic operator demonstrate the existence of the associated two-parameter semigroup by which the solutions of the nonautonomous infinite-dimensional system is provided. These results enabled the optimal control problem to be considered in the context of time-varying infinite-dimensional systems theory. The direct application of the results to the Czochralski crystal growth process crystal temperature regulation problem with numerical results demonstrated the effectiveness of the regulator formulation.

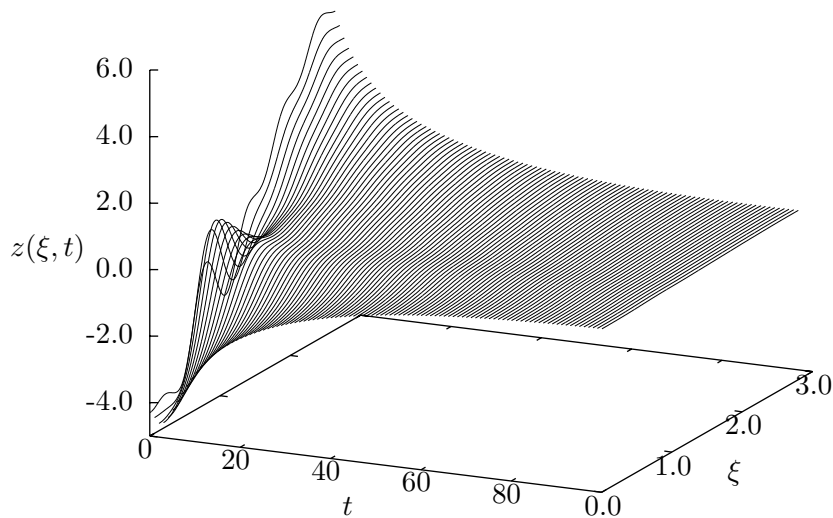


Figure 3.4: Crystal temperature evolution in the time-dependent spatial domain with input applied at $\xi_c = 0.875$.

Bibliography

- [1] Ng J, Dubljevic S. Multiscale dynamics and optimal control of parabolic PDE with time varying spatial domain (crystal growth process). In: *Proceedings of the 19th International Symposium on Mathematical Theory of Networks and Systems*. 2010; pp. 999–1006.
- [2] Ng J, Dubljevic S, Aksikas I. Multiscale optimal control of transport-reaction system with time varying spatial domain. In: *Proceedings of the 49th IEEE Conference on Decision and Control (CDC)*. 2010; pp. 858–863.
- [3] Ng J, Aksikas I, Dubljevic S. Control of parabolic PDEs with time-varying spatial domain: Czochralski crystal growth process. *International Journal of Control*. 2013;0(0):1–12.
- [4] Rubenstein LI. *The Stefan problem*. Providence, R.I.: Amer. Math. Soc. 1971. Translated from the Russian by A. D. Solomon, Trans. of Math. Mono., Vol. 27.
- [5] Dunbar W, Petit N, Rouchon P, Martin P. Motion Planning For A Non-linear Stefan Problem. *ESAIM: Contr Optim and Cal of Var*. 2003;9:275–296.
- [6] Cannon JR, Cavendish JC, Fasano A. A Free Boundary-Value Problem Related to the Combustion of a Solid. *SIAM J Appl Math*. 1985;45(5):798–809.
- [7] Marsden J, Hughes T. *Mathematical Foundations of Elasticity*. New York, U.S.A.: Dover Publications. 1983.

- [8] Kloeden P, Marn-Rubio P, Real J. Pullback attractors for a semilinear heat equation in a non-cylindrical domain. *Journal of Differential Equations*. 2008;244(8):2062 – 2090.
- [9] Kato T. *Perturbation theory for linear operators*. New York: Springer-Verlag. 1966.
- [10] Lasiecka I. Unified theory for abstract parabolic boundary problems: A semigroup approach. *Appl Math & Optim*. 1980;6:287–333.
- [11] Acquistapace P, Terreni B. A unified approach to abstract linear non-autonomous parabolic equations. *Rend Sem Univ Padova*. 1987;78:47–107.
- [12] Tanabe H. *Functional analytic methods for partial differential equations*. New York: Marcel Dekker Inc. 1997.
- [13] Triggiani R. Boundary feedback stabilization of parabolic equations. *Appl Math Optim*. 1980;6:201–220.
- [14] Acquistapace P, Flandoli F, BTerreni. Initial boundary value problems and optimal control for nonautonomous parabolic systems. *SIAM J Math Anal*. 1991;29:89–118.
- [15] Da Prato G, Kunstmann PC, Weis L, Lasiecka I, Lunardi A, Schnaubelt R, Lunardi A. An Introduction to Parabolic Moving Boundary Problems. In: *Functional Analytic Methods for Evolution Equations*, vol. 1855 of *Lecture Notes in Mathematics*, pp. 23–31. Springer Berlin / Heidelberg. 2004;.

- [16] Baconneau O, Lunardi A. Smooth Solutions to a Class of Free Boundary Parabolic Problems. *Transactions of the American Mathematical Society*. 2004;356(3):pp. 987–1005.
- [17] Burdzy C, Chen ZQ, Sylvester J. The heat equation in time dependent domains with insulated boundaries. *Journal of Mathematical Analysis and Applications*. 2004;294(2):581 – 595.
- [18] Kloeden PE, Real J, Sun C. Pullback attractors for a semilinear heat equation on time-varying domains. *Journal of Differential Equations*. 2009;246(12):4702 – 4730.
- [19] Bonaccorsi S, Guatteri G. A Variational Approach to Evolution Problems with Variable Domains. *Journal of Differential Equations*. 2001;175(1):51 – 70.
- [20] Savaré G. Parabolic problems with mixed variable lateral conditions: An abstract approach. *Journal de Mathématiques Pures et Appliquées*. 1997; 76(4):321 – 351.
- [21] Wang PKC. Stabilization and Control of Distributed Systems with Time-Dependent Spatial Domains. *J Optim Theor & Appl*. 1990;65:331–362.
- [22] Armaou A, Christofides PD. Crystal temperature control in the czochralski crystal growth process. *AIChE J*. 2001;47:79–106.
- [23] Armaou A, Christofides PD. Robust Control of Parabolic PDE Systems with Time-Dependent Spatial Domains. *Automatica*. 1999;.
- [24] Derby J, Brown R. Thermal-capillary analysis of Czochralski and Liquid Encapsulated Czochralski Crystal Growth. I. Simulation. *J Cryst Growth*. 1986;74:605–624.

- [25] Derby J, Brown R. On the Dynamics of Czochralski Crystal Growth. *J Cryst Growth*. 1987;83:137–151.
- [26] Derby JJ, Atherton LJ, Thomas PD, Brown RA. Finite-element methods for analysis of the dynamics and control of Czochralski Crystal Growth. *J Sci Comput*. 1987;2:297–343.
- [27] Adams R. *Sobolev Spaces*. New York, U.S.A.: Academic Press. 1978.
- [28] Evans L. *Partial differential equations*. USA: American Mathematical Society. 1998.
- [29] McOwen R. *Partial differential equations: methods and applications, 2nd ed.* USA: Prentice Hall. 2002.
- [30] Pazy A. *Semigroups of Linear Operators and Applications to Partial Differential Equations*. New York, U.S.A.: Springer-Verlag. 1983.
- [31] Ray WH. *Advanced Process Control*. New York: McGraw-Hill. 1981.
- [32] Winkin J, Dochain D, Ligarius P. Dynamical analysis of distributed parameter tubular reactors. *Automatica*. 2000;36:349–361.
- [33] Cedric D, Dochain D, Winkin J. Sturm-Liouville systems are Riesz-spectral operators. *Int J Appl Math Comput Sci*. 2003;13:481–484.
- [34] Curtain RF, Zwart H. *An introduction to infinite-dimensional linear systems theory*. New York, NY, USA: Springer-Verlag New York, Inc. 1995.
- [35] Bensoussan A, Prato GD, Delfour M, Mitter S. *Representation and Control of Infinite Dimensional Systems*. Boston: Birkhäuser. 2007.

- [36] Abou-Kandil H, Freiling G, Ionescu V, Jank G. *Matrix Riccati Equations in Control and Systems Theory*. Systems & control. Germany: Birkhäuser Verlag. 2003.

- [37] Sussmann HJ, Kokotovic PV. The peaking phenomenon and the global stabilization of nonlinear systems. *IEEE Trans Automat Contr*. 1991; 36:424–440.

Chapter 4

Optimal control of convection-diffusion process with time-varying spatial domain: Czochralski crystal growth process

The material presented in this chapter has been published as the following:

- [1] J. Ng and S. Djurjebic, “Optimal control of convection-diffusion process with time-varying spatial domain: Czochralski crystal growth,” *Journal of Process Control*, vol. 21, no. 10, pp. 1361-1369, 2011.

4.1 Introduction

A large number of industrial systems exhibit time-varying features in which certain parameters of the system change over the course of the process. The methods employed in the formation and treatment of materials may result in,

for example, chemical reactions, phase transitions, deformations or a combination of these behaviours, and therefore introduce complexities in model-based controller design. The Czochralski (CZ) crystal growth process, utilized for the production of semiconductor materials for the microelectronics industry, is a prime example in which a time-dependent feature of the system is the change in material domain and is the motivating example behind our study.

In the CZ crystal growth process, large boules of single crystals, typically Si, GaAs, InP, and CdTe, are formed in a thermal environment, whereby a seed crystal is slowly drawn from a pool of melt by a mechanical pulling arm. The material growth by solidification at the crystal-melt interface is affected by variations in the thermal fields of the ambient and melt temperatures, as well as the rate of pulling. These conditions are significant factors which contribute to the overall product quality where the objective of the batch processing strategy is to yield high-purity, defect and dislocation free crystals with constant diameter. The latter specification is vulnerable to fluctuations in heat transfer caused by turbulent convection in the melt environment, and also to longer term disturbances in the ambient temperature and changes in the melt level.

The complexity in modelling the dynamics of the CZ crystal growth process is reflected in the numerous works dedicated to the analyses of the multi-physics system which include studies of the transport phenomena associated with the crystal temperature, crystal-melt interface, melt dynamics, and crystal pull rate. A more complete survey of the modelling and dynamical analyses of the process is contained in the review articles [2, 3], which also describe the uses and challenges in the design and implementation of active control methodologies for single crystal growth. For example, the maintenance of the crystal shape is a subject of considerable interest. Several controlled growth methods

are based on models which incorporate the relationships between the crystal, ambient and melt temperatures, and have led to proposed strategies in which diameter control is achieved via combinations of crucible heater, bottom heater and crystal pull rate actuation [4, 5, 6].

Another important control problem which has garnered less attention is the regulation of the crystal temperature distribution during the process which is important in counteracting the fluctuations in the rate at which the crystal cools which can cause large thermoelastic stresses leading to micro-defect and dislocation generation [7, 8]. The transport phenomena models of the crystal temperature dynamics are determined through mass and energy balance relations which yield parabolic partial differential equations (PDEs) defined on time-varying spatial domains [6]. In the process control field there are several works which consider various model representations and control strategies for parabolic PDEs with time-varying spatial domains along with different control objectives which include the temperature regulation problem using robust control methods [9], the boundary stabilization by manipulation of the temperature field [10], and the inverse Stefan problem in which the boundary evolution is known *a priori* [11]. Another approach considers the optimal stabilization of the temperature distribution of a material, for example in annealing type processes, by varying the spatial domain in which the domain motion is described by a finite-dimensional mechanical subsystem [12, 13].

Motivated by the complexity of the process of crystal growth, in this work we provide a model development for the parabolic PDE on the time-varying spatial domain, and consider the optimal control formulation for the CZ crystal temperature regulation problem. As previously mentioned, it is of interest to control the rate at which the crystal cools in order to prevent material defects and dislocation generation and it is also of interest to stabilize the

rate of pulling around some desired value. Therefore, the optimal regulation of the temperature distribution in the time-varying spatial domain around a pre-specified nominal distribution is required. The system is characterized by the unidirectional coupling of the domain motion, which is determined by the mechanical pulling which draws the crystal from the melt with dynamics described by a second order ODE, to the parabolic PDE system which describes the transient temperature of the crystal region. The controller synthesis for the crystal temperature regulation problem is considered from the perspective of infinite-dimensional systems theory whereby the PDE is represented as an evolutionary equation on an appropriately defined function space with nonautonomous operator which generates a two-parameter semigroup. In this form, the control problem is considered using linear-quadratic optimal control theory for nonautonomous infinite-dimensional systems. To address the issue of practical realization, the finite-dimensional system representation of the PDE system is obtained, and we consider the simultaneous control problem of the crystal temperature regulation and the stabilization of the domain motion around a nominal steady state value. A low order controller for the crystal temperature regulation problem is proposed and numerical results are provided including the comparison of the optimal controller to conventional proportional controllers.

This chapter is organized as follows: In Section 4.2 the boundary evolution due to the mechanical pulling arm is described in terms of a second order ODE and the crystal temperature dynamics are described by a parabolic PDE defined on the time-varying spatial domain. In Section 4.3, the PDE is represented as an abstract evolution equation on an infinite-dimensional space with nonautonomous parabolic operator which generates a two-parameter semigroup. This representation enables the use of time-varying infinite-dimensional

systems theory to pose the time-varying optimal control problem in Section 4.4. In Section 4.5, the finite-dimensional system representation of the PDE is determined and augmented with the mechanical pulling arm subsystem, to facilitate the numerical implementation of the control problem for the temperature regulation and domain motion. The optimal control synthesis of the augmented system is presented and numerical results are provided in Section 4.6. Finally, Section 4.7 concludes the chapter with a summary of results.

4.2 Model description

The crystal region is considered as an axisymmetric and time-varying spatial domain with unit radius $R_c = 1$ and length $l(t)$. The spatial domain motion is due to the crystal pull rate $v(t)$ which determines the growth in the crystal at the boundary $\xi = l(t)$ where $l(t) > 0$ is the crystal length, see Fig.4.1. The boundary evolution is determined by a mechanical actuator pulling the crystal from the melt. In practice the crystal pull rate is slow, and we approximate the dynamics of the mechanical subsystem around some nominal pull rate by the second order ordinary differential equation (ODE) for rigid body mechanics:

$$m_s \frac{d^2 \tilde{l}}{dt^2} + a_d \frac{d\tilde{l}}{dt} + b_e \tilde{l} = f_{\text{mec}} \quad (4.2.1)$$

where m_s , a_d and b_e are finite and represent constant mass, damping, and elastic coefficients of the rigid body system, f_{mec} is the force applied by the actuator, and $\tilde{l}(t)$ is the deviation form of $l(t)$.

The function $z : \Omega \times [0, T] \rightarrow \mathbb{R}$ represents the temperature of the time dependent spatial domain, denoted $\Omega := \{(r, \xi) : 0 < r < 1, 0 < \xi < l(t)\}$ at some time $t \in [0, T]$, around the desired nominal distribution in dimensionless

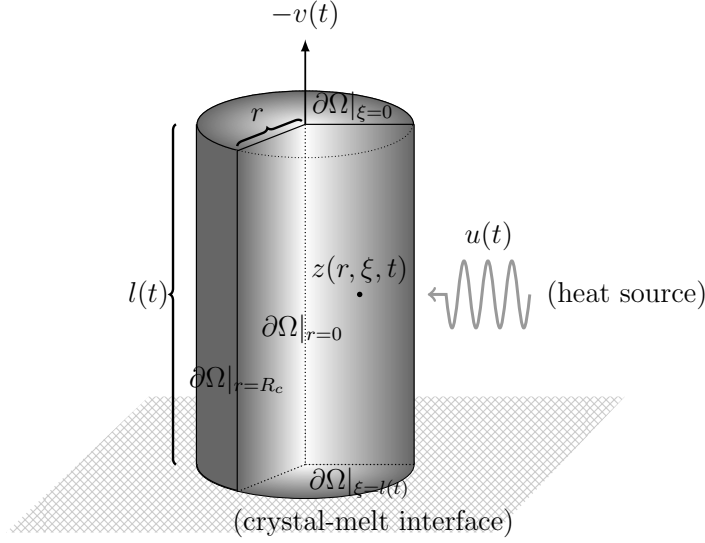


Figure 4.1: Cutaway of general process diagram of axisymmetric cylindrical slab with radius R_c , length $l(t)$, and temperature distribution $z(r, \xi, t)$ for $(r, \xi) \in \Omega$ at time $t \in [0, T]$. The spatial domain time-dependence is due to the change in the boundary at $\partial\Omega|_{z=l(t)}$ which is moving with velocity $v(t)$. The temperature distribution of the slab is regulated by heat input $u(t)$ applied to the boundary at $\partial\Omega|_{r=R_c}$.

form with dynamics described by the parabolic PDE model:

$$\begin{aligned} \text{Pe} \frac{\partial z}{\partial t} &= \nabla \cdot \kappa_s \nabla z - \text{Pe} v(t) \frac{\partial z}{\partial \xi} \quad \text{in } \Omega \times (0, T] \\ z(r, \xi, 0) &= z_0(r, \xi) \quad \text{in } \Omega \end{aligned} \quad (4.2.2)$$

where $z_0(r, \xi)$ is the initial condition. The Peclet number $\text{Pe} = v_0 R_{cruc} C_p \rho_c > 0$ is the dimensionless variable with constants v_0 , R_{cruc} , and C_p denoting the nominal pull rate, scaled crucible radius and crystal specific heat capacity, respectively. It is assumed that as the crystal is pulled from the melt, solidification at the solid-melt interface results in a crystal structure of constant density ρ_c . The Eq.4.2.2, which is derived in the Appendix 4.8, is similar to the model utilized in [6] and [14] with the exception that the scaled thermal conductivity

in these works is a function of the temperature, i.e. $\kappa_s = \kappa_s(z)$. In this work it is assumed that the thermal effects on κ_s are sufficiently small due to the high crystal purity such that κ_s is homogeneous and constant throughout Ω for all $t \in [0, T]$. One can notice that the PDE in the Eq.4.2.2 is characterized by the presence of the boundary velocity term $v(t)$. In particular, the convective transport term $v(t)\partial z/\partial \xi$ is due to the underlying spatial domain motion which vanishes if the domain motion becomes isochronic, and is time-invariant if the pull rate is constant.

The crystal temperature at the crystal-melt interface is assumed to be equal to the melt temperature, and similarly across the crystal-ambient temperature fields [6]. Then the boundary conditions imposed on the Eq.4.2.2 are expressed as:

$$\left. \frac{\partial z}{\partial n} \right|_{\partial \Omega} = 0, \quad \text{on } \partial \Omega \times (0, T] \quad (4.2.3)$$

where n is the unit outward normal to $\partial \Omega$.

Remark 4.2.1. One can impose more general boundary conditions of the Robin type which will not substantially change the results of the subsequent sections except that the eigenfunctions in the Eq.4.3.9 with the associated eigenvalues in the Eq.4.3.11 will not be analytically expressed.

4.3 Infinite-dimensional system representation

The optimal control formulation proposed in the subsequent section requires the representation of the PDE in Eq.4.2.2 as an evolution system on some appropriate Banach space. In order to handle the time-dependence of the spatial domain, the following function space description provides a suitable framework such that the representation of the PDE in Eq.4.2.2 can be handled

using standard infinite-dimensional systems theory.

4.3.1 Function space description

Let \mathcal{Z} and \mathcal{Y} denote two general Banach spaces and $\mathcal{L}(\mathcal{Z}, \mathcal{Y})$ denotes the space of bounded linear operators $\mathcal{T} : \mathcal{Z} \rightarrow \mathcal{Y}$ and $\mathcal{L}(\mathcal{Z}) = \mathcal{L}(\mathcal{Z}, \mathcal{Z})$. At some time $t \in [0, T]$, the spatial domain $\Omega \subset \mathbb{R}^2$ is a bounded open set with smooth boundary $\partial\Omega$. The largest spatial domain configuration is denoted $\mathbf{\Omega} \subset \mathbb{R}^2$ where for all $t \in I_j$, $I_j \subset [0, T]$, there is a sequence of subdomains $\{\Omega_j\} \subset \mathbb{R}^2$ such that $\Omega_{j_1} \subset \Omega_{j_2} \subset \dots \subset \mathbf{\Omega}$ for each j . The space $L^2(\Omega_j)$ of measurable functions $\phi(r, \xi, t)$ and $\psi(r, \xi, t)$ with $\int_{\Omega} |\phi|^2 d\mu < \infty$ at each time $t \in I_j$, is a Hilbert space with inner product:

$$\langle \phi, \psi \rangle_{L^2(\Omega_j)} = \int_{\Omega_j} \alpha_j \phi \psi dr d\xi \quad (4.3.1)$$

where:

$$\alpha_j(t) = \begin{cases} 1 & t \in I_j \\ 0 & t \notin I_j \end{cases} \quad (4.3.2)$$

That is, $L^2(\Omega_j)$ forms a family of function spaces for ϕ and ψ defined for each $t \in I_j$ and is generalized as follows: For spatial domain Ω at some time $t \in [0, T]$ the $L^2(\Omega)$ inner product $\langle \cdot, \cdot \rangle$ is given by:

$$\langle \phi, \psi \rangle = \int_{\Omega} \alpha(t) \phi(r, \xi, t) \psi(r, \xi, t) dr d\xi \quad (4.3.3)$$

4.3.2 Nonautonomous evolution system representation

The PDE in the Eq.4.2.2 is expressed as:

$$\frac{\partial z}{\partial t} = A(r, \xi, t)z \quad (4.3.4)$$

with the boundary conditions in the Eq.4.2.3. In cylindrical coordinates, the operator $A(r, \xi, t)$ is defined as:

$$A(r, \xi, t)z := \frac{1}{r} \frac{\partial}{\partial r} \left(\kappa_0 r \frac{\partial z}{\partial r} \right) + \kappa_0 \frac{\partial^2 z}{\partial \xi^2} - v(t) \frac{\partial z}{\partial \xi} \quad (4.3.5)$$

for $\kappa_0 = \kappa_s/\text{Pe}$. The expression of the PDE in the Eq.4.3.4 as an abstract evolution system requires the establishment of the following properties. For each $t \in [0, T]$, the coefficients of the principle part of the operator $A(r, \xi, t)$ satisfy:

$$\kappa_0(\eta_1^2 + \eta_2^2) \neq 0, \quad \text{for all } (\eta_1, \eta_2) \neq (0, 0) \in \Omega \quad (4.3.6)$$

which is equivalent to $\kappa_0^2 > 0$ since κ_s and Pe are each positive. The Eq.4.3.6 implies that there are no real characteristics of the operator $A(r, \xi, t)$ given in the Eq.4.3.5 such that:

- E1. The operator $A(r, \xi, t)$ is an *elliptic operator* of second order for each $t \in [0, T]$.

The description of the boundary motion with dynamics governed by the second order ODE in the Eq.4.2.1 implies that:

- E2. The boundary velocity $v(t)$ is a smooth function (sufficiently Hölder continuous) which satisfies:

$$|v(t) - v(s)| \leq L|t - s|^\beta \quad (4.3.7)$$

for $s, t \in [0, T]$ and constants $L > 0$ and $\beta \in (0, 1]$.

It is known from [15, Chapter 7.6, Lemma 6.1,] that the properties E1-E2 are sufficient in the expression of the initial and boundary value problem in the Eq.4.3.4 as an abstract evolution system on the infinite-dimensional function space $L^2(\Omega)$ with solution provided in terms of a two-parameter semigroup. In order to obtain the explicit expression of this two-parameter semigroup, the eigenfunctions and eigenvalues of the operator $A(r, \xi, t)$ and the adjoint $A^*(r, \xi, t)$ are determined by standard methods (e.g. separation of variables) and application of the appropriate boundary conditions at each $t \in [0, T]$. For $0 \leq r \leq 1$, the eigenfunctions are determined as:

$$\phi_m^{(1)}(r) = \frac{\sqrt{2}}{J_0(\alpha_m)} J_0(\alpha_m r) \quad (4.3.8)$$

for $m \in \mathbb{N}$, where J_p are Bessel functions of the first kind and p^{th} order, and $\alpha_m = \{0, 3.83, 7.016, 10.173, 13.323 \dots\}$ are the m^{th} zeros of J_1 . The functions $\phi_m^{(1)}(r)$ in the Eq.4.3.8 are orthonormal to the eigenfunctions $\psi_m^{(1)}(r) := r\phi_m^{(1)}(r)$ of the corresponding adjoint operator. For $0 \leq \xi \leq l(t)$ and each $t \in [0, T]$, the eigenfunctions are determined as:

$$\begin{aligned} \phi_n^{(2)}(\xi, t) &= A_n e^{\frac{1}{2}\kappa_0^{-1}v(t)\xi} \left(\cos\left(\frac{n\pi}{l(t)}\xi\right) - \frac{1}{2}\kappa_0^{-1} \frac{v(t)}{\left(\frac{n\pi}{l(t)}\right)} \sin\left(\frac{n\pi}{l(t)}\xi\right) \right) \\ A_n(t) &= \sqrt{\frac{2}{l(t)}} \left(1 + \left(\frac{v(t)}{2\kappa_0 \left(\frac{n\pi}{l(t)}\right)} \right)^2 \right)^{-\frac{1}{2}} \end{aligned} \quad (4.3.9)$$

for $n \in \mathbb{N}$ and are orthonormal to the adjoint eigenfunctions $\psi_n^{(2)}(\xi) = \exp(-\kappa_0^{-1}v(t)\xi)\phi_n^{(2)}(\xi)$. We remark here that the notations (1) and (2) are utilized only to distinguish arguments of the functions $\phi^{(1)}(r)$ and $\phi^{(2)}(\xi, t)$. The

family of eigenvalues $\{\Lambda_{mn}(t)\}_{t \in [0, T]}$, $m, n = 1, 2, \dots$ of the operator $A(r, \xi, t)$ and adjoint $A^*(r, \xi, t)$ are:

$$\Lambda_{mn}(t) = \lambda_n(t) - \kappa_0 \alpha_m^2 \quad (4.3.10)$$

where,

$$\lambda_n(t) = -\kappa_0 \left(\frac{n\pi}{l(t)} \right)^2 - \frac{1}{2} \kappa_0^{-1} \frac{v(t)^2}{2} \quad (4.3.11)$$

which correspond at each $t \in [0, T]$ to the set of eigenfunctions of the operator $A(r, \xi, t)$:

$$\phi_{mn}(r, \xi, t) := \phi_m^{(1)}(r) \phi_n^{(2)}(\xi, t) \quad (4.3.12)$$

and the adjoint $A^*(r, \xi, t)$:

$$\psi_{mn}(r, \xi, t) := \psi_m^{(1)}(r) \psi_n^{(2)}(\xi, t) \quad (4.3.13)$$

For all $t \in [0, T]$, the eigenfunctions in the Eqs.4.3.12-4.3.13 form a family of time-dependent functions $\{\phi_{mn}(t)\}_{t \in [0, T]}$ and $\{\psi_{mn}(t)\}_{t \in [0, T]}$ which form an orthonormal basis of $L^2(\Omega)$, and at each $t \in [0, T]$, correspond to the family of time-dependent functions $\{\Lambda(t)\}_{t \in [0, T]}$.

Consider the family of linear operators $A(t)$, $t \in [0, T]$ which is associated with the operator $A(r, \xi, t)$ in the Eq.4.3.5. The domain of $A(t)$ is defined as:

$$D(A(t)) := \left\{ z \in L^2(\Omega), z, z_r, z_\xi \text{ are a.c., } z_{rr}, z_{\xi\xi} \in L^2(\Omega) \right. \quad (4.3.14)$$

$$\left. z_r|_{r=0} = 0, z_r|_{r=1} = 0, z_\xi|_{\xi=0} = 0, z_\xi|_{\xi=l(t)} = 0 \right\}$$

where z_r, z_{rr} denote the first and second order partial derivatives with respect to r , respectively (similarly for z_ξ and $z_{\xi\xi}$), and a.c. means absolutely continuous. Then for $z(t) \in D(A(t))$, we define:

$$A(t)z := A(r, \xi, t)z \quad (4.3.15)$$

The initial and boundary value problem in the Eq.4.3.4 is expressed in terms of the nonautonomous evolution system:

$$\frac{dz}{dt} = A(t)z, \quad z(0) = z_0 \quad (4.3.16)$$

where the operator $A(t) : D(A(t)) \subset L^2(\Omega) \rightarrow L^2(\Omega)$ in the Eq.4.3.14, satisfies the following properties [15, Chapter 5.6]:

- F1. For every $t \in [0, T]$, the resolvent $R(\lambda, A(t))$ exists for all λ with $\operatorname{Re}\lambda \leq 0$ and

$$R(A(t), \mu) \leq \max_{m,n,t \in [0,T]} (\Lambda_{mn}(t) - \mu)^{-1} \quad (4.3.17)$$

which gives that $\|R(A(t), \lambda)\| \leq L_1(|\mu| + 1)^{-1}$. Then $A(t)$ is a sectorial operator of $L^2(\Omega)$ for every $t \in [0, T]$.

- F2. Since $\{0\} \neq \sigma(A(\cdot))$ for all $t \in [0, T]$ the operator $A(t)$ has a bounded inverse $A(t)^{-1}$ on $L^2(\Omega)$ such that

$$\|(A(t) - A(s))A(\tau)^{-1}\| \leq L_2|t - s|^\alpha \quad (4.3.18)$$

for $s, t, \tau \in [0, T]$, and constants $L_2 > 0$ and $\alpha \in (0, 1]$.

Then by [15, Chapter 5.1; Chapter 5.6, Theorem 6.1] the solution of the non-homogeneous initial value problem in the Eq.4.3.16 is expressed as:

$$z(t) = U(t, s)z_0, \quad 0 \leq s \leq t \leq T \quad (4.3.19)$$

where $U(t, s)$ is a unique two-parameter semigroup with analytic expression provided in the following Theorem 4.3.1.

Theorem 4.3.1. The eigenfunctions in the Eqs.4.3.12-4.3.13 form a family of time-dependent functions with members denoted as $\phi_{mn}(t) = \phi_m^{(1)}(r)\phi_n^{(2)}(\xi, t)$ and $\psi_{mn}(t) = \psi_m^{(1)}(r)\psi_n^{(2)}(\xi, t)$ and at each $t \in [0, T]$, correspond to the family of time-dependent functions $\{\Lambda(t)\}_{t \in [0, T]}$ with members $\Lambda_{mn}(t) \in C^1([0, T])$. For $D(A(t))$ given in the Eq.4.3.14, consider the operator $A(t) : D(A(t)) \rightarrow L^2(\Omega)$ defined as:

$$A(t) := \sum_{m,n=1}^{\infty} \mathcal{F}_{mn}(t) \langle \cdot, \psi_{mn}(t) \rangle \phi_{mn}(t) \quad (4.3.20)$$

with

$$\mathcal{F}_{mn}(t) = \left\{ \left[t \frac{d}{dt} \lambda_n(t) + \lambda_n(t) - \kappa_0 \alpha_m^2 \right] \phi_n^{(2)}(t) + \frac{\partial}{\partial t} \phi_n^{(2)}(t) \right\} \phi_n^{(2)}(t)^{-1}$$

The operator $A(t) : D(A(t)) \subset L^2(\Omega) \rightarrow L^2(\Omega)$ is the infinitesimal generator of the two-parameter semigroup $U(t, s)$ defined as:

$$U(t, s)z(s) := \sum_{m,n=1}^{\infty} e^{\Lambda_{mn}(t)t - \Lambda_{mn}(s)s} \langle z(s), \psi_{mn}(s) \rangle \phi_{mn}(t) \quad (4.3.21)$$

for $0 \leq s \leq t \leq T$ and $z(s) \in L^2(\Omega)$.

To demonstrate that $A(t)$ is the infinitesimal generator of the two-parameter semigroup $U(t, s)$, one needs to check if the operator $U(t, s)$ satisfies the following: G1. $U(t, s)$ is bounded; G2. $U(t, t) = I$, $U(t, s) = U(t, s^*)U(s^*, s)$ for $0 \leq s \leq s^* \leq t \leq T$; and G3. $U(t, s)$ is differentiable for $0 \leq s \leq t \leq T$ with:

$$\frac{\partial U(t, s)}{\partial t} = A(t)U(t, s) \quad \text{and} \quad \frac{\partial U(t, s)}{\partial s} = -U(t, s)A(s)$$

which are verified in the Appendix 4.8. The crystal temperature regulation problem is considered in the following section in terms of the two-parameter semigroup.

Remark 4.3.2. One can recall that the notion of the energy of a parabolic PDE system is usually described by the eigenvalue spectrum. A unique transport-phenomena associated with the spectral characteristic of the operator $A(t)$ is that the contribution of the domain motion is manifested in the eigenvalues $\Lambda_{mn}(t)$ as the addition additional term in Eq.4.3.11 which has the features of the kinetic energy associated with the boundary motion, i.e. $E_k = v(t)^2/2$. The eigenvalues evolve over time as determined by the boundary velocity and the eigenfunctions in the Eqs.4.3.12-4.3.13 depend on both the velocity $v(t)$ and length of the domain, $l(t)$. One also notes that as the boundary motion approaches zero, $v(t) \rightarrow 0$ and $l(t) \rightarrow l_c$ where l_c is constant, the eigenfunctions $\phi_m(r, \xi, t)$ and $\psi_n(r, \xi, t)$ and eigenvalues converge to those of the standard parabolic PDE on a fixed spatial domain.

4.4 Controller design

In this section, we consider the optimal control problem for the PDE system given by Eq.4.2.2. Although in several works the boundary control problem for nonautonomous systems of parabolic type has been explored within different frameworks [16, 17, e.g.], in this work, we consider the approach to the boundary control formulation which is proposed in [18].

4.4.1 Optimal boundary control formulation

The input $u(t) \in \mathbb{R}$ is applied at $r = 1$ with function $b(\xi_c) = (1/2\varepsilon_1)\delta_{[\xi_c - \varepsilon_1, \xi_c + \varepsilon_1]}(\xi)$, $\varepsilon_1 > 0$ on some finite interval $[\xi_c - \varepsilon_1, \xi_c + \varepsilon_1]$ around the point $\xi_c \in (0, l(t))$. The boundary control problem is converted to a distributed control problem (inside the domain) by use of the Dirac delta function denoted $\delta(r - 1)$. The input operator $B(t)$ is the linear and bounded, i.e. $B(t) \in \mathcal{L}(\mathbb{R}, \mathcal{Z})$ where:

$$\begin{aligned} B(t)u(t) &:= \int_{\Omega} b(\xi_c)\delta(r - 1)\phi_{mn}(r, \xi, t)u(t)dr d\xi \\ &= \int_{\Omega} b(\xi_c)\phi_{mn}(1, \xi, t)u(t)dr d\xi \end{aligned} \tag{4.4.1}$$

The output measurement $y(t) = C(t)z(t)$ is taken at the radial boundary $r = 1$ around the point $z_o \in (0, l(t))$ and it is similarly defined as the function $b(\xi)$. The boundary control problem is then expressed as:

$$\begin{aligned} \frac{dz}{dt} &= A(t)z + B(t)u(t) \\ y(t) &= C(t)z \end{aligned} \tag{4.4.2}$$

In this form, we consider the finite-time horizon LQ-optimal state feedback control problem for the system in Eq.4.4.2 which is based on the minimization

of the cost functional:

$$J(z, u) = \int_0^T (|C(\tau)z(\tau)|^2 + |u(\tau)|^2) d\tau + \langle Qz(T), z(T) \rangle \quad (4.4.3)$$

for any initial state $z_0 \in \mathcal{Z}$ and weight $Q \in \mathcal{L}(\mathcal{Z})$. The minimizing input is denoted $u_{\text{opt}}(t) \in L^2([0, T]; \mathbb{R})$ and is associated with the input penalty term $R \in \mathbb{R}$ and the optimal pair $u_{\text{opt}}(t)$ and $z_{\text{opt}}(t)$ are related by the feedback formula:

$$u_{\text{opt}}(t) = -R^{-1}B^*(t)\Pi(t)z_{\text{opt}}(t) \quad (4.4.4)$$

The minimizing solution to Eq.4.4.3 is determined by the operator $\Pi(t) \in \mathcal{L}(\mathcal{Z})$ which is the unique nonnegative solution of the differential Riccati equation:

$$\begin{aligned} \dot{\Pi}(t) + A^*(t)\Pi(t) + \Pi(t)A(t) \\ - \Pi(t)B(t)R^{-1}B^*(t)\Pi(t) + C^*(t)C(t) = 0 \end{aligned} \quad (4.4.5)$$

with $\Pi(T) = Q$ and where $\dot{\Pi}(t)$ is the derivative of $\Pi(t)$ with respect to time [19, 20, see,]. The mild form expression of the Eq.4.4.5 is given in terms of $U(t, s)$ as:

$$\begin{aligned} \Pi(t)z = U^*(T, t)QU(T, t)z + \int_t^T U^*(\tau, t)U(\tau, t)z d\tau \\ - \int_t^T U^*(\tau, t)\Pi(\tau)B(\tau)R^{-1}B^*(\tau)\Pi(\tau)U(\tau, t)z d\tau \end{aligned} \quad (4.4.6)$$

Solving the Eq.4.4.5 yields the optimal input $u_{t \in [0, T]}^{\min}$ and the optimal state trajectory as the mild solution of the state feedback system $dz/dt = (A(t) -$

$B(t)R^{-1}B^*(t)\Pi(t)z(t)$, $0 \leq \tau < t \leq T$, $z(0) = z_0$ which is expressed as:

$$z(t) = \sum_{m,n}^{\infty} e^{\Lambda_{mn}(t)t} \langle z_0, \psi_{mn}(0) \rangle \phi_{mn}(t) - \int_0^t U(t, \tau) \sum_{m,n}^{\infty} B(t)R^{-1}B^*(t)\Pi(t) \langle z(\tau), \psi_{mn}(\tau) \rangle \phi_{mn}(\tau) d\tau \quad (4.4.7)$$

The numerical solution for the optimal input u_{opt} can be determined by utilizing the eigenfunctions in Eq.4.3.12-4.3.13 which form an orthonormal basis of $L^2(\Omega)$ at each $t \in [0, T]$ in order to reduce the Eq.4.4.5 to an infinite dimensional system of quadratic equations which can then be solved. However, implementation to a physical system requires truncation of terms in the optimal control law which is given as an infinite sum. The numerical approach in the following section provides both the foundation to simulate the closed loop PDE system in Eqs.4.2.2-4.2.3 and also an appropriate method to compute the optimal stabilizing input based on the finite-dimensional differential matrix Riccati equation.

4.5 Numerical implementation

This section provides an overview of the numerical approach utilized to simulate the closed loop PDE system in Eqs.4.2.2-4.2.3. A more thorough treatment of the Galerkin method pertaining to the variational form of the problem and existence and uniqueness of solutions is omitted [21, 22, 23].

4.5.1 Galerkin approximation

In this section, we invoke the Galerkin method in order to approximate the infinite-dimensional system representation of the PDE as a finite-dimensional

problem by projection of the PDE onto a finite-dimensional vector space Z utilizing the complete set of eigenfunctions in Eqs.4.3.12-4.3.13 which together form an orthonormal basis of $L^2(\Omega)$ at each time $t \in [0, T]$. Consider the finite set of the first M eigenfunctions $\phi_{mn}(r, \xi, t)$ with $m, n = 1, \dots, M$, and note that by using the weight function $w(\xi, t) = \exp(-(v(t)/\kappa_0)\xi)$, then $\langle w(\xi, t)\phi_{mn}(r, \xi, t), \phi_{ps}(r, \xi, t) \rangle = \delta_{mp}\delta_{ns}$. We assume a solution of the form:

$$z(r, \xi, t) = \sum_{m,n=0}^M a_{mn}(t)\phi_{mn}(r, \xi, t) \quad (4.5.1)$$

where the coefficients $a_{mn}(t)$ are to be determined. Restricting $z(r, \xi, t)$ to the finite-dimensional space Z which is spanned by $\phi_{mn}(r, \xi, t)$, then for each $t \in [0, T]$:

$$\begin{aligned} & \int_{\Omega} w(\xi, t)\phi_{mn}(r, \xi, t)z(r, \xi, t)drd\xi \\ &= \sum_{p,q=0}^M a_{pq}(t) \int_{\Omega} w(\xi, t)\phi_{pq}(r, \xi, t)\phi_{mn}(r, \xi, t)drd\xi \quad (4.5.2) \\ &= a_{mn}(t)\delta_{mp}\delta_{nq} \end{aligned}$$

with the indices $p, q = 1, \dots, M$. The initial state is given by:

$$a_{mn}(0) = \int_{\Omega} \phi_{mn}(r, \xi, t)z_0(r, \xi)drd\xi \quad (4.5.3)$$

and the projection of the Eq.4.4.2 on Z yields the system of M ordinary differential equations:

$$\frac{da_{mn}}{dt} = \Lambda_{mn}(t)a_{mn} + b_{mn}(t)u(t) \quad (4.5.4)$$

where:

$$b_{mn}(t) = \int_{\Omega} b(\xi_c) w(\xi, t) \phi_{mn}(1, \xi, t) \phi_{mn}(r, \xi, t) dr d\xi \quad (4.5.5)$$

The problem of determining a sufficiently large M such that the dominant dynamics of the PDE system may be captured in a finite set of M modes is considered in several other works [24, 25].

4.5.2 Optimal control problem for coupled systems

As previously stated, the crystal temperature dynamics are coupled to the domain motion through the boundary evolution at $z = l(t)$ and the boundary velocity $v(t)$ which are determined by the mechanical pulling arm and correspond to the states $x_1(t)$ and $x_2(t)$ in the Eq.4.5.6, respectively. The coupling of the infinite-dimensional system and the finite-dimensional subsystem is unidirectional since the crystal temperature does not affect the boundary motion. Therefore, one can consider the simultaneous stabilization of the domain motion and the crystal temperature regulation in the following setup. The finite-dimensional state system representation of the Eq.4.2.1 which is used to model the pulling arm subsystem dynamics is given by:

$$\begin{pmatrix} \dot{x}_1 \\ \dot{x}_2 \end{pmatrix} = \begin{pmatrix} 0 & 1 \\ -b_e/m_s & -a_d/m_s \end{pmatrix} \begin{pmatrix} x_1 \\ x_2 \end{pmatrix} + \begin{pmatrix} 0 \\ 1/m_s \end{pmatrix} f_{\text{mec}} \quad (4.5.6)$$

where $x_1(t) = \tilde{l}(t)$ and $x_2(t) = \dot{\tilde{l}}(t) = v(t)$ are the states of the system denoted as:

$$\dot{x} = A_m x + B_m f_{\text{mec}} \quad (4.5.7)$$

The optimal control input for each of the systems is then simultaneously determined by augmenting Eq.4.5.4 with Eq.4.5.7 in the following setup:

$$\begin{pmatrix} \dot{x} \\ \dot{a} \end{pmatrix} = \begin{pmatrix} A_m & 0 \\ 0 & \Lambda(t) \end{pmatrix} \begin{pmatrix} x \\ a \end{pmatrix} + \begin{pmatrix} B_m & 0 \\ 0 & b \end{pmatrix} \begin{pmatrix} f_{\text{mec}} \\ u \end{pmatrix} \quad (4.5.8)$$

which is represented by $\dot{\mathbf{x}}(t) = A_c(t)\mathbf{x}(t) + B_c(t)F(t)$. The feedback control law for the augmented system in Eq.4.5.8 is given by:

$$F_{\text{opt}}(t) = -R_c^{-1}B_c^T\Pi_c\mathbf{x} = \begin{pmatrix} f_{\text{opt}}(t) \\ u_{\text{opt}}(t) \end{pmatrix} \quad (4.5.9)$$

where Π_c is determined from the solution of the augmented finite-dimensional differential Riccati equation analogous to the Eq.4.4.5.

4.6 Simulation and results

In this section, the numerical simulation of the crystal temperature regulation problem in the presence of the time-varying spatial domain is provided. We consider the situation in which a perturbation has occurred in the crystal temperature distribution which arises, for example, from fluctuations in the melt environment. It is of interest to optimally stabilize the crystal temperature around the nominal steady state distribution of $z(r, \xi, t) = 0$ throughout the crystal region which is approximated as an axisymmetric cylinder with radius $R_c = 1$ and initial length $l(t = 0) = 3.5$ where the moving boundary at $\xi = l(t)$ and boundary velocity of $v(t)$ which are determined by the mechanical pulling arm at $\xi = 0$ drawing the crystal from the melt. To demonstrate the regulation of the crystal temperature in the presence of the time-varying spatial

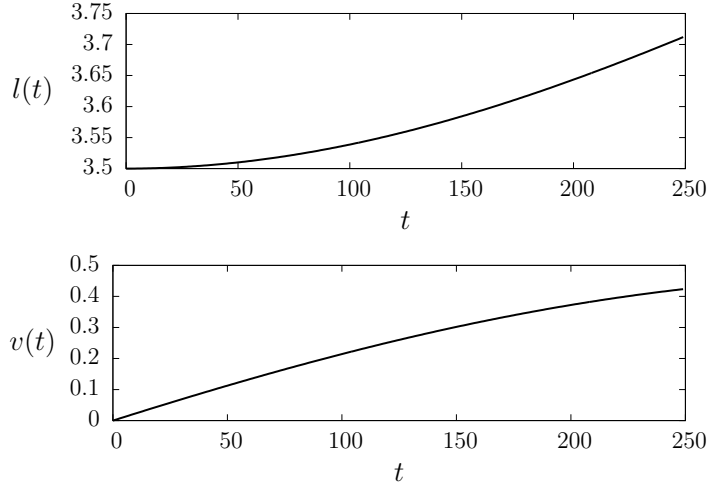


Figure 4.2: Domain length and boundary velocity evolution. Dimensionless system parameters: $m_s = 0.75$, $a_e = 1$, $b_d = -2.5$. Control parameters: $Q_m = 0.5I_{2 \times 2}$, $R_m = 1.5$.

domain, the controller for the mechanical pulling arm is detuned such that the domain growth is non-constant throughout the simulation and this point is further discussed in the following section.

4.6.1 Crystal temperature regulation

To capture the dominant dynamics of the crystal temperature evolution, the number of modes utilized was $M = 10$ for the finite-dimensional system representation of the PDE as described in the Section 4.5.1 with spatial discretization $\Delta r = 0.01$ for $[0 \leq r \leq 1]$ and $\Delta \xi = 0.025$ for $[0 \leq \xi \leq 3.5]$. The total simulation time of 250 time units t is representative of a physical processing time of 8 minutes, or 1.92 seconds per time unit. The domain length and boundary velocity evolution are shown in the Fig.4.2. The total change in crystal length from $t = 0$ to $t = 250$ is approximately 0.21 units of length which corresponds to a physical system growth of 0.67 cm based on an average crystal pull rate of 5.0 cm per hour [6]. From a practical point of view, the

slow growth of the crystal is essential in preventing the occurrence of “necking” which results in crystals of non-uniform diameter. Aggressive control action on the crystal pull rate may also lead to undesirable instabilities in the meniscus shape whereby the melt separates from the solidified crystal [2].

The initial deviation form for the temperature distribution of the crystal is shown in the Fig.4.3 where the region on the side of the crystal-melt interface at $z = 3.5$ is higher than on the side of the pulling arm at $\xi = 0$. The optimal control law in Eq.4.5.9 was numerically determined utilizing the first three modes of the finite-dimensional system representation of the PDE, with control parameters $Q(1,1) = 10$, $Q(2,2) = 1$, $Q(3,3) = 0.0001$ and $R = 0.005$. This was done to yield a low dimensional controller and also to prevent the peaking phenomena in the controller input to the system Sussmann,1991. The optimal feedback control u_{opt} is calculated by solving the analogous finite-dimensional form of the time-varying differential Riccati equation in the Eq.4.4.5 at each time instance. The resulting input is applied at the $r = 1$ boundary of the crystal in the region $[0.2 \leq \xi_c \leq l(t)]$ and the output is measured at $r = 1$ and $\xi_o = 2.5$. The Figs.4.4-4.6 show the closed

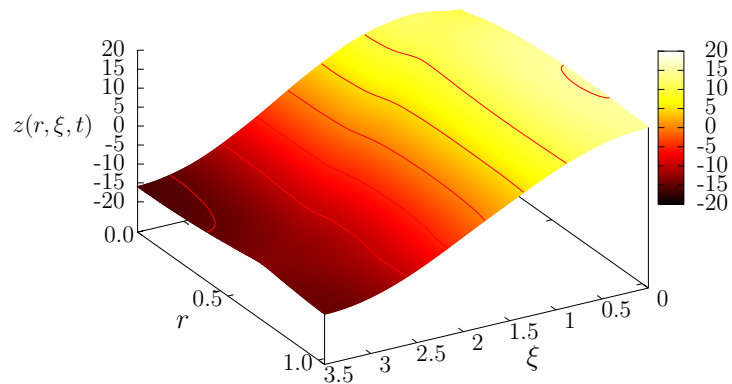


Figure 4.3: Initial deviation form for the temperature distribution of crystal at $t = 0$. Crystal conductivity ratio $\kappa_0 = 0.39$.

loop system temperature distribution $z(r, \xi, t)$ of the crystal at six different time instances: $t = 5, 25, 50, 75, 100, 150$ under the optimal control regulator. One can again notice the temperature on the side of the crystal-melt interface at $\xi = l(t)$ is higher than on the side of the pulling arm at $\xi = 0$. At $t = 5$, the temperature difference between the highest and lowest regions within the crystal is approximately 40 with the contours providing an indication of the overall temperature gradient across the crystal regions throughout the process.

The temperature distribution becomes progressively uniform and stabilizes around the nominal distribution $z(r, \xi, t) = 0$ throughout almost the entire time-dependent region with crystal length $l(t) = 3.579$ at the time $t = 150$. The input profile generated by the optimal control scheme and the total system energy evolution are shown in the following section with comparisons to simpler control strategies.

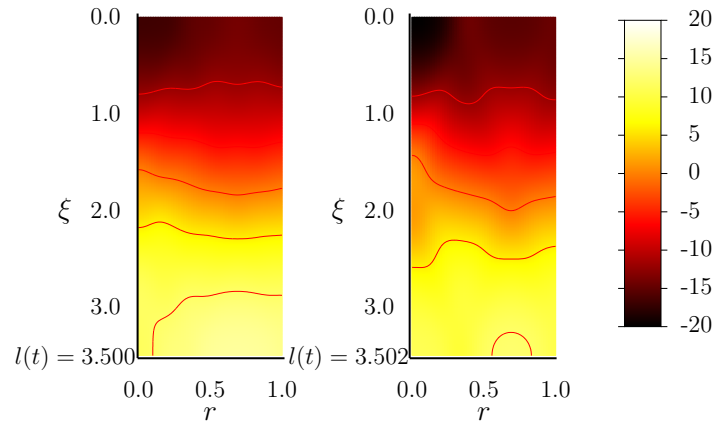


Figure 4.4: Crystal temperature distribution at $t = 5$ (Left) and at $t = 25$ (Right).

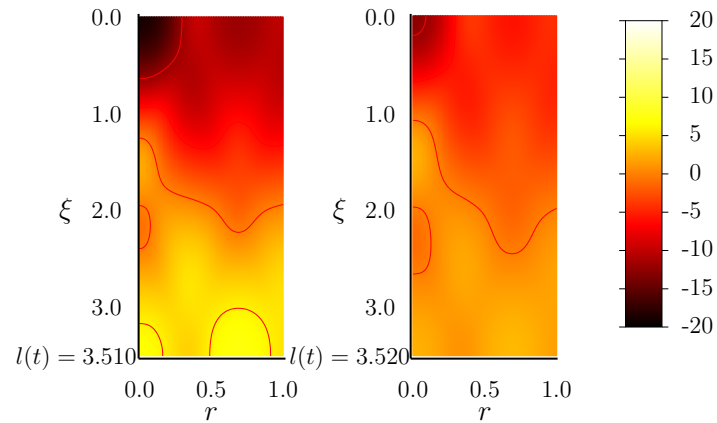


Figure 4.5: Crystal temperature distribution at $t = 50$ (Left) and at $t = 75$ (Right).

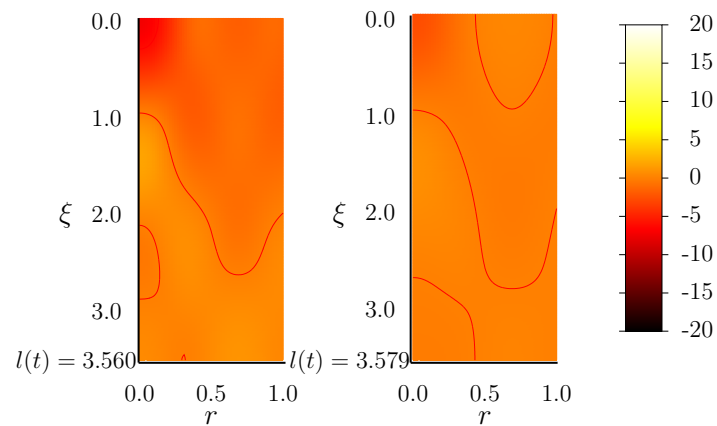


Figure 4.6: Crystal temperature distribution at $t = 100$ (Left) and at $t = 150$ (Right).

4.6.2 Comparison to fixed-gain controllers

To evaluate the performance of the optimal controller for the crystal temperature regulation problem, we consider the input and total energy profiles of the

closed loop system as compared with two fixed-gain controllers. In contrast to the optimal controller, with time-varying gain $K_{\text{opt}}(t)$ which is determined from the solution of the differential Riccati equation, the two low dimensional modal based proportional controllers for the PDE system with time-invariant gains are selected as: $K_1 = (8 \ -1 \ -10)$; and $K_2 = (1 \ -0.5 \ -1)$. Each of K_1

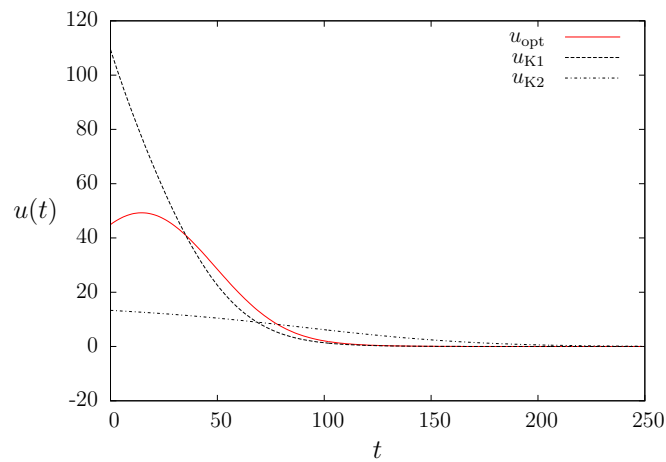


Figure 4.7: Input profiles $u_{K1}(t)$, $u_{K2}(t)$, and $u_{\text{opt}}(t)$ applied to boundary of the crystal.

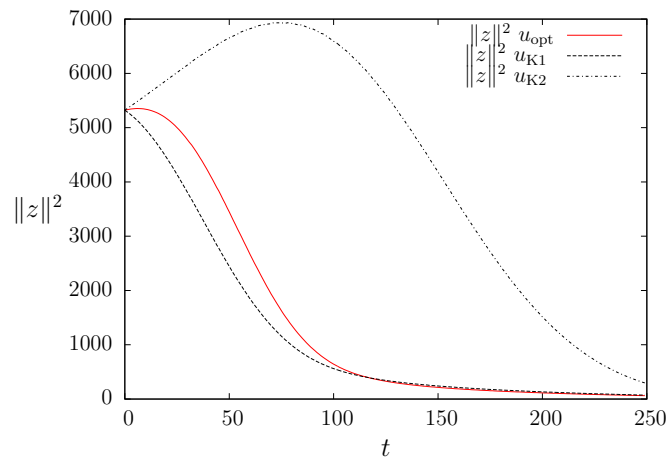


Figure 4.8: Total system energy profiles for closed loop systems under $u_{K1}(t)$, $u_{K2}(t)$, and $u_{\text{opt}}(t)$.

and K_2 results in a control input $u_{K_1}(t)$ and $u_{K_2}(t)$. Each of the fixed-gain controllers, where the rate of temperature regulation is fixed such that the input evolution cannot be adjusted during the process, is not optimal, i.e. the gains are not chosen from any model based control criteria to incorporate any performance characteristics. The closed loop systems under each regulator with inputs $u_{K_1}(t)$ and $u_{K_2}(t)$ are simulated under the same conditions as the closed loop system under the optimal control law with input $u_{\text{opt}}(t)$.

The Fig.4.7 shows the input profiles $u_{K_1}(t)$, $u_{K_2}(t)$, and $u_{\text{opt}}(t)$. One can notice that the input generated using the fixed-gain controller K_1 resulted in a relatively more aggressive controller and highest initial input $u(t)$ as compared to each of $K_{\text{opt}}(t)$ and K_2 . The least aggressive controller K_2 generated the input profile $u_{K_2}(t)$. These results are consistent to what was expected due to the choice of entries in the gain vectors K_1 and K_2 .

The total system energy profiles of the closed loop systems under each of the controllers $u_{K_1}(t)$, $u_{K_2}(t)$, and $u_{\text{opt}}(t)$ is shown in the Fig.4.8. It can be seen that aggressive controller resulted in the system initially being stabilized to a lower total energy than both of the controllers K_1 and $K_{\text{opt}}(t)$. The least aggressive controller K_2 resulted in a total system energy profile which initially increases even though the system is inherently dissipative. This phenomena is due to the growth in the crystal domain from the melt which contributes to the total system energy. In contrast, the optimal controller $K_{\text{opt}}(t)$, which accounts for the crystal domain evolution, is less aggressive than the controller K_1 , and results in the input profile shown in the Fig.4.7. The total system energy profile for the optimal controller is initially greater than the profile generated by the aggressive controller K_1 . At approximately $t = 100$ one can see that the two profiles are essentially the same until the systems are each stabilized to the zero distribution at approximately $t = 250$. One can notice

that the optimal and time-varying control strategy with milder input profile resulted in the same temperature regulation performance over the simulation time-frame as the aggressive fixed-gain controller. These results suggests that the optimal control law would be better suited as a temperature regulator where it is undesirable to subject the crystal boundary to high temperature inputs.

4.7 Conclusions

In this work, we considered the optimal control of the CZ crystal growth and temperature regulation problem. The convection-diffusion parabolic PDE process model of the crystal temperature dynamics defined on the time-varying spatial domain was derived from first principles continuum mechanics. The domain evolution was described by a second order ODE model for the mechanical pulling arm subsystem which is unidirectionally coupled to the crystal temperature dynamics. The representation of the parabolic PDE as a nonautonomous operator on an infinite-dimensional space was developed and the analytic expression and properties of the associated two-parameter semigroup were presented. The optimal control problem for the time-varying system was provided in terms of the two-parameter semigroup based on the LQR formulation for infinite-dimensional time-varying systems theory. A numerical scheme was provided to facilitate the realization of the control problem by approximation of the PDE as a finite-dimensional system. The optimal control problem setup for the finite-dimensional representation of the PDE augmented with the finite-dimensional subsystem for the mechanical pulling arm was presented. The numerical simulation of the CZ crystal growth process demonstrated the regulation of the crystal temperature using the optimal control formulation

developed in this work. A comparison of the optimal and time-varying regulator performance to simple fixed-gain controllers showed the advantages of the optimal control strategy.

4.8 Appendix

Formulation of the PDE model

The parabolic PDE of a material domain with moving boundary can be derived directly from first-principles continuum mechanics [26, 27] and yields a convection-diffusion model which is consistent with the governing equations of heat transfer which are utilized in previous works to describe the CZ crystal temperature dynamics [5].

Let the simple body $\Omega \subset \mathbb{R}^3$ with material points, $\zeta = (\zeta_1, \zeta_2, \zeta_3) \in \Omega$, volume element dV and smooth boundary $\partial\Omega$, denote the crystal body with spatial points $\xi = (\xi_1, \xi_2, \xi_3) \in \mathbb{R}^3$ and volume element dv . Let Ω_0 be the initial configuration and $\Omega_t \subset \mathbb{R}^3$ be the configuration at time $t \in [0, T]$. The regular motion of Ω is determined by the C^1 mapping $\varphi_t : \Omega \rightarrow \mathbb{R}^3$ such that $\xi = \varphi_t(\zeta)$ and $\Omega_t = \varphi_t(\Omega)$, with C^1 inverse, $\varphi_t^{-1} : \varphi_t(\Omega_t) \rightarrow \Omega$. The material velocity of the motion $\mathbf{V} : \Omega \times [0, T] \rightarrow \mathbb{R}^3$ is defined by:

$$\mathbf{V}(\zeta, t) = \mathbf{V}_t(\zeta) = \frac{\partial \varphi}{\partial t}(\zeta, t) = \frac{d}{dt} \varphi_\zeta(t) \quad (4.8.1)$$

The spatial velocity of motion $\mathbf{v} : \varphi_t(\Omega) \rightarrow \mathbb{R}^3$ defines the spatial velocity field \mathbf{v} with relation $\mathbf{v} = \mathbf{V}_t \circ \varphi_t^{-1}$ where \circ is the composition operator. The regularity of the motion presumes that Ω is never divided or penetrated and the continuous mapping φ_t allows one to describe the configuration of Ω at time $t \in [0, T]$ in terms of a fixed configuration by change of variables Marsden1983.

We define the following standard identities: The Jacobian of $\varphi_t(\zeta)$ is $J(\zeta, t) = \det\left(\frac{\partial\varphi}{\partial\zeta}\right)$ with derivative $\frac{\partial J}{\partial t} = \nabla \cdot \mathbf{v} J(\zeta, t)$. Under the assumption that mass is conserved, one obtains that $\frac{D\rho}{Dt} + \rho \nabla \cdot \mathbf{v} = 0$, where $\frac{D}{Dt} = \frac{\partial}{\partial t} + \mathbf{v} \cdot \nabla$ is the material derivative operator.

The Transport Theorem which describes the rate of change of the crystal temperature z in Ω_t with respect to time is given by:

$$\begin{aligned} \frac{d}{dt} \int_{\varphi_t(\Omega)} \rho(\xi, t) z(\xi, t) dv &= \frac{d}{dt} \int_{\Omega} \rho(\varphi_t, t) z(\varphi_t, t) J(\zeta, t) dV \\ &= \int_{\Omega} \left(\frac{D\rho}{Dt}(\varphi_t, t) z(\varphi_t, t) J(\zeta, t) \right. \\ &\quad \left. + \rho(\varphi_t, t) \frac{Dz}{Dt}(\varphi_t, t) J(\zeta, t) + \rho(\varphi_t, t) z(\varphi_t, t) \frac{\partial J}{\partial t}(\zeta, t) \right) dV \end{aligned} \quad (4.8.2)$$

Using the identities and change of variables where the differentiation and integration operations may be interchanged [27] we have:

$$\begin{aligned} \frac{d}{dt} \int_{\varphi_t(\Omega)} \rho(\xi, t) z(\xi, t) dv &= \int_{\Omega} \rho(\varphi_t, t) \left(-z(\varphi_t, t) \nabla \cdot \mathbf{v}(\varphi_t, t) + \frac{\partial z}{\partial t} \right. \\ &\quad \left. + \mathbf{v}(\varphi_t, t) \cdot \nabla z(\varphi_t, t) + z(\varphi_t, t) \nabla \cdot \mathbf{v}(\varphi_t, t) \right) J(\zeta, t) dV \\ &= \int_{\Omega} \rho(\varphi_t, t) \left(\frac{\partial z}{\partial t}(\varphi_t, t) + \mathbf{v}(\varphi_t, t) \cdot \nabla z(\varphi_t, t) \right) J(\zeta, t) dV \\ &= \int_{\varphi_t(\Omega)} \rho(\xi, t) \left(\frac{\partial z}{\partial t}(\xi, t) + \mathbf{v}(\xi, t) \cdot \nabla z(\xi, t) \right) dv \end{aligned} \quad (4.8.3)$$

Then by the Conservation Law the total heat balance in the region is expressed as $\frac{d}{dt} \int_{\Omega_t} \rho z dv = \int_{\partial\Omega_t} \kappa \nabla z \cdot \mathbf{n} ds$, where κ is the thermal conductivity

constant, and n is the normal component of ds . Substitution of the Eq.4.8.3 yields the expression:

$$\int_{\Omega_t} \rho(\xi, t) \left(\frac{\partial z}{\partial t}(\xi, t) + \mathbf{v}(\xi, t) \cdot \nabla z(\xi, t) \right) dv = \int_{\Omega_t} \nabla \cdot \kappa \nabla z(\xi, t) dv \quad (4.8.4)$$

From a physical point of view of the CZ crystal growth process, the following assumptions are made: The density of the solidified material at the crystal-melt interface is equal to that of the preexisting crystal such that $\rho(\xi, t) = \rho$ is constant. Secondly, the material growth is due to the motion of the boundary at the crystal-melt interface whereby $\mathbf{v}(\xi, t) = v(t)$. Furthermore, one can regard the element dv as the crystal regions itself which yields the differential form of the Eq.4.8.4:

$$\rho \left(\frac{\partial z}{\partial t} + v(t) \cdot \nabla z \right) = \nabla \cdot \kappa \nabla z \quad (4.8.5)$$

whereby the Eq.4.8.5 is the PDE which describes the temperature dynamics in the time-dependent spatial domain Ω_t where the domain deformation is due to the motion of the boundary with velocity $v(t)$. The scaling of the Eq.4.8.5 by the constant Peclet number, Pe , converts the PDE to the dimensional form in the Eq.4.2.2 which describes the CZ crystal temperature dynamics [6, 14].

The temperature field across the crystal boundary in the axisymmetric radial direction and at the side of the pulling arm is assumed to be zero-flux [14]. The melt temperature z_m is assumed to be a constant C and equal to the crystal temperature at the melt-crystal interface boundary, i.e. $z_m = z(r, l(t), t) = C$ at $\xi = l(t)$ such that $\partial z / \partial \xi = 0$ at $z = l(t)$. Then the boundary conditions imposed on the PDE are prescribed as in the Eq.4.2.3.

Properties of $U(t, s)$

The property G1 is determined from the relation $\|U(t, s)\| \leq \exp \left\{ \int_s^t \|A(\tau)\| d\tau \right\}$ which follows from the Contraction mapping principle where $z(t)$ is a fixed point associated with the homogeneous form of the initial value problem [22]. By Gronwall's inequality $\|U(t, s)z_0\| = \|z(t)\| \leq \|z_0\| \exp \left(\int_s^t \|A(\tau)\| d\tau \right)$ whereby $U(t, s)$ is bounded [15].

The property G2 is determined as follows: Consider the family of eigenfunctions in the Eqs.4.3.12-4.3.13 with indices $m, m', n, n' = 1, 2, \dots$ and let $h_{mn}(t, s) = \lambda_n(t)t - \lambda_n(s)s - \kappa_0 \alpha_m^2(t - s)$. One can note that the sets $\{\phi_{mn}(t)\}_{t \in [0, T]}$ and $\{\psi_{m'n'}(t)\}_{t \in [0, T]}$ are pairwise orthonormal for each $t \in [0, T]$:

$$\int_{\Omega} \phi_{mn}(r, \xi, t) \psi_{m'n'}(r, \xi, t) dr d\xi = \begin{cases} 1 & m = m' \text{ and } n = n' \\ 0 & \text{otherwise} \end{cases}$$

The identity $U(t, t) = I$ is easily deduced by inspection. It follows that for $z \in L^2(\Omega)$ and $0 \leq s \leq s^* \leq t \leq T$:

$$\begin{aligned} & U(t, s^*)U(s^*, s)z \\ &= \sum_{m,n=1}^{\infty} e^{h_{mn}(t, s^*)} \left\langle \sum_{p,q=1}^{\infty} e^{h_{pq}(s^*, s)} \langle z, \psi_{pq}(s) \rangle \phi_{pq}(s^*), \psi_{mn}(s^*) \right\rangle \phi_{mn}(t) \\ &= \sum_{m,n=1}^{\infty} e^{h_{mn}(t, s)} \langle z, \psi_{mn}(s) \rangle \phi_{mn}(t) = U(t, s)z \end{aligned}$$

The property G3 is verified by direct calculation with:

$$\begin{aligned} A(t)U(t, s) &= \sum_{m,n=1}^{\infty} \mathcal{F}_{mn}(t) \left\langle \sum_{p,q=1}^{\infty} e^{h_{pq}(t,s)} \langle \cdot, \psi_{pq}(s) \rangle \phi_{pq}(t), \psi_{mn}(t) \right\rangle \phi_{mn}(t) \\ &= \sum_{m,n=1}^{\infty} \mathcal{F}_{mn}(t) e^{h_{mn}(t)} \langle \cdot, \psi_{mn}(s) \rangle \phi_{mn}(t) \end{aligned}$$

The operator $U(t, s)$ is differentiable in $t \in [0, T]$ and straightforward calculations yields:

$$\begin{aligned} \frac{\partial U(t, s)}{\partial t} &= \sum_{m,n=1}^{\infty} \left\{ \left(t \frac{d}{dt} \lambda_n(t) + \lambda_n(t) - \kappa_0 \alpha_m^2 \right) \phi_n^{(2)}(t) \right. \\ &\quad \left. + \frac{\partial \phi^{(2)}(t)}{\partial t} \right\} e^{h_{mn}(t,s)} \langle \cdot, \psi_n(s) \rangle \phi_m^{(1)} = A(t)U(t, s) \end{aligned}$$

The derivative of $U(t, s)$ with respect to $s \in [0, T]$ is similarly determined.

Bibliography

- [1] Ng J, Dubljevic S. Optimal control of convection-diffusion process with time-varying spatial domain: Czochralski crystal growth. *Journal of Process Control*. 2011;21(10):1361–1369.
- [2] Brown R. Theory of transport processes in single crystal growth from the melt. *AIChE J*. 1988;34:881–911.
- [3] Lan CW. Recent progress of crystal growth modeling and growth control. *Chemical Engineering Science*. 2004;59(7):1437 – 1457.
- [4] Derby J, Brown R. Thermal-capillary analysis of Czochralski and Liquid Encapsulated Czochralski Crystal Growth. I. Simulation. *J Cryst Growth*. 1986;74:605–624.
- [5] Derby J, Brown R. Thermal-capillary analysis of Czochralski and Liquid Encapsulated Czochralski Crystal Growth. II. Processing Strategies. *J Cryst Growth*. 1986;75:227–240.
- [6] Derby J, Brown R. On the Dynamics of Czochralski Crystal Growth. *J Cryst Growth*. 1987;83:137–151.
- [7] Sinno T, Brown RA. Modeling Microdefect Formation in Czochralski Silicon. *Journal of The Electrochemical Society*. 1999;146(6):2300–2312.
- [8] Szabo G. Thermal Strain during Czochralski Crystal Growth. *J Cryst Growth*. 1985;73:131–141.
- [9] Armaou A, Christofides PD. Robust Control of Parabolic PDE Systems with Time-Dependent Spatial Domains. *Automatica*. 1999;.

- [10] Hinze M, Ziegenbalg S. Optimal control of the free boundary in a two-phase Stefan problem. *Journal of Computational Physics*. 2007;223(2):657 – 684.
- [11] Dunbar W, Petit N, Rouchon P, Martin P. Boundary control of a nonlinear Stefan problem. In: *Decision and Control, 2003. Proceedings. 42nd IEEE Conference on*, vol. 2. 2003; pp. 1309 – 1314 Vol.2.
- [12] Wang PKC. Stabilization and Control of Distributed Systems with Time-Dependent Spatial Domains. *J Optim Theor & Appl*. 1990;65:331–362.
- [13] Wang PKC. Feedback Control of a Heat Diffusion System with Time-Dependent Spatial Domains. *Optim Contr Appl & Meth*. 1995;16:305–320.
- [14] Derby JJ, Atherton LJ, Thomas PD, Brown RA. Finite-element methods for analysis of the dynamics and control of Czochralski Crystal Growth. *J Sci Comput*. 1987;2:297–343.
- [15] Pazy A. *Semigroups of Linear Operators and Applications to Partial Differential Equations*. New York, U.S.A.: Springer-Verlag. 1983.
- [16] Acquistapace P, Flandoli F, BTerreni. Initial boundary value problems and optimal control for nonautonomous parabolic systems. *SIAM J Math Anal*. 1991;29:89–118.
- [17] Acquistapace P, Terreni B. Infinite-horizon linear-quadratic regulator problems for nonautonomous parabolic systems with boundary control. *SIAM J Math Anal*. 1996;34:1–30.
- [18] Ray W. *Advanced Process Control*. New York: McGraw-Hill. 1981.

- [19] Bensoussan A, Prato GD, Delfour M, Mitter S. *Representation and Control of Infinite Dimensional Systems*. Boston: Birkhäuser. 2007.
- [20] Naidu D. *Optimal control systems*. Electrical engineering textbook series. CRC Press. 2003.
- [21] Evans L. *Partial differential equations*. USA: American Mathematical Society. 1998.
- [22] McOwen R. *Partial differential equations: methods and applications, 2nd ed.* USA: Prentice Hall. 2002.
- [23] Hughes T. *The Finite Element Method*. New York, U.S.A.: Dover Publications. 2000.
- [24] Balas M. Exponentially stabilizing finite-dimensional controllers for linear distributed parameter systems: Galerkin approximation of infinite-dimensional controllers. *J Math Anal Appl.* 1986;117:358–384.
- [25] Ito K. Finite-Dimensional Compensators for Infinite-Dimensional Systems via Galerkin-Type Approximation. *SIAM J Control Optim.* 1990; 28:1251–1269.
- [26] Marsden J, Hughes T. *Mathematical Foundations of Elasticity*. New York, U.S.A.: Dover Publications. 1983.
- [27] Marsden J, Ratiu T, Abraham R. *Manifolds, Tensor Analysis and Applications*. New York, U.S.A.: Springer-Verlag. 2001.

Chapter 5

Optimal boundary control of a diffusion-convection-reaction PDE model with time-dependent spatial domain: Czochralski crystal growth process

The material presented in this chapter has been published as the following:

- [1] J. Ng and S. Dubljevic, “Optimal boundary control of a diffusion convection-reaction PDE model with time-dependent spatial domain: Czochralski crystal growth process,” *Chemical Engineering Science*, vol. 67, no. 1, pp. 111-119, 2012.

5.1 Introduction

A large number of industrial processes such as metal casting, operating the tubular and packed-bed reactors, metal or glass annealing and crystal growth,

involve phase transitions, material deformation and chemical reactions. The occurrence of these changes in the state, shape or other time-dependent material property during its processing regime introduce complexities in the modeling of the process dynamics. The first principle models arising from fundamental transport and balance principles usually yield the dissipative transport-reaction models given by the parabolic partial differential equations (PDEs) with appropriately defined boundary conditions and domains [2, 3, 4]. In many cases the transport-reaction models exhibits nonlinear dynamics due to, for example, chemical reactions with Arrhenius type dependence on temperature and/or concentration and which therefore introduces the complexity in model description [5, 6]. In addition, for models of transport-reaction systems defined on fixed spatial domains, the possible time-dependence of system parameters, for example catalyst deactivation, yields nonautonomous parabolic evolution system representations of the PDE and induces significant mathematical complexity in the process characterization. Currently, the general theory which treats time-varying parabolic PDEs is already well established [7, 8, 9, 10], and it has been extended to distributed and boundary control problems including linear quadratic regulator synthesis [11, 12, 13]. However, only a relatively small number of contributions have considered the control of PDEs defined on time-dependent spatial domain [14, 15, 16, 17, 18] like in the case of Czochralski (CZ) crystal growth process in which the crystal is grown by pulling out of the melt crucible, and also in the representative case of phase transition problems modelled by Stefan model [19], which is suitable for describing processes such as the vertical Bridgman-Stockbarger crystal growth method depicted in Fig.5.1.

In this chapter, we consider the CZ crystal growth problem in which the type of material boundary motion considered arises due to the pulling out

of crystal motion and it is independent of the temperature and/or concentration profile at the the melt-solid phase interface and material regions itself. However, the melt-solid interface boundary motion contributes to the underlying transport phenomena determining the true process dynamics. Therefore, a thermal-capillary Czochralski (CZ) crystal growth method for single crystal growth is representative physical system modeled as a moving boundary problem and is one of the most important industrial process utilized for the production of semiconductor materials for the microelectronics industry [20, 21, 22, 23]. The CZ crystal growth process is a thermal-capillary method whereby, large boules of single crystals, typically silicon (Si) and gallium arsenide (GaAs), are formed in a thermal environment through the action of a mechanical pulling arm which draws a seed crystal from a pool of melt in a heated crucible, and as the melt solidifies around the solid-melt interface, the crystal is formed (see Fig.5.2 for general setup). The principle factors contributing to the overall crystal quality include variations in the thermal fields of the ambient and melt temperatures, and the crystal pull rate where fluctuations in the crystal temperature distribution and the rate at which the crystal cools can cause large thermoelastic stresses leading to defect and dislocation generation [24]. One proposed method to realize the crystal temperature regulation is by distributed heat input allocated along the crystal domain by a heat pipe which is inserted between the growing crystal and the crucible [23]. However, technical limitations may prohibit the effective temperature regulation by heaters along the domain. For example, at the initial stage of the CZ process, the crystal seed is placed in the crucible below the level of an encapsulant which prevents evaporation of the crystal melt from the crucible.

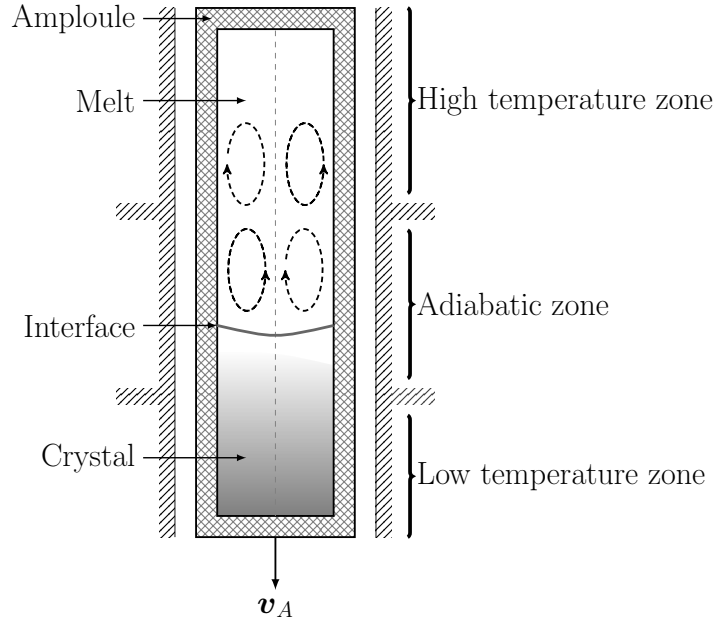


Figure 5.1: The schematics of Bridgman-Stockbarger crystal growth method.

From an industrial processing point of view it is of interest to obtain the desired temperature or concentration profile in the time varying region over the course of the process in order to achieve the desired purity, structural and metallurgical properties in the final product and to decrease overall production cost. Therefore, we consider the optimal boundary control of a general class of diffusion-convection-reaction system defined on a time-dependent spatial domain with moving boundary describing the CZ process. Although the main motivation is to design the optimal boundary controller for the 2D Czochralski crystal growth process, one may consider the proposed methodology design to be applied to the general class of diffusion-convection-reaction PDEs model with time varying spatial domain, since the methodology provided in this work allows for a broad number of processes to be treated (annealing type of processes) within the proposed optimally boundary control framework.

This chapter is organized as follows: Section 5.2 introduces the derivation of the time varying parabolic PDE starting from the *Conservation Law* and principles of *Continuum mechanics*, then the basic notation and definitions from functional analysis necessary in describing the properties of the class of PDE system with time varying domain and its subsequent representation as a nonautonomous evolution system on an appropriately defined function space. In Section 5.3 the boundary control formulation will be presented and applied in the Section 5.4 in the context of the crystal temperature regulation problem for the CZ crystal growth process with numerical simulation results included. Finally, Section 5.5 concludes this chapter with a brief summary of results. Formal proofs and definitions will be included in the Appendices.

5.2 Preliminaries

In this section, we formulate a model starting from basic dynamical equations for continuum mechanics for the purpose of incorporating the time-dependent evolution of the spatial domain into the model dynamics for the diffusion-reaction process. In particular, we utilize the Reynolds Transport Theorem in ensuing model development. We also provide the notation and the functional space setting associated with the time-varying parabolic PDE. While the definitions are purely formal and well known [25, Chapters 2-5] they enable us to consider this class of PDE defined on a time-dependent spatial domain within the context of standard infinite-dimensional systems theory. Then by using the results of [26] and [10], the PDE properties relevant to the subsequent abstract representation as a nonautonomous parabolic evolution system on an infinite-dimensional function space will be included.

5.2.1 Model formulation

Let denote a simple body Ω with material points, $X = \{X_1, X_2, X_3\} \in \Omega$, volume element dV and smooth boundary $\partial\Omega$, be an open subset in \mathbb{R}^3 with spatial points $\xi = \{\xi_1, \xi_2, \xi_3\} \in \mathbb{R}^3$ and volume element dv . Let Ω_0 be the initial configuration and $\Omega_t \subset \mathbb{R}^3$ be the configuration at time $t \in [0, T] \subset \mathbb{R}$, so that simple motion (material velocity motion-deformation) from one body configuration to another one can be described by introducing the following well defined mapping.

Definition 5.2.1. The regular motion of Ω is determined by the continuous mapping $\varphi_t : \Omega \rightarrow \mathbb{R}^3$ such that $z = \varphi_t(X)$ and $\Omega_t = \varphi_t(\Omega)$, with continuous inverse, $\varphi_t^{-1} : \varphi_t(\Omega) \rightarrow \Omega$. The material velocity of the motion $\mathbf{V} : \Omega \rightarrow \mathbb{R}^3$ is defined by

$$\mathbf{V}(X, t) = \mathbf{V}_t(X) = \frac{\partial \varphi}{\partial t}(X, t) = \frac{d}{dt} \varphi_X(t) \quad (5.2.1)$$

The spatial velocity of motion $\mathbf{v} : \varphi_t(\Omega) \rightarrow \mathbb{R}^3$ defines the spatial velocity field $\mathbf{v}(\xi, t)$ with relation $\mathbf{v}(\xi, t) = \mathbf{V}_t \circ \varphi_t^{-1}$.

The regularity of the motion defined in Definition 5.2.1 presumes that Ω is never divided or penetrated. Moreover, Definition 5.2.1 gives that the evolution of Ω is described by the semi-flow ($t \geq 0$) property. In other words, there is a collection of maps $\varphi_{t,s}$ such that for each s and z , the integral curve of flow $t \mapsto \varphi_{t,s}(X)$ is given by $\varphi_{t,s} \circ \varphi_{s,r} = \varphi_{t+r}$ for all r, s, t , such that the configuration Ω_t at time $t \in [0, T]$ can be described in terms of a fixed configuration by change of variables [2]. Utilizing these general results, the *Transport Theorem* for a time-dependent spatial domain is given as follows.

Proposition 6. Let $z(\xi, t)$ be the bounded and continuous function on Ω for all $t \in [0, T]$, and continuous on $\partial\Omega_t$, which represents the concentration or

temperature. The rate of change of x with respect to time in Ω_t is expressed as

$$C_p \frac{d}{dt} \int_{\Omega_t} \rho(\xi, t) z(\xi, t) dv = C_p \int_{\Omega_t} \rho(\xi, t) \left(\frac{\partial z}{\partial t}(\xi, t) + \mathbf{v}(\xi, t) \cdot \nabla z(\xi, t) \right) dv \quad (5.2.2)$$

where the density $\rho : \Omega_t \times [t_0, t_f] \rightarrow \mathbb{R}$ is bounded $C^1(\Omega_t)$ and satisfies $\frac{\partial \rho}{\partial t}(\xi, t) + \nabla \cdot \rho(\xi, t) \mathbf{v}(\xi, t) = 0$, (conservation of mass), and the specific heat capacity C_p is constant.

Proof. The Jacobian of $\varphi_t(X)$ is the determinant of the deformation gradient, i.e. $J(\xi, t) = \det \left(\frac{\partial \varphi}{\partial X}(\xi, t) \right)$ and $\frac{\partial J}{\partial t}(\xi, t) = \nabla \cdot \mathbf{v}(\xi, t) J(\xi, t)$. Under the assumption that mass is conserved in Ω_t then $\frac{D\rho}{Dt}(\xi, t) + \rho(\xi, t) \nabla \cdot \mathbf{v}(\xi, t) = 0$ where $\frac{D(\cdot)}{Dt} = \partial_t(\cdot) + \mathbf{v} \cdot \nabla(\cdot)$ is the material derivative operator, and by change of variables

$$\begin{aligned} \frac{d}{dt} \int_{\varphi_t(\Omega)} \rho(\xi, t) z(\xi, t) dv &= \frac{d}{dt} \int_{\Omega} \rho(\varphi_t, t) z(\varphi_t, t) J(\xi, t) dV \\ &= \int_{\Omega} \left(\frac{D\rho}{Dt}(\varphi_t, t) z(\varphi_t, t) J(\xi, t) + \rho(\varphi_t, t) \frac{Dz}{Dt}(\varphi_t, t) J(\xi, t) \right. \\ &\quad \left. + \rho(\varphi_t, t) z(\varphi_t, t) \frac{\partial J}{\partial t}(\xi, t) \right) dV \\ &= \int_{\Omega} \rho(\varphi_t, t) \left(\frac{\partial z}{\partial t}(\varphi_t, t) + \mathbf{v}(\varphi_t, t) \cdot \nabla z(\varphi_t, t) \right) J(\xi, t) dV \end{aligned}$$

where Ω is fixed such that the differentiation and integration operations may be interchanged. Changing the variables back in terms of ξ gives the result in Eq.5.2.2. \square

Proposition 7. The PDE system describing the temperature dynamics $z = z(\xi, t)$ in a region Ω_t undergoing deformation along a velocity field $\mathbf{v} = \mathbf{v}(\xi, t)$ is given by

$$\rho C_p \frac{\partial z}{\partial t} = \nabla \cdot (\kappa \nabla z) - \rho C_p \mathbf{v} \cdot \nabla z + Gz \quad (5.2.3)$$

with initial condition $z(\xi, 0) = z_0$ and general boundary conditions:

$$\kappa \nabla z = \rho C_p \mathbf{v} \cdot (z - z_B) \quad (5.2.4)$$

where κ is the thermal conductivity constant, $G = G(\xi, t)$ is a continuous function which represents the linearized reaction-generation factor, $z(\xi, 0)$ is the initial temperature distribution, and $\kappa \nabla z(\xi, t)$ relates the flux over the boundary to the difference between z and the bulk temperature z_B , which gives the generalized boundary condition on $\partial\Omega_t$.

Proof. The *Conservation Law* describes the total heat balance in Ω_t as

$$C_p \frac{d}{dt} \int_{\Omega_t} \rho(\xi, t) z(\xi, t) dv = \int_{\partial\Omega_t} \kappa \nabla z(\xi, t) \cdot \nu ds + \int_{\Omega_t} G(\xi, t) z(\xi, t) dv$$

where ν is the normal component of ds . Substituting the expression in Eq.5.2.2 to the L.H.S. and the application of the *divergence theorem* for the integral over $\partial\Omega_t$ give Eq.5.2.3. The general boundary condition expression in Eq.5.2.4 similarly follows from the following expression for the total heat flux over $\partial\Omega_t$

$$\int_{\partial\Omega_t} \kappa \nabla z(\xi, t) ds = C_p \int_{\partial\Omega_t} \rho(\xi, t) \mathbf{v}(\xi, t) \cdot (z(\xi, t) - z_B) ds$$

□

One can note in Eq.5.2.3 that the convective transport phenomena given by

$$\mathbf{v} \cdot \nabla z = \frac{d\xi_i}{dt} \frac{\partial z_i}{\partial \xi_j}, \quad i, j = \{1, 2, 3\}$$

arises from the domain deformation [2], and vanishes if the motion of Ω is isochronic, i.e. Ω_t is constant for all $t \in [0, T]$ which is the case of the crystal growth processes in which material coordinates are fixed and only boundary undergoes motion. In the case when the boundary is time invariant, above expression leads to the well known expression of the reaction-diffusion parabolic PDE system with fixed domain since neither internal material points nor the boundary undergo motion.

In general, one needs to introduce the most general type of boundary conditions in the form of the Eq.5.2.4 in order to account for the transport of heat or concentration across the boundary interface which impacts the temperature or concentration inside the material region. Also, one might consider a combination of boundary conditions which reflect the process setup, for example, the presence of an encapsulation along a portion of the boundary. However, in this work, we relax this restriction and consider the boundary conditions associated with the Eq.5.2.3 to be of homogeneous Neumann type which represent zero-flux across the boundary interfaces.

5.2.2 Notation and function space description

In this section, we introduce necessary functional space notations which will enable the representation of the PDE system as an evolution type of equation on a Banach space [25, 27, 28]. The primary motivation for this comes from the necessity to define a single inner product space for which time dependent operators and associated spatially dependent functions which also evolve in

time, can be handled in consistent way.

A general Banach space is denoted as \mathcal{Z} . If \mathcal{Y} is a Banach space, $\mathcal{L}(\mathcal{Z}, \mathcal{Y})$ denotes the space of bounded linear operators $\mathcal{T} : \mathcal{Z} \rightarrow \mathcal{Y}$ and $\mathcal{L}(\mathcal{Z}) = \mathcal{L}(\mathcal{Z}, \mathcal{Z})$. The time index t is taken in the interval $[0, T]$ for notational convenience. The spatial domain at some time $t \in [0, T]$ is an open set of \mathbb{R}^n and will be denoted as Ω with smooth boundary $\partial\Omega$. The largest time-dependent spatial domain will be denoted as $\mathbf{\Omega}$ with boundary $\partial\mathbf{\Omega}$ such that $\Omega \subset \mathbf{\Omega}$ for all $t \in [0, T]$ and the initial configuration is denoted by Ω_0 . Spatial points are denoted by $z \in \Omega$. We use the notion of the function space imbedding to generalize the inner product since Ω changes over time. In this way the time-dependent functions and operators defined on Ω at each $t \in [0, T]$ can be considered by using the $L^2(\mathbf{\Omega})$ inner product. The space of interest consists of the functions having all derivatives up to order k continuous on Ω and $L^p(\mathbf{\Omega})$, $1 \leq p < \infty$ denotes the set of all measurable functions $\phi \in C^0(\mathbf{\Omega})$ with

$$\int_{\Omega} |\phi(\xi)|^p d\xi < \infty \quad \text{and} \quad \|\phi\|_p = \left\{ \int_{\Omega} |\phi(\xi)|^p d\xi \right\}^{\frac{1}{p}}$$

where $\|\phi\|_p$ is the norm on $L^p(\mathbf{\Omega})$. Then the space formed by functions defined on the time-varying spatial domain can be handled by use of the *zero extension* [25, Chapters 2-5]. Consider the family of functions $\phi(\xi, t)$ with members $\phi(\xi)$ defined for each $t \in [0, T]$ and on the associated subdomain $\Omega_t \subset \mathbf{\Omega}$. Then the zero extension is given by

$$\phi(\xi, t) = \begin{cases} \phi(\xi) & \text{for } z \in \Omega_t \\ 0 & \text{for } z \in \Omega_t^c \end{cases}$$

where $\Omega_t^c \subset \Omega$ is the complement of Ω_t . Then $L^p(\Omega_t)$ forms a family of function spaces which are precompact and imbedded in $L^2(\Omega)$. For arbitrary subdomain, $\Omega \subset \Omega$, we mean that $L^p(\Omega) \subset L^p(\Omega)$. Then the inner product $\langle \cdot, \cdot \rangle_{L^2(\Omega)}$ of the functions $\phi(\xi, t) \in L^2(\Omega)$ and $\psi(\xi, t) \in L^2(\Omega)$ at some time $t \in [0, T]$ is given by

$$\langle \phi, \psi \rangle_{L^2(\Omega)} = \int_{\Omega} \phi(\xi, t)\psi(\xi, t)d\xi = \int_{\Omega} \phi(\xi)\psi(\xi)d\xi + \int_{\Omega^c} 0 d\xi$$

Therefore, the above conditions provide a single inner product structure on $L^2(\Omega)$ which accounts for the time varying nature of the spatial domain and avoids the use of inner product spaces defined for each $t \in [0, T]$. We also denote the Hilbert space $H^{1,2}(\Omega)$ and $H^{2,2}(\Omega)$ with standard definitions and only remark here that $H^{1,2}(\Omega)$ and $H^{2,2}(\Omega)$ are dense in $L^2(\Omega)$ [25, 27, 28].

5.2.3 Parabolic PDE with time-dependent spatial domain

The initial and boundary value problem associated with Eq.5.2.3 is restated in the following form

$$\begin{aligned} \frac{\partial z(\xi, t)}{\partial t} &= A(\xi, t)z(\xi, t) \quad \text{on } \Omega \times [0, T] \\ \frac{\partial z(\xi, t)}{\partial \nu} &= 0 \quad \text{on } \partial\Omega \times [0, T], \\ z(\xi, 0) &= z_0(\xi) \quad \text{in } \Omega_0 \end{aligned} \tag{5.2.5}$$

where the operator $A(\xi, t) = \kappa_s \nabla^2 - \mathbf{v} \cdot \nabla + G_s$ is the spatial operator of the PDE which is defined on the time dependent domain $\Omega \subset \Omega$, with $\kappa_s = \kappa/(C_p \rho)$ and $G_s = G/(C_p \rho)$. As previously mentioned, we consider homogeneous Neumann

boundary conditions, where ν is the outward normal component of $\partial\Omega$ and $z_0(\xi)$ is the initial condition. In this work, we restrict the operator $A(\xi, t)$ to the class of operators which are linear, and strongly elliptic at each $t \in [0, T]$ [28]. This conditions enables the representation of the initial and boundary value problem in the Eq.5.2.5 as an initial value problem given by the nonautonomous evolution system on the state space $\mathcal{Z} = L^2(\Omega)$ in the following way.

First, we consider the family of linear operators $A(t)$ associated with the domain $D(A(t)) := H^{1,2}(\Omega) \cap H^{2,2}(\Omega)$. The operator $A(t) : D(A(t)) \subset L^2(\Omega) \rightarrow L^2(\Omega)$ defines an unbounded linear operator on $L^2(\Omega)$. For a state function $[z(t)](\cdot) = z(\xi, t)$ with $z(t) \in D(A(t))$ the operator $A(t)$ is defined as

$$A(\xi, t)z = A(t)z \quad (5.2.6)$$

Now we develop some of the technical aspects of the operator $A(t)$ beginning with the spectral properties. Let $\mu > 0$ be a constant where $G - \mu \leq 0$ for each $t \in [0, T]$. The operator $A(t)$ is closed and densely defined and the resolvent of $A(t)$ defined as $R_\mu(A(t), \mu) = (A(t) - \mu)^{-1}$ is compact. Then the resolvent set of $A(t)$, defined as $\rho(A(t)) := \{\lambda \in \mathbb{C} : (A(t) - \lambda) \text{ is one to one } (A(t) - \lambda)^{-1} : D \rightarrow D \text{ is bounded}\}$, consists of λ such that $R_\mu(A(t), \mu)$ is defined and compact. Since $A(t)$ satisfies assumption of strong elliptic property, the spectrum of $A(t)$, denoted $\sigma(A(t))$ consists of isolated eigenvalues $\{\lambda_n\}_{n=1}^\infty$ with finite multiplicity and no finite accumulation points [28]. This means that the spectrum $\sigma(A(t))$ is discrete for each $t \in [0, T]$ and moreover, that the eigenspace associated with a given eigenvalue is finite-dimensional. Denote the projection on the n^{th} eigenfunction as $E_n(\cdot) = \langle \phi_n, \cdot \rangle \phi_n$ where ϕ_n are the set of eigenfunctions associated with $\lambda(t)$.

We have that for all $t \in [0, T]$ and $z \in D(A(t))$

$$\begin{aligned} R_\mu(A(t), \mu)z &= (A(t) - \mu)^{-1}z = \sum_n (\lambda_n(t) - \mu)^{-1}E_n(z) \\ &\leq \max_{t \in [0, T]} (\lambda_n(t) - \mu)^{-1} \sum_n E_n(z) \\ &= \max_{t \in [0, T]} (\lambda_n(t) - \mu)^{-1}z \end{aligned}$$

Then there exist positive constants M and k such that

$$\|(A(t) - \mu)^{-1}\| \leq M(\mu - k)^{-1}$$

It follows that there exists a sector

$$S_\omega = \{\lambda \in \mathbb{C} : |\arg \lambda| < \frac{\pi}{2} + \omega\} / \{0\}, \quad \omega \in (0, \pi/2]$$

in the resolvent set $\rho(A(t))$ in which the spectrum of $A(t)$ is contained, i.e. $\sigma(A(t)) \subset \mathbb{C}/S_\omega$, which means that $A(t)$ is a *sectorial operator*. Moreover, $\{0\} \notin \sigma(A(t))$ so that the operator $A(t)$ has bounded inverse, i.e. $A(t)^{-1} \leq L$ for constant $L > 0$.

We have established some properties of the nonautonomous parabolic operator $A(t)$ on time-independent spatial domains [26] which provides that for *each* $t \in [0, T]$ the operator $A(t)$ is the infinitesimal generator of an analytic semigroup on $L^2(\Omega)$ and that $A(t)$ is the infinitesimal generator of a *family* of analytic semigroups of bounded linear operators on $L^2(\Omega)$. The initial and boundary value problem in Eq.5.2.5 is restated as the initial value problem given by the nonautonomous evolution system on the state space $\mathcal{Z} = L^2(\Omega)$

$$\frac{dz(t)}{dt} = A(t)z(t), \quad z(s) = z_s \quad (5.2.7)$$

for $0 \leq s < t \leq T$ and where $z_0 \in L^2(\Omega)$ is the initial condition. The solution of the Eq.5.2.7 can be represented by way of the following Theorem [26, Chapter 5, Theorem 6.1, Theorem 6.8].

Theorem 5.2.2. The operator $A(t)$ with domain $D(A(t))$ is dense in $L^2(\Omega)$ and independent of $t \in [0, T]$, gives that for every $0 \leq s < t \leq T$ and $z(s) \in L^2(\Omega_s)$, there exists a unique solution of the initial value problem in the Eq.5.2.7 expressed as

$$z(t) = U(t, s)z_s, \quad \text{for } 0 \leq s \leq t \leq T \quad (5.2.8)$$

where $U(t, s)$, $0 \leq s < t \leq T$, is a two parameter evolution operator.

The operator $U(t, s)$ can be explicitly determined, but its construction is not essential in this work, however by using the operator $U(t, s)$ one can define the input driven solution to the Eq.5.2.7 in terms of the two-parameter evolutionary system as

$$z(t) = U(t, s)z_s + \int_s^t U(t, \tau)u(\tau)d\tau, \quad \text{for } 0 \leq s \leq t \leq T \quad (5.2.9)$$

5.3 Optimal boundary controller synthesis

We consider the boundary control problem for the PDE system in which the boundary conditions in the Eq.5.2.5 are replaced with

$$\frac{\partial z}{\partial \nu} = u(t) \quad \text{on } \partial\Omega \times [0, T] \quad (5.3.1)$$

where the continuous function $u(t)$ is the manipulated input at the domain's boundary. In contrast to the case of distributed control, i.e. control within

the spatial domain, the application of control to the boundary requires some additional modifications to the original system. This is also motivated by consideration of more realistic two dimensional crystal growth process in which one rarely can consider the process model with the distributed actuation since the process has inherently boundary applied actuation.

5.3.1 System representation

The formulations proposed in [29] and [30] are explored and utilized in finding a transformation which enables the representation of the boundary control problem as a distributed control problem. To this end, we consider the following linear system on the state space $\mathcal{Z} = L^2(\Omega)$ for each $t \in [0, T]$:

$$\begin{aligned}\frac{dz(t)}{dt} &= \mathfrak{A}(t)z(t) \\ \mathfrak{B}u(t) &= u(t)\end{aligned}\tag{5.3.2}$$

The operator \mathfrak{A} is closed on \mathcal{Z} , and the boundary operator $\mathfrak{B} : \mathcal{Z} \rightarrow \mathbb{R}$ is linear with $D(\mathfrak{A}) \subseteq D(\mathfrak{B})$. It is assumed that the function $b(\xi, t)$ exists such that for all $u(t)$ and $\mathfrak{B}u(t) \in D(\mathfrak{A})$ we have,

$$\mathfrak{B}b(\xi, t)u(t) = u(t)\tag{5.3.3}$$

We introduce the transformation $p(t) = z(t) - b(t)u(t)$ which leads to the following system,

$$\begin{aligned}\frac{dp(t)}{dt} &= A(t)p(t) + (\mathfrak{A}(t)b(t))u(t) - b(t)\dot{u}(t) \\ p(0) &= p_0 \in D(A)\end{aligned}\tag{5.3.4}$$

where the function $\dot{u}(t) = du(t)/dt$ is the time derivative of the input. The associated operator $A(t)$ is defined on the state space \mathcal{Z} such that:

$$D(A(t)) = \{z \in D(\mathfrak{A}(t)) / \mathfrak{B}z = 0\} \quad (5.3.5)$$

and

$$A(t)z = \mathfrak{A}(t)z \quad \text{in} \quad D(A(t)) \quad (5.3.6)$$

The conditions assumed are that $A(t)$ is an infinitesimal generator of a family of strongly continuous semigroup for each $t \in [0, T]$ and that the operators $b(\xi, t)$ and $\mathfrak{A}(t)b(\xi, t)$ are bounded and continuous on $s \leq \tau \leq T$ such that the Eq.5.3.4 has the unique solution:

$$p(t) = U(t, s)p_0 - \int_s^t U(t, \tau)b(\tau)\dot{u}(\tau)d\tau + \int_s^t U(t, \tau)(\mathfrak{A}(\tau)b(\tau))u(\tau)d\tau \quad (5.3.7)$$

where for $0 \leq s \leq t \leq T$ the operator $U(t, s)$ is the two parameter evolution operator from the Eq.5.2.8. The solution of the system in the Eq.5.3.2 takes the form:

$$z(t) = p(t) + b(t)u(t) \quad (5.3.8)$$

where $z_0 = p_0 + b(0)u(0)$ is the initial condition of the Eq.5.3.2. Then the original boundary control problem can be then represented as a distributed control problem by the following system on the extended state space $\mathbb{R} \oplus \mathcal{Z}$,

$$\frac{dp^e(t)}{dt} = \begin{pmatrix} 0 & 0 \\ \mathfrak{A}(t)b(t) & A(t) \end{pmatrix} p^e(t) + \begin{pmatrix} 1 \\ -b(t) \end{pmatrix} u^e(t) \quad (5.3.9)$$

where the state and the input are given by:

$$p^e(t) = \begin{pmatrix} u(t) \\ p(t) \end{pmatrix}, \quad p^e(0) = \begin{pmatrix} u(0) \\ p(0) \end{pmatrix}, \quad \text{and} \quad u^e(t) = \frac{du(t)}{dt} \quad (5.3.10)$$

We represent the abstract boundary control system representation in the Eq.5.3.9 as:

$$\frac{dp^e(t)}{dt} = A^e(t)p^e(t) + B^e(t)u^e(t) \quad (5.3.11)$$

and one can notice that the time derivative of $u(t)$ appears as the input to the system in the Eq.5.3.11 which corresponds to integral feedback of the state $z(t)$ by the input and is expressed as:

$$u^e = \left\langle \begin{pmatrix} h \\ g \end{pmatrix}, \begin{pmatrix} u(t) \\ p(t) \end{pmatrix} \right\rangle_{\mathbb{R} \oplus \mathcal{Z}} = hu(t) + \langle g, p(t) \rangle_{\mathcal{Z}} \quad (5.3.12)$$

where $h \in \mathbb{R}$, $g \in \mathcal{Z}$ such that $(h \ g)^T \in \mathbb{R} \oplus \mathcal{Z}$.

5.3.2 Linear Quadratic Regulator synthesis

In order to obtain a stabilizing feedback regulator for above boundary control formulation, we consider the following quadratic optimization problem,

$$\min_{u^e} \int_0^T (|Qp^e(\tau)|^2 + |Ru^e(\tau)|^2) d\tau + \langle Qp^e(T), p^e(T) \rangle$$

subject to (5.3.13)

$$\frac{dp^e(t)}{dt} = A^e(t)p^e(t) + B^e(t)u^e(t)$$

where $p^e(t)$ and $u^e(t)$ are the input and state defined in the Eq.5.3.10, [31] and $p^e(0) \in \mathbb{R} \oplus \mathcal{Z}$. The input is minimized over all possible controls $u^e(t)$

subject to the differential constraint given by the boundary control system. The operator $Q \in \mathcal{L}(\mathbb{R} \oplus \mathcal{Z})$ is self-adjoint and nonnegative and $R \in \mathcal{L}(\mathbb{R})$ is coercive, where Q is the state weight operator, R is the input penalty operator. Since $A(t)$ generates a C_0 -semigroup on $L^2(\Omega)$ for all $t \in [0, T]$ which gives the state evolution in the Eq.5.3.7, the optimization problem in the Eq.5.3.13 has the continuous and unique minimizing solution $u^e(t)$ given by the feedback formula

$$u_{\min}^e(t) = -R^{-1}(B^e(t))^T \Pi(t) p_{\min}^e(t) \quad (5.3.14)$$

where the operator $\Pi(t) \in \mathcal{L}(\mathbb{R} \oplus \mathcal{Z})$ is the strongly continuous, self adjoint, nonegative solution of the differential Riccati equation

$$\dot{\Pi}(t) + (A^e)^* \Pi(t) + \Pi(t) A^e - \Pi(t) B^e(t) (B^e(t))^T \Pi(t) + Q = 0 \quad (5.3.15)$$

with final value $\Pi(T) = \Pi_0$, where $(A^e)^*$ is the conjugate transpose of A^e [30, 31].

5.4 Application of optimal boundary control to CZ crystal growth process

In this section, we apply the abstract results of in the previous section to the 2D representation of the Czochralski (CZ) crystal temperature boundary control problem which is depicted in the Fig.5.2. The spatial domain Ω is considered as an axisymmetric region with radius $R = 1$, time-dependent length $l(t)$, and the spatial points are denoted $r \in [0, 1]$ and $z \in [0, l(t)]$ where $l(t)$ is continuous and bounded with maximum length L . The temperature dynamics are governed by the PDE system in the Eq.5.2.3 with $G = 0$ and

$dl(t)/dt = \mathbf{v}_\xi(t)$ is the boundary velocity at $l(t)$. The resulting PDE expression coincides with the CZ crystal temperature model utilized by [21, 22]

$$\text{Pe} \frac{\partial z}{\partial t} = \nabla \cdot \kappa_r \nabla z - \text{Pe} \mathbf{v}_\xi(t) \frac{\partial z}{\partial \xi} \quad (5.4.1)$$

where the Peclet number $\text{Pe} = \rho C_p v_0 R_c / \kappa_s$ is a dimensionless variable determined by the parameters v_0 , R_c , κ_s and κ_r which are positive constants and denote the nominal growth rate, crucible radius, regional thermal conductivity and crystal thermal conductivity ratio, respectively. For this example, the boundary velocity $\mathbf{v}_\xi(t)$ of the crystal region is due to the action of a mechanical pulling arm which draws the crystal from a melt and the spatial domain grows as the melt solidifies at the melt-crystal interface. Therefore, given an initial temperature perturbation in the crystal region Ω_0 at $t = 0$, we wish to optimally stabilize the temperature distribution in the time-dependent spatial domain Ω around some nominal profile using the control formulation the Section 5.3.2. The temperature $z(r, \xi, t)$ governed by the PDE in the Eq.5.4.1 is in deviation form such that the stabilized temperature will be $z(r, \xi, t) = 0$ throughout all Ω at some time $t \in (0, T]$.

5.4.1 Eigenfunctions and eigenvalues

The operator of the PDE in Eq.5.4.1 takes the form of the general operator considered in the Eq.5.2.5 with $A(\xi, t) = A(r, \xi, t)$. For smooth function $\phi(r, \xi, t)$, the associated operator linear operator $A(t)$ on the state space $\mathcal{Z} = L^2(\Omega)$ is expressed in cylindrical coordinates as

$$A(t)\phi = \frac{1}{r} \frac{\partial}{\partial r} \left(\kappa_0 r \frac{\partial \phi}{\partial r} \right) + \kappa_0 \frac{\partial^2 \phi}{\partial \xi^2} - \mathbf{v}_\xi(t) \frac{\partial \phi}{\partial \xi} \quad (5.4.2)$$

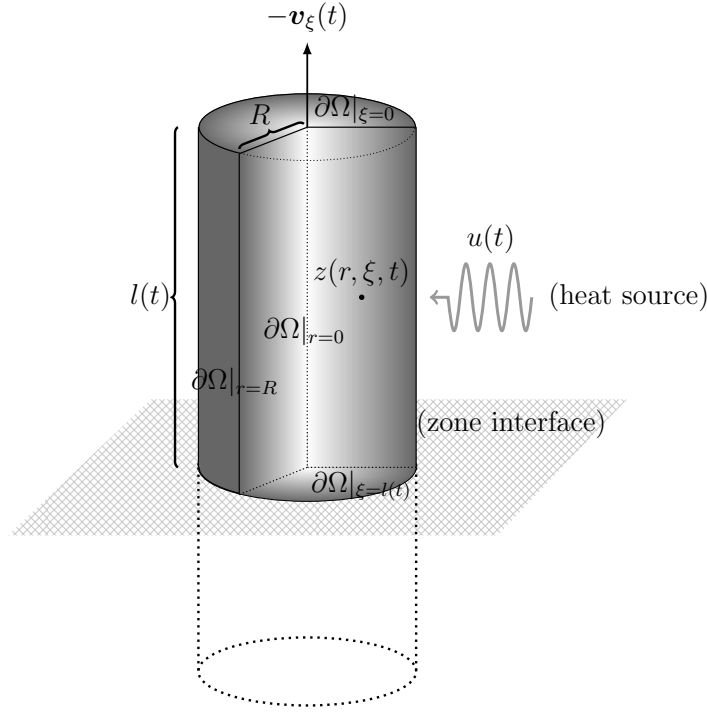


Figure 5.2: Cutaway of general process diagram of axisymmetric cylindrical slab with radius R , length $l(t)$, and temperature distribution $z(r, \xi, t)$ for $(r, \xi) \in \Omega$ at time $t \in [0, T]$. The spatial domain time-dependence is due to the change in the boundary at $\partial\Omega|_{\xi=l(t)}$ which is moving with velocity $\mathbf{v}_\xi(t)$. The temperature distribution of the slab is controlled by heat input $u(t)$ applied to the boundary at $\partial\Omega|_{r=R}$.

with $\kappa_0 = \kappa_s/\text{Pe}$. For each $t \in [0, T]$, we consider the eigenvalue problem $A(t)\phi(r, \xi, t) = \lambda(t)\phi(r, \xi, t)$ subject to the set of homogeneous Neumann boundary conditions

$$\frac{\partial\phi}{\partial z}(r, 0, t) = 0, \quad \frac{\partial\phi}{\partial z}(r, l(t), t) = 0 \quad (5.4.3)$$

$$\frac{\partial\phi}{\partial r}(0, \xi, t) = 0, \quad \frac{\partial\phi}{\partial r}(1, \xi, t) = 0 \quad (5.4.4)$$

The Eq.5.4.2 is separable and subject to the boundary conditions in the Eq.5.4.3 yields the family of time-dependent eigenfunctions $\phi_m^{(1)}(\xi, t)$ with $m \in \mathbb{N}$

$$\begin{aligned} \phi_m^{(1)}(\xi, t) = & \\ B_m(t)e^{\frac{1}{2}\kappa_0^{-1}\mathbf{v}_\xi(t)\xi} & \left(\cos\left(\frac{m\pi}{l(t)}\xi\right) - \frac{1}{2}\kappa_0^{-1}\frac{\mathbf{v}_\xi(t)}{(m\pi/l(t))}\sin\left(\frac{m\pi}{l(t)}\xi\right) \right) \end{aligned} \quad (5.4.5)$$

The coefficients

$$B_m(t) = \sqrt{\frac{2}{l(t)}} \left(1 + \left(\frac{\mathbf{v}_\xi(t)}{2\kappa_0(m\pi/l(t))} \right)^2 \right)^{-\frac{1}{2}} \quad (5.4.6)$$

orthonormalize $\phi_n(\xi, t)$ with respect to the adjoint eigenfunctions $\psi_m^{(1)}(\xi, t)$ determined as

$$\psi_m^{(1)}(\xi, t) = e^{-\kappa_0^{-1}\mathbf{v}_\xi(t)\xi}\phi_m^{(1)}(\xi, t) \quad (5.4.7)$$

At each $t \in [0, T]$, the set of adjoint eigenfunctions ψ_m are associated with the eigenvalue problem $A^*(t)\psi(r, \xi, t) = \lambda(t)\psi(r, \xi, t)$ with imposed boundary conditions in the Eqs.5.4.4-5.4.3, where the adjoint operator $A^*(t)$ is given by

$$A^*(t)\psi = \frac{1}{r}\frac{\partial}{\partial r}\left(\kappa_0 r \frac{\partial \psi}{\partial r}\right) + \kappa_0 \frac{\partial^2 \psi}{\partial \xi^2} + \mathbf{v}_\xi(t) \frac{\partial \psi}{\partial \xi} \quad (5.4.8)$$

Subject to the boundary conditions in the Eq.5.4.4, the eigenfunctions in $r \in [0, R]$ for all $t \in [0, T]$ and $n \in \mathbb{N}$ are given in terms of Bessel functions J_p of

the first kind and p^{th} order, and are determined as

$$\begin{aligned} \phi_n^{(2)}(r) &= \frac{\sqrt{2}}{J_0(\alpha_n)} J_0(\alpha_n r) \\ \alpha_0 &= 0, \quad \alpha_1 = 3.83, \quad \alpha_2 = 7.016, \quad \alpha_3 = 10.173, \\ \alpha_4 &= 13.323, \quad \alpha_5 = 16.471, \quad \alpha_6 = 19.616, \dots \end{aligned} \tag{5.4.9}$$

with adjoints $\psi_n^{(2)}(r) = r\phi_n^{(2)}(r)$. The coefficients α_n are the n^{th} zeros of J_1 type Bessel functions which are readily available from appropriate tables, and both of $\phi_n^{(2)}$ and the corresponding adjoints $\psi_n^{(2)}$ are of class $C^\infty(0, 1)$.

The time-dependent eigenvalues associated with $\phi(r, \xi, t)$ and $\psi(r, \xi, t)$ are determined as

$$\lambda_{mn}(t) = -\kappa_0 \left\{ \left(\frac{m\pi}{l(t)} \right)^2 + \alpha_n^2 \right\} - \frac{1}{2} \kappa_0^{-1} \frac{\mathbf{v}_\xi(t)^2}{2} \tag{5.4.10}$$

One can note that the eigenvalues in the Eq.5.4.10 are real and negative for all $t \in [0, T]$ so that the spectrum $\sigma(A(t))$, which is the same as $\sigma(A^*(t))$, is discrete and lies in the left half-plane of \mathbb{C} , with $\{0\} \notin \sigma(A(t))$ for $\mathbf{v}_\xi(t) \neq 0$, and the eigenspaces are one dimensional. Then the growth bound $\omega_0 \in \mathbb{R}$ is given by

$$\omega_0 = \sup_{m,n \geq 1, t \in [0, T]} \text{Re}(\lambda_{mn}(t)) < 0 \tag{5.4.11}$$

and the PDE in the Eq.5.4.1 is dissipative. Moreover, the operator $A(t)$ in the Eq.5.4.2, is the infinitesimal generator of a family of stable C_0 -semigroups (and similarly the same holds for the adjoint operator $A^*(t)$ in the Eq.5.4.8).

Remark 5.4.1. In order to clarify the notation with respect to the application considered in this Section 5.4 we note the following. For $z(r, \xi) \in L^2(\Omega)$ and length $l(t)$ at time $t \in [0, T]$, the inner product with the eigenfunction $\phi(r, \xi, t)$

is given by

$$\begin{aligned} \langle z, \phi \rangle &= \int_0^L \int_0^1 z(r, \xi) \phi^{(1)}(\xi, t) \phi^{(2)}(r) dr d\xi \\ &= \begin{cases} \int_0^{l(t)} \int_0^1 z(r, \xi) \phi^{(1)}(\xi) \phi^{(2)}(r) dr d\xi, & \text{for } (r, \xi) \in \Omega \\ 0 & \text{for } (r, \xi) \in \Omega^c \end{cases} \end{aligned} \quad (5.4.12)$$

due to the definition of functions defined on the time-dependent spatial domain in the Section 5.2. Also, since $\phi_m^{(1)}$ and $\phi_n^{(2)}$ are orthogonal to $\psi_i^{(1)}$ and $\psi_j^{(2)}$, respectively, we have that

$$\langle \phi_{mn}, \psi_{ij} \rangle = \begin{cases} 1 & \text{if } m = n = i = j \\ 0 & \text{otherwise} \end{cases} \quad (5.4.13)$$

and denote this relation $\langle \phi_{mn}, \psi_{ij} \rangle = \delta_{mn}$. Then for each $t \in [0, T]$, the projection of the operator $A(t)$ and $A^*(t)$ on to the eigenspaces formed by the basis functions ϕ_m and ψ_n is given as the following

$$\langle A(t)\phi_m(r, \xi, t), \psi_n(r, \xi, t) \rangle = \lambda_{nn}(t) \quad (5.4.14)$$

5.4.2 The optimal boundary control problem synthesis

The control input $u(t)$ is applied to the crystal boundary at $R = 1$ as depicted in the Fig.5.2 and one needs to determine the necessary functions to transform the system in the boundary control problem. Therefore, the boundary conditions in the Eq.5.4.4 are modified to include the input and are then prescribed

by the following

$$\frac{\partial z}{\partial r}(0, \xi, t) = 0, \quad \frac{\partial z}{\partial r}(1, \xi, t) = u(t) \quad (5.4.15)$$

For each $t \in [0, T]$, the operator $\mathfrak{A}(t)$ is defined as

$$\mathfrak{A}(t)\phi := \frac{1}{r} \frac{\partial}{\partial r} \left(\kappa_0 r \frac{\partial \phi}{\partial r} \right) + \kappa_0 \frac{\partial^2 \phi}{\partial \xi^2} - \mathbf{v}_\xi(t) \frac{\partial \phi}{\partial \xi} \quad (5.4.16)$$

with the domain

$$D(\mathfrak{A}(t)) = \left\{ \phi \in L^2(\Omega) : \phi, \frac{\partial \phi}{\partial r}, \frac{\partial \phi}{\partial \xi} \text{ are a.c.}, \frac{\partial^2 \phi}{\partial r^2}, \frac{\partial^2 \phi}{\partial \xi^2} \in L^2(\Omega), \right. \\ \left. \text{and } \frac{\partial \phi}{\partial r}(0, \xi, t) = 0, \frac{\partial \phi}{\partial \xi}(r, 0, t) = 0, \frac{\partial \phi}{\partial \xi}(r, l(t), t) = 0 \right\} \quad (5.4.17)$$

where a.c. means absolutely continuous. The boundary operator $\mathfrak{B} : L^2(\Omega) \rightarrow \mathbb{R}$ is defined as

$$\mathfrak{B}\phi := \frac{\partial \phi}{\partial r}(1, \xi, t), \quad D(\mathfrak{B}) = D(\mathfrak{A}) \quad (5.4.18)$$

The function b is selected as $b(r, \xi, t) = \frac{1}{2}r^2 - \frac{3}{2}l(t)\xi^2 + \xi^3$ which satisfies the relation $\mathfrak{B}bu(t) = u(t)$ with $b(r, \xi, t) \in D(\mathfrak{A}(t))$. By using the transformation $p(t) = z(t) - bu(t)$, the Eq.5.3.4 and the operator $A(t)\phi = \mathfrak{A}(t)\phi$ is obtained with domain in the Eq.5.3.5 defined as

$$D(A(t)) = D(\mathfrak{A}(t)) \cap \ker(\mathfrak{B}) \\ = \left\{ \phi \in L^2(\Omega) : \phi, \frac{\partial \phi}{\partial r}, \frac{\partial \phi}{\partial \xi} \text{ are a.c.}, \frac{\partial^2 \phi}{\partial r^2}, \frac{\partial^2 \phi}{\partial \xi^2} \in L^2(\Omega), \text{ and} \right. \quad (5.4.19) \\ \left. \frac{\partial \phi}{\partial r}(0, \xi, t) = 0, \frac{\partial \phi}{\partial r}(1, \xi, t) = 0, \frac{\partial \phi}{\partial \xi}(r, 0, t) = 0, \frac{\partial \phi}{\partial \xi}(r, l(t), t) = 0 \right\}$$

Finally, the boundary control system representation in the Eq.5.3.1 is then obtained as the following:

$$\frac{dp^e(t)}{dt} = \begin{pmatrix} 0 & 0 \\ \mathfrak{A}(t)b & A(t) \end{pmatrix} \begin{pmatrix} u(t) \\ p(t) \end{pmatrix} + \begin{pmatrix} 1 \\ -b \end{pmatrix} \dot{u}(t) \quad (5.4.20)$$

Remark 5.4.2. In this example the process model for the crystal temperature distribution is dissipative since generation terms are not present in the PDE system given in the Eq.5.4.1. The control objective becomes one of stability enhancement and to achieve or maintain a desired nominal temperature distribution in order to avoid the proliferation of crystal defects, for example, due to thermoelastic stresses as discussed in the introduction. Other control design features, such as the problem of optimal actuator placement [32, 33], as well as the optimization problem in the presence of prescribed input and state constraints [34], can be incorporated into the boundary control framework presented in this work.

5.4.3 Numerical implementation

We apply the Galerkin method in order to simulate the temperature dynamics governed by the PDE in the Eq.5.4.1 defined on the time-dependent spatial domain Ω_t which has also been utilized by [14] to prove existence of solutions to the nonhomogeneous form of the Eq.5.2.5. In this approach, we seek solutions of the Eq.5.2.5 in the form of

$$z_n(t) = \sum_{n=1}^{\infty} a_n(t) \phi_n(\xi, t) \quad (5.4.21)$$

where $\phi_n(\xi, t) = \{\phi_1(t), \dots, \phi_n(t), \dots\}$ form a time-dependent countable basis of $L^2(\Omega)$ for each $t \in [0, T]$.

The coefficients $a_n(t) = \{a_1(t), \dots, a_n(t), \dots\}$ are determined from the projection of the system on $L^2(\Omega)$ at each $t \in [0, T]$

$$\left\langle \frac{dz}{dt}, \phi_n(t) \right\rangle = \langle A(t)\phi_n(t), \phi_n(t) \rangle + \langle u(t), \phi_n(t) \rangle \quad (5.4.22)$$

where $u(t) \in L^2(\Omega)$ is some nonhomogeneous function. For our particular system, one obvious choice is for $\phi_n(\xi, t)$ is the set of orthogonalized eigenfunctions $\phi(r, \xi, t)$ and $\psi(r, \xi, t)$ in the Section 5.4.1 such that the system in the Eq.5.2.7 is reduced to a system of ordinary differential equations. The Galerkin approximations of solutions take a finite set of the first N basis functions which span a finite-dimensional time-dependent vector space H . The number of modes N is chosen to provide a balance between numerical accuracy and computational efficiency. The boundary control system representation in the Eq.5.4.20 is determined as

$$\frac{d\tilde{p}(t)}{dt} = \tilde{A}^e(t)\tilde{p}(t) + \tilde{B}^e\dot{u}(t) \quad (5.4.23)$$

where $\tilde{p}(t) = (u(t) \ a_1(t) \ \dots \ a_n(t))^T$, $\tilde{A}^e = \begin{pmatrix} 0 & \\ \tilde{\mathfrak{A}}(t)b(r, \xi) & \tilde{A}(t) \end{pmatrix}$ and $\tilde{B}^e = (1 \ \tilde{B})^T$, with $\tilde{\mathfrak{A}}(t)b(r, \xi) = \langle \tilde{\mathfrak{A}}(t)b(r, \xi), \phi(r, \xi, t) \rangle$ and

$\tilde{B}_n = \langle -(\frac{1}{2}r^2 - \frac{3}{2}l(t)\xi^2 + \xi^3), \phi_n(r, \xi, t) \rangle$ as vectors of size $N \times 1$, and $\tilde{A}(t)$ is the $N \times N$ diagonal matrix with elements as the finite set of the first N eigenvalues in the Eq.5.4.10. One can note that the control law developed in the Section 5.3.2 is based on the solution of the operator Riccati equation on the infinite-dimensional state space \mathcal{Z} . Even though an analytic solution of this equation can be determined, the resulting expression contains an infinite number of terms which is not suitable in practical applications. Other

works have considered related approaches to developing finite-dimensional regulators for infinite-dimensional systems [35, 36]. In our present case, we use the finite-dimensional system representation determined in this section such that the controller synthesis then takes on the finite-dimensional form of the optimization problem in the Eq.5.3.13 where operator $\Pi(t)$ in the Eq.5.3.14 is calculated as the solution to the analogous differential matrix Riccati equation at each time instance and we assume full state feedback. The structure of the extended state system in the Eq.5.4.23 plays a role in the choice of state weights in the finite-dimensional control parameter $\tilde{Q}^e = \begin{pmatrix} Q_{11} & 0 \\ 0 & Q_{NN} \end{pmatrix}$ which is typically taken with only positive entries along its main diagonal. In particular, the first entry \tilde{Q}_{11} influences the first state of the extended state system $\tilde{p}_1 = u(t)$ and therefore acts as the input penalty term to the extended state system.

5.4.4 Simulation results

We follow the procedure described in the previous section and utilize the set of $N = 10$ time-dependent eigenfunctions determined in the Section 5.4.1 to approximate the original PDE system. Increasing this number of modes showed no significant change in the simulation results which indicates that the chosen value of N is sufficient in capturing the dominant dynamics of the system. The control parameter \tilde{Q} is taken with a weight on the states $\tilde{Q}_{NN} = 10 I_{10 \times 10}$ and the input penalty term is taken as $Q_{11} = 0.1$. The Table 5.1 contains numerical and physical process model parameters for the Czochralski crystal growth method used in the simulated process model [23].

The domain length $l(t)$ and boundary velocity $v_\xi(t)$ evolution are shown in the Fig.5.3. In this case, the crystal length is increasing at the corresponding velocity so the spatial domain is growing during the entire simulation. The input profile $u(t)$ generated by the finite-dimensional version of the optimization problem in the Eq.5.3.13 for the system in the Eq.5.4.20 is shown in Fig.5.4, which is applied to the boundary at the crystal boundary at $r = 1$ and distributed along the crystal length $l(t)$. As previously mentioned, the crystal is formed in a thermal environment and one method of control actuation proposed in [23] is via a heating source placed along the crystal length. The input is interpreted from a physical point of view as a change from a nominal heater temperature u_{nominal} which implies adjusting the input accordingly.

Table 5.1: Table of physical and numerical parameters

Parameter	Value	Dimensionless value
Ambient temperature, z_{ref}	1430 K [†]	0
Heater temperature, u_{nominal}	1935 K [†]	0
Crystal temperature, z	-	z
Length, $l(t = 0)$	10.95 cm [†]	2.64
Peclet number, Pe	-	0.1
Scaled conductivity, κ_s	-	0.025
Time scale, t	8.3 min	100
Sampling time, dt	5 samples/ s	1
Spatial discretization, r, ξ	-	200, 600

[†] Parameters obtained from [23].

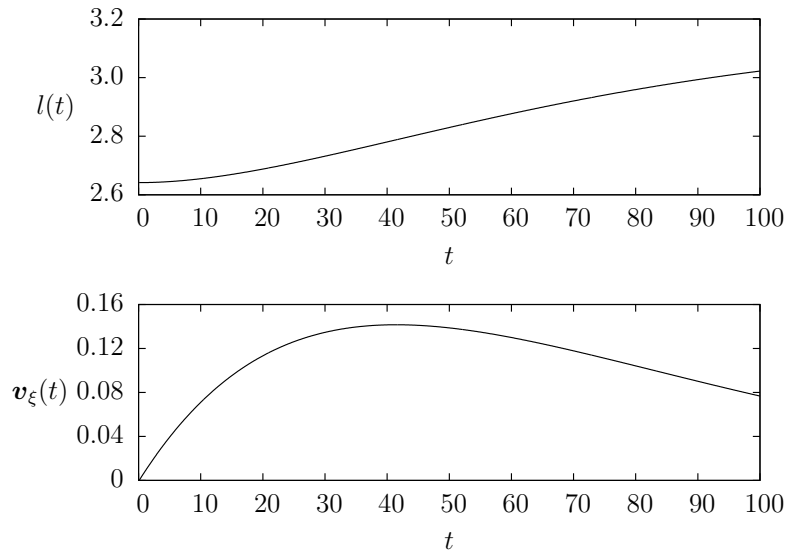


Figure 5.3: Crystal length $l(t)$ and boundary velocity $v_\xi(t)$ evolution.

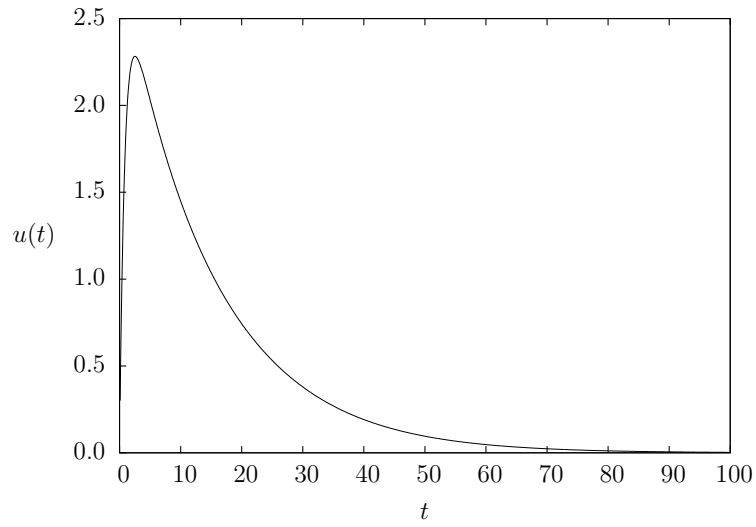


Figure 5.4: Boundary Input $u(t)$

The closed loop system crystal temperature distributions for $(r, \xi) \in [0, 1] \times [0, l(t)]$ at the time-instances $t = 0$, $t = 5$, $t = 20$ and $t = 50$ are shown in the Figs.5.6-5.7. From the input profile, it can be seen that the controller response converges towards zero which corresponds to the stabilization of the crystal temperature to the nominal zero distribution which can be seen from the Figs.5.6-5.7 where the range of the distribution is significant less in the second set of plots than the initial distribution. The overall temperature profile is captured in the plot of the total energy of the system which is shown in the Fig.5.5. The total energy of the open loop system with no input $u(t)$ applied at the boundary is also depicted alongside the closed loop temperature profile in the Fig.5.5. The closed loop system shows a faster convergence to the nominal temperature distribution than the open loop system which clearly demonstrates that the derived controller is effective in enhancing the stability of the system in the time-dependent region, through boundary control actuation.

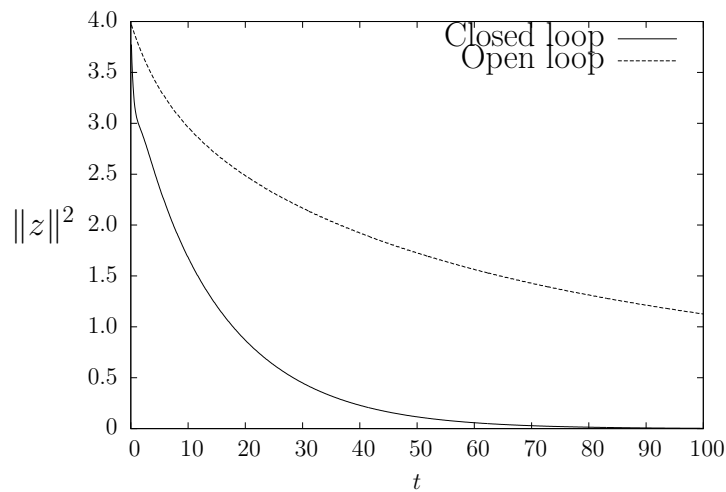


Figure 5.5: Total system energy for closed and open loop systems.

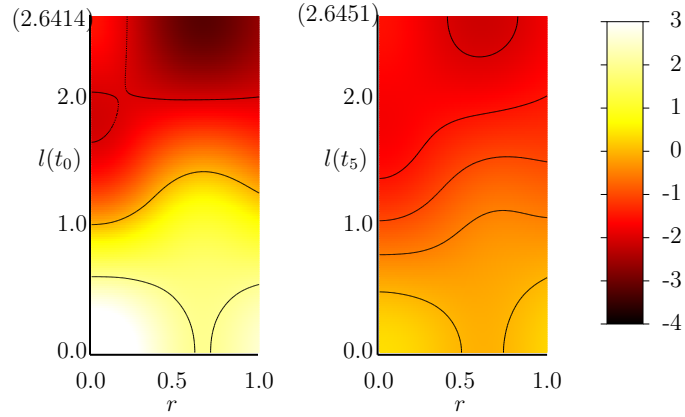


Figure 5.6: (Left) Initial crystal temperature distribution at $t = 0$. (Right) Temperature distribution at $t = 5$.

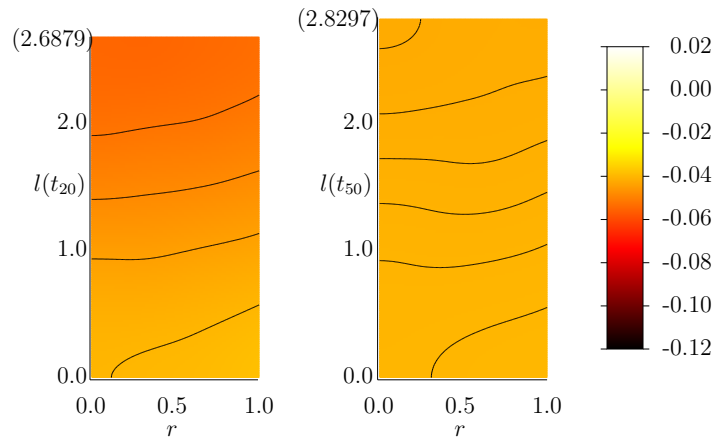


Figure 5.7: (Left) Initial crystal temperature distribution at $t = 20$. (Right) Temperature distribution at $t = 50$.

5.5 Summary

This chapter considered the control problem with boundary actuation for a class of diffusion-convection-reaction process modelled by parabolic PDEs defined on time-dependent spatial domains where the change in the spatial domain is due to the time-evolution of the boundary. The properties of the PDE spatial operator were discussed which enabled the representation of the PDE as a nonautonomous parabolic evolution system on an appropriately defined function space. The transformation of this parabolic system into a boundary control problem facilitated the synthesis of a feedback regulator based on a quadratic minimization scheme. The Czochralski crystal growth process with 2D crystal temperature regulation problem was considered as an illustrative example and the proposed controller formulation was applied. The numerical results of the simulated system demonstrated the stabilization of the temperature distribution in the time-dependent crystal region by the optimal feedback regulator through the boundary control actuation.

Bibliography

- [1] Ng J, Dubljevic S. Optimal boundary control of a diffusion-convection-reaction PDE model with time-dependent spatial domain: Czochralski crystal growth process. *Chemical Engineering Science*. 2012;67(1):111–119.
- [2] Marsden J, Hughes T. *Mathematical Foundations of Elasticity*. New York, U.S.A.: Dover Publications. 1983.
- [3] Chorin AJ, Marsden JE. *A Mathematical Introduction to Fluid Mechanics 3rd Ed*. New York, U.S.A.: Springer. 1983.
- [4] Leal G. *Laminar Flow and Convective Transport Processes*. Boston, U.S.A: Butterworth-Heinemann. 1992.
- [5] Christofides PD. *Nonlinear and Robust Control of PDE Systems: Methods and Applications to Transport-Reaction Processes*. Boston: Birkhäuser. 2001.
- [6] Ray WH. *Advanced Process Control*. New York: McGraw-Hill. 1981.
- [7] Kato T. *Perturbation theory for linear operators*. New York: Springer-Verlag. 1966.
- [8] Lasiecka I. Unified theory for abstract parabolic boundary problems: A semigroup approach. *Appl Math & Optim*. 1980;6:287–333.
- [9] Acquistapace P. Evolution operators and strong solutions of abstract linear parabolic equations. *Diff Int Eqns*. 1988;1:433–457.
- [10] Tanabe H. *Functional analytic methods for partial differential equations*. New York: Marcel Dekker Inc. 1997.

- [11] Triggiani R. Boundary feedback stabilization of parabolic equations. *Appl Math Optim.* 1980;6:201–220.
- [12] Acquistapace P, Flandoli F, BTerreni. Initial boundary value problems and optimal control for nonautonomous parabolic systems. *SIAM J Math Anal.* 1991;29:89–118.
- [13] Acquistapace P, Terreni B. Infinite-horizon linear-quadratic regulator problems for nonautonomous parabolic systems with boundary control. *SIAM J Math Anal.* 1996;34:1–30.
- [14] Wang PKC. Stabilization and Control of Distributed Systems with Time-Dependent Spatial Domains. *J Optim Theor & Appl.* 1990;65:331–362.
- [15] Wang PKC. Feedback Control of a Heat Diffusion System with Time-Dependent Spatial Domains. *Optim Contr Appl & Meth.* 1995;16:305–320.
- [16] Armaou A, Christofides PD. Robust Control of Parabolic PDE Systems with Time-Dependent Spatial Domains. *Automatica.* 1999;.
- [17] Armaou A, Christofides PD. Crystal temperature control in the czochralski crystal growth process. *AIChE J.* 2001;47:79–106.
- [18] Armaou A, Christofides PD. Nonlinear feedback control of parabolic partial differential equation systems with time-dependent spatial domains. *Chem Eng Sci.* 2002;57:5083–5114.
- [19] Dunbar W, Petit N, Rouchon P, Martin P. Boundary control of a nonlinear Stefan problem. In: *Decision and Control, 2003. Proceedings. 42nd IEEE Conference on*, vol. 2. 2003; pp. 1309–1314 Vol.2.

- [20] Brown R. Theory of transport processes in single crystal growth from the melt. *AIChE J.* 1988;34:881–911.
- [21] Derby J, Brown R. Thermal-capillary analysis of Czochralski and Liquid Encapsulated Czochralski Crystal Growth. I. Simulation. *J Cryst Growth.* 1986;74:605–624.
- [22] Derby J, Brown R. Thermal-capillary analysis of Czochralski and Liquid Encapsulated Czochralski Crystal Growth. II. Processing Strategies. *J Cryst Growth.* 1986;75:227–240.
- [23] Derby J, Brown R. On the Dynamics of Czochralski Crystal Growth. *J Cryst Growth.* 1987;83:137–151.
- [24] Szabo G. Thermal Strain during Czochralski Crystal Growth. *J Cryst Growth.* 1985;73:131–141.
- [25] Adams R. *Sobolev Spaces.* New York, U.S.A.: Academic Press. 1978.
- [26] Pazy A. *Semigroups of Linear Operators and Applications to Partial Differential Equations.* New York, U.S.A.: Springer-Verlag. 1983.
- [27] Evans L. *Partial differential equations.* USA: American Mathematical Society. 1998.
- [28] McOwen R. *Partial differential equations: methods and applications, 2nd ed.* USA: Prentice Hall. 2002.
- [29] Fattorini HO. Boundary control systems. *SIAM Journal on Control.* 1968; 6:349–385.
- [30] Curtain RF. On stabilizability of linear spectral systems via state boundary feedback. *SIAM J Control and Optimization.* 1985;23:144–152.

- [31] Bensoussan A, Prato GD, Delfour M, Mitter S. *Representation and Control of Infinite Dimensional Systems*. Boston: Birkhäuser. 2007.
- [32] Antoniadis C, Christofides P. Integrated optimal actuator placement and robust control of uncertain transport-reaction processes. *In Proc Amer Contr Conf, Arlington, VA*. 2001;3:1942–1947.
- [33] Demetriou MA, Borggaard J. Optimization of an integrated actuator placement and robust control scheme for distributed parameter processes subject to worst case spatial disturbance distribution. *In Proceedings of the American Control Conference, Denver, Colorado*. 2003;6:3894–3899.
- [34] Dubljevic S, Christofides P. Predictive control of parabolic PDEs with boundary control actuation. *Chemical Engineering Science*. 2006;61:6239–6248.
- [35] Balas MJ. Finite-Dimensional Control of Distributed Parameter Systems by Galerkin Approximation of Infinite Dimensional Controllers. *J Math Anal Appl*. 1986;114:17–36.
- [36] Ito K. Finite-Dimensional Compensators for Infinite-Dimensional Systems via Galerkin-Type Approximation. *SIAM J Control Optim*. 1990; 28:1251–1269.

Chapter 6

Conclusions and Future Work

Parabolic PDEs are used as models of transport-reaction phenomena in a variety of different industrial chemical and materials engineering processes, and can provide precise descriptions of process variables with complex temporal and spatially dependent system dynamics which are unattainable alternative modelling methodologies. The analysis of these models provides a fundamental basis for both the understanding the process dynamics and also the design and implementation of control schemes. While a comprehensive approach to model based control synthesis for PDEs is yet to be developed, there are several frameworks which are applicable to a large number of problems. One such framework is infinite-dimensional systems control theory which provides a convenient method of control design for parabolic PDEs. However, there are obstacles in the application of this approach which have also hindered the adoption and application in mainstream industrial settings. The issues related to analysis and control synthesis for already complex PDE initial and boundary value problems which often contain nonlinear or time-varying parameters terms, are further compounded by the inherently abstract nature of the infinite-dimensional systems approach which relies heavily on functional analytic methods. The feasible application of such control designs including

the formulation of the boundary control problem, output feedback, optimality, late lumping and the numerical realization of the system, are required to at least demonstrate the practicality of the design. One of the underlying themes of this thesis was to maintain a balance between the abstract nature of the general framework utilized in the analysis control synthesis and the applications to relevant industrial systems. Moreover, new methods are required in considering the application to particular classes of parabolic PDE systems. A systematic treatment and realization within this framework is provided for two general classes of control problems: 1) The optimal boundary control of unstable parabolic PDEs with nonautonomous and nonhomogeneous infinite-dimensional system representation; and 2) the optimal distributed and boundary control of parabolic PDEs on time-varying spatial domains with nonautonomous infinite-dimensional system representation. These two classes of problems were presented in the context of a Li-ion battery temperature regulation problem, and the feedback control of a class of convection-diffusion process in the context of the CZ crystal temperature stabilization problem.

6.1 Conclusions

A methodology to handle the output feedback boundary control of a class of unstable parabolic PDEs with nonautonomous and nonhomogeneous infinite-dimensional system representations was developed in Chapter 2 in the context of a Li-ion battery thermal regulation problem. The parabolic PDE model of the battery temperature dynamics is characterized by the presence of a time varying state related heat generation term, and a time varying non state related (non homogeneous) heat generation term which are sources of the dynamical instability of the system. To represent physical limitations in the

control system setup, the input was restricted along a portion of the domain boundary, and the sensor locations were specified only on small regions within the spatial domain itself. The state-feedback boundary control problem was represented by a nonautonomous infinite-dimensional system utilizing an exact boundary control transformation. The observer based optimal boundary control design was considered where the separation principle was utilized to demonstrate the stability of the closed loop time-varying system. Determination of the input profile was based on the infinite-dimensional LQR quadratic minimization problem, and required solving both a time-varying differential Riccati equation related to the state evolution, and an auxiliary differential Riccati equation related to the time-evolution of the non-state related heat generation term. The output feedback control problem was realized using a state measurement and temperature field interpolation methodology, and numerical results for simulation case studies demonstrated the stabilization of the temperature field by boundary control actuation utilizing different controller tuning designs and limitations in the sensor placements.

In Chapters 3-5, a methodology to handle the state feedback optimal distributed and boundary problems for a class of parabolic PDEs defined on time-varying spatial domains was developed within the context of the CZ crystal temperature stabilization problem. The distinguishing features of this class of PDE are the presence of a time-dependent convective-transport term which is associated with the time-evolution of the spatial domain boundary, and the definition of the PDE on a time-varying spatial domain. In the context of the CZ crystal growth process, the change in the spatial domain was due to the motion a mechanical pulling arm such that the dynamics of the mechanical

subsystem, together with the dynamics of crystal temperature, were represented by a unidirectionally coupled ODE and PDE system. The representation of the convection-diffusion PDE as an infinite-dimensional system was accomplished through the development of a nested-spatial domain approach which provide the basis for the definition of an appropriate function space setting in which the control problems can be considered within the infinite-dimensional systems framework. These concepts were detailed in Chapter 3 along with an introduction to the model formulation for PDEs defined on time-varying spatial domains from the first principles continuum mechanics. The optimal distributed control problem was considered for the PDE model posed on a 1-dimensional time-varying spatial domain and the numerical realization was provided. Chapter 4 considered the boundary control problem where the PDE model of the CZ crystal temperature is posed on a 2-dimensional time-varying spatial domain with dynamics coupled with those of the mechanical subsystem. The optimal control problem setup for the PDE coupled with the finite-dimensional subsystem is presented, and numerical results demonstrate the stabilization of the crystal temperature distribution in the time-varying spatial domain. Chapter 5 also considers the boundary control of the CZ crystal temperature on a 2-dimensional time-varying spatial domain but utilized an exact transformation of the PDE into an infinite-dimensional boundary control system. The LQR optimal control synthesis for the infinite-dimensional system and finite-dimensional subsystem were provided and numerical results demonstrated the stabilization of the crystal temperature distribution.

6.2 Future Work

This thesis was based on a series of papers [1, 2, 3, 4] which developed a set of methodologies devoted to the optimal distributed and boundary control problems for two important classes of transport-reaction systems modelled by parabolic PDEs within the context of two representative processes. Partial and preliminary results in each chapter can also be found in [5, 6, 7, 8, 9, 10]. In each work the feedback control designs were provided by considering the nonautonomous infinite-dimensional system representations of the PDE systems and the related infinite-dimensional LQR quadratic minimization problems. However, there remain many open questions regarding fundamental mathematical control issues in practical applications of infinite-dimensional systems theory for including exponential stability, stabilizability, and detectability conditions especially for nonautonomous and boundary control problems.

At present, there are very few results and examples on these subjects in addition to the associated controllability and observability conditions for practical problems. Some preliminary work is provided by the [11, 12] but the formalization of these notions and their application to physical systems has yet to be completed. A parallel branch of applied mathematical control theory considers discrete time infinite-dimensional systems [13, 14, 15, 16].

This area has important implications in the development of late lumping control methods for discretized PDE systems. One other extremely important are is the development of Model Predictive Control (MPC) strategies for nonautonomous infinite-dimensional systems as an extension of the celebrated works for finite-dimensional linear systems [17, 18, 19]. Preliminary work which considers the MPC formulation for the CZ crystal temperature

stabilization problem within the context of this thesis can be found in [20] along with a realization of the problem on a 2-dimensional spatial domain with state and input constraints [21]. Some recent results on MPC for PDEs in general can also be found in [22, 23, 24, 25].

Bibliography

- [1] Ng J, Dubljevic S. Boundary control synthesis for a lithium-ion battery thermal regulation problem. *AIChE Journal*. 2013;.
- [2] Ng J, Aksikas I, Dubljevic S. Control of parabolic PDEs with time-varying spatial domain: Czochralski crystal growth process. *International Journal of Control*. 2013;0(0):1–12.
- [3] Ng J, Dubljevic S. Optimal control of convection-diffusion process with time-varying spatial domain: Czochralski crystal growth. *Journal of Process Control*. 2011;21(10):1361–1369.
- [4] Ng J, Dubljevic S. Optimal boundary control of a diffusion-convection-reaction PDE model with time-dependent spatial domain: Czochralski crystal growth process. *Chemical Engineering Science*. 2012;67(1):111–119.
- [5] Ng J, Dubljevic S, Aksikas I. Optimal control of transport-reaction system with time varying spatial domain (keynote paper). In: *Proceedings of the 9th International Symposium on Dynamics and Control of Process Systems*. 2010; pp. 587–592.
- [6] Ng J, Dubljevic S. Multiscale dynamics and optimal control of parabolic PDE with time varying spatial domain (crystal growth process). In: *Proceedings of the 19th International Symposium on Mathematical Theory of Networks and Systems*. 2010; pp. 999–1006.
- [7] Ng J, Dubljevic S, Aksikas I. Multiscale optimal control of transport-reaction system with time varying spatial domain. In: *Proceedings of*

- the 49th IEEE Conference on Decision and Control (CDC)*. 2010; pp. 858–863.
- [8] Ng J, Dubljevic S. Optimal boundary control of parabolic PDE with time-varying spatial domain. In: *Advanced Control of Industrial Processes (ADCONIP), 2011 International Symposium on*. 2011; pp. 216–221.
- [9] Ng J, Aksikas I, Dubljevic S. Application of optimal boundary control to reaction-diffusion system with time-varying spatial domain. In: *American Control Conference (ACC), 2011*. 2011; pp. 2528–2533.
- [10] Ng J, Dubljevic S, Aksikas I. Optimal control of a class of linear nonautonomous parabolic PDE via two-parameter semigroup representation. In: *Decision and Control and European Control Conference (CDC-ECC), 2011 50th IEEE Conference on*. 2011; pp. 6997–7002.
- [11] Ng J, Dubljevic S, Aksikas I. Aspects of controllability and observability for time-varying PDE systems. In: *American Control Conference (ACC), 2012*. 2012; pp. 2220–2225.
- [12] Ng J, Dubljevic S, Aksikas I. Exponential stability and stabilizability conditions for a class of nonautonomous parabolic system, submitted. In: *Decision and Control Conference (CDC), 2012 51th IEEE Conference on*. 2012; .
- [13] Zabczyk J. Remarks on the control of discrete-time distributed parameter systems. *SIAM Journal on Control*. 1974;12(4):721–735.
- [14] Bamieh B, Pearson J J. A general framework for linear periodic systems with applications to H/sup infinity / sampled-data control. *Automatic Control, IEEE Transactions on*. April;37(4):418–435.

- [15] Logemann H. Stability and stabilizability of linear infinite-dimensional discrete-time systems. *IMA Journal of Mathematical Control and Information*. 1992;9(3):255–263.
- [16] Maciej Przyłuski K, Rolewicz S. On stability of linear time-varying infinite-dimensional discrete-time systems. *Systems & Control Letters*. 1984;4(5):307–315.
- [17] Rawlings JB, Muske KR. The Stability of Constrained Receding Horizon Control. *IEEE Trans Automat Contr*. 1993;38:1512–1516.
- [18] Muske KR, Rawlings JB. Model predictive control with linear models. *AIChE J*. 1993;39:262–287.
- [19] Muske KR. Linear Model Predictive Control of Chemical Processes. Ph.D. thesis, The University of Texas. 1995.
- [20] Ng J, Aksikas I, Dubljevic S. Model predictive control formulation for a class of time-varying linear parabolic PDEs. In: *American Control Conference (ACC), 2011*. 29 2011-July 1; pp. 2963–2968.
- [21] Ng J, Dubljevic S, Aksikas I. Model predictive control of Czochralski crystal growth process. In: *Control Automation (MED), 2011 19th Mediterranean Conference on*. June; pp. 825–831.
- [22] Shang H, Forbes JF, Guay M. Model Predictive Control for Quasilinear Hyperbolic Distributed Parameter Systems. *Industrial & Engineering Chemistry Research*. 2004;43(9):2140–2149.
- [23] Dubljevic S, Mhaskar P, El-Farra NH, Christofides PD. Predictive control of transport-reaction processes. *Computers & Chemical Engineering*. 2005;29(1112):2335 – 2345.

- [24] Dubljevic S, El-Farra NH, Mhaskar P, Christofides PD. Predictive control of parabolic PDEs with state and control constraints. *International Journal of robust and nonlinear control*. 2006;16(16):749–772.
- [25] Ishida M, Zhan J. Neural model-predictive control of distributed parameter crystal growth process. *AIChE Journal*. 1995;41(10):2333–2336.